AD-A256 740

TATION PAGE

Form Approved
OMB No. 0704-0188

(2)

to average 1 hour per response, including the time for reviewing instructions, searching existing data sources, wing the collection of information. Send comments regarding this burden estimate or any other aspect of this en, to Washington Headquarters Services, Directorate for information Operations and Reports, 1215 Jefferson e of Management and Budget, Paperwork Reduction Project (0704-0188), Washington, DC 20503

OATE	3. REPORT TYPE AND DATES COVERED
August 28, 1992	Final Report; 7/89-6/92

4. TITLE AND SUBTITLE
HIGHLY ACCURATE ADAPTIVE FINITE ELEMENT SCHEMES FOR NONLINEAR HYPERBOLIC PROBLEMS

5. FUNDING NUMBERS
DAAL03-89-K-0120

6. AUTHOR(S)
J. Tinsley Oden

7. PERFORMING ORGANIZATION NAME(S) AND ADDRESS(ES)
Texas Institute for Computational Mechanics
The University of Texas at Austin
Austin, TX 78712-1085

8. PERFORMING ORGANIZATION REPORT NUMBER

DTIC ELECTE OCT 22 1992

9. SPONSORING/MONITORING AGENCY NAME(S) AND ADDRESS(ES)
U. S. Army Research Office
P. O. Box 12211
Research Triangle Park, NC 27709-2211

10. SPONSORING/MONITORING AGENCY REPORT NUMBER
ARO 26821.5-MA

11. SUPPLEMENTARY NOTES
The view, opinions and/or findings contained in this report are those of the author(s) and should not be construed as an official Department of the Army position, policy, or decision, unless so designated by other documentation.

12a. DISTRIBUTION/AVAILABILITY STATEMENT
Approved for public release; distribution unlimited.

12b. DISTRIBUTION CODE

13. ABSTRACT *(Maximum 200 words)*

This document is a final report of research activities supported under General Contract DAAL03-89-K-0120 between the Army Research Office and The University of Texas at Austin from July 1, 1989 through June 30, 1992. The project supported several Ph.D. students over the contract period, two of which are scheduled to complete dissertations during the 1992-93 academic year. Research results produced during the course of this effort led to 6 journal articles, 5 research reports, 4 conference papers and presentations, 1 book chapter, and two dissertations (nearing completion).

It is felt that several significant advances were made during the course of this project that should have an impact on the field of numerical analysis of wave phenomena. These include the development of high-order, adaptive, *hp*-finite element methods for elastodynamic calculations and high-order schemes for linear and nonlinear hyperbolic systems. Also, a theory of multi-stage Taylor-Galerkin schemes was developed and implemented in the analysis of several wave propagation problems, and was configured within a general *hp*-adaptive strategy for these types of problems. Further details on research results and on areas requiring additional study are given in the Appendix.

92-27594

14. SUBJECT TERMS	15. NUMBER OF PAGES
stress waves, adaptive methods, hp version finite elements, error estimation	103
	16. PRICE CODE

17. SECURITY CLASSIFICATION OF REPORT	18. SECURITY CLASSIFICATION OF THIS PAGE	19. SECURITY CLASSIFICATION OF ABSTRACT	20. LIMITATION OF ABSTRACT
UNCLASSIFIED	UNCLASSIFIED	UNCLASSIFIED	UL

HIGHLY ACCURATE ADAPTIVE FINITE ELEMENT SCHEMES FOR NONLINEAR HYPERBOLIC PROBLEMS

FINAL REPORT

J. TINSLEY ODEN

AUGUST, 1992

THE ARMY RESEARCH OFFICE

CONTRACT DAAL03–89–K–0120

Texas Institute for Computational Mechanics
The University of Texas at Austin

Approved for Public Resease

Distribution Unlimited

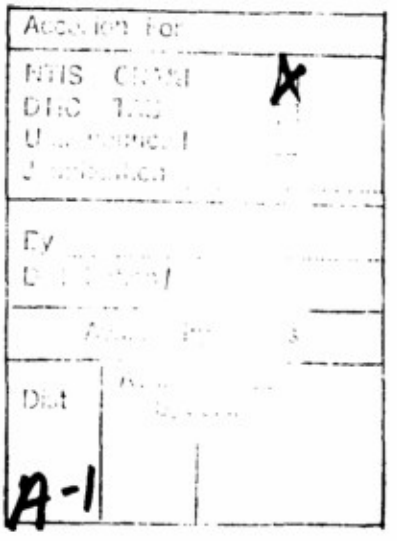

Contents

Final Report
on
Highly Accurate Adaptive Finite Element Schemes for Nonlinear Hyperbolic Problems

1 Introduction

This document is a final report of research activities supported under General Contract DAAL03-89-K0120 between the Army Research Office and The University of Texas at Austin. The report describes work performed during the period July 1, 1989 and June 30, 1992. The Principal Investigator of the project was Professor J. T. Oden. The project supported several Ph.D. students over the contract period, two of which are scheduled to complete dissertations during the 1992–93 academic year. Research results produced during the course of this effort led to six journal articles, five research reports, four conference papers and presentations, one book chapter, and two dissertations (nearing completion). More complete summaries of these documents are given later in this report.

It is felt that several significant advances were made during the course of this project that should have an impact on the field of numerical analysis of wave phenomena. These include the development of high–order, adaptive, *hp*-finite element methods for elastodynamic calculations and high–order schemes for linear and nonlinear hyperbolic systems. Also, a theory of multi-stage Taylor-Galerkin schemes was developed and implemented in the analysis of several wave propagation problems, and was configured within a general *hp*-adaptive strategy for these types of problems. Further details on research results and on areas requiring additional study are given in the next section of this report and in an appendix.

2 Review of Research Results

2.1 *General Goals*

Despite a half century of study, despite the introduction of modern computational techniques and machines, and despite a multitude of papers, conferences, and journals on the subject, the field of numerical analysis of complex wave phenomena has actually not progressed much beyond its glorious beginnings in the pre–World War II era of computational modeling. In a sense, the basic issues today are the same as they have been for a half century: accuracy, stability, and consistency of the numerical approximation of the propogations of functions which possibly possess discontinuities. Many textbooks are filled with examples of successful schemes for a simple one–dimensional linear wave equation, or perhaps Burger's equation in one dimension. Indeed, the theory of numerical analysis of wave phenomena, as it exists today, is still basically a one–dimensional theory, and the most significant advances in the subject over the last decade are the introduction of methods which seem to work well for certain one–dimensional cases.

Among major goals of research in this area are the development of highly accurate, stable, non–oscillatory, and convergent numerical approximations to study a multitude of features of solutions of hyperbolic systems of conservation laws that can be used efficiently to model wave phenomena of interest in science and engineering. But these goals have proved to be paradoxical; e.g., monotone schemes may non–oscillatory and stable, but they are only first–order accurate, and higher order schemes, while providing higher accuracy, are almost always oscillatory and frequently unstable. Moreover, for nonlinear hyperbolic systems, questions of uniqueness of solutions arise and the additional requirement that the numerical solution be "physically meaningful" must be added to the list of criteria.

The emergence of adaptive computational schemes over the last decade has provided a possible basis for achieving the historical goals in the numerical analysis of wave phenomena: manipulate mesh parameters in such a way that both high–order accuracy and stability can somehow be achieved. In this way, the computational process is optimized, and any tendency of the scheme to oscillate or to lose accuracy would, in theory, be compensated by appropriate adaptation of the control parameters. A key to this approach is the basic idea of developing reliable *a posteriori* estimates of the numerical error in a finite element approximation, mesh parameters such as the mesh size h, spectral order of approximation p, or the location or the relocation of nodes, can be adapted to keep error within preset tolerances. Importantly, the computational cost can also be added to the cost functional so that, at least in theory, highly efficient schemes can be used to achieve these classical goals.

The project summarized in this final report had as its basic objective the exploration of new types of hp-finite element methods for the analysis of wave propagation problems, with

particular emphasis on stress waves in solids. The starting points for all of the studies in this effort were the following: a high-level *hp* data structure was constructed in which the mesh size h and the spectral order p within a finite element mesh were designed to be free parameters. The capability for either using h-refinement, p-enrichment, or hp-refinements was embodied in the data structure, the data structure was designed to admit fairly general *a posteriori* error estimates, so that some research and experimentation could be done on the calculation of errors to drive any adaptive process. Finally, the specifics of the adaptive process were left open so that a number of different strategies could be explored. With regard to the general approaches considered in the research, two were explored:

1. Use of discontinuous *hp*-finite element methods for nonlinear hyperbolic systems, and
2. the use of continuous *hp*-approximations with very high-order implicit schemes for the particular classes of hyperbolic systems that arise in the study of stress waves in solids.

These two approaches are discussed in more detail in the following sections and some technical details are given in the appendices.

2.2 *Stress Waves in Solids: RK and TG Schemes*

We briefly outline here the approach and some results of the research on high-order schemes for calculation of transient phenomena in elastic solids.

To construct a successful adaptive scheme for the hyperbolic partial differential equations that occur in linear elastodynamics, the basic ingredients mentioned above must first be addressed: 1), a functional *hp*-adaptive data structures in hand, a high-order temporal scheme must be identified to advance the solution in time; 2), an efficient method of *a posteriori* error estimation must be developed to provide the data for controlling the numerical process; 3), an adaptive strategy must be developed to control (optimize) the mesh during the evolution of the wave phenomena.

In the early months of this phase of the project, considerable effort was spent exploring classical high-order methods for time integration. Surprisingly, relatively few existing methods survive our criteria for efficiency and applicability to very large systems. The classical Adams-Bashforth methods, for example, require a significant amount of memory and are only conditionally stable. The Runge-Kutta methods, however, do seem to offer a number of advantages. They are implemented locally over a time step, which was convenient for *hp*-adaptive schemes, and they could be used to produce results of arbitrary order in time. A great deal of time was spent during early phases of this project encoding and experimenting various forms of Runge-Kutta methods, including the singly-implicit Runge-Kutta schemes, implicit Runge-Kutta schemes, and traditional semi-implicit Runge-Kutta schemes. These

proved to be somewhat effective, but in many cases also were accompanied by unpleasant oscillations for very high order schemes.

A new study was initiated on a completely new family of methods which are of a form similar to so–called Taylor-Galerkin methods used in certain flow calculations. Traditionally, Taylor-Galerkin methods no higher than third–order appear in the literature, and these are known to be very inefficient and expensive. However, it was observed that by reducing the elastodynamics problem to a first–order hyperbolic system and then applying the Taylor-Galerkin strategy, a recurrence formula could be derived which could produce very robust and stable schemes of arbitrary high order. Thus was invented the first high–order Taylor-Galerkin schemes for wave propagation. These schemes are still under study, but they are known to possess many attractive features and have proved to be quite superior to traditional Runge-Kutta methods in a number of numerical experiments.

In the final months of this phase of the project, still another version of the implicit, high–order, multi-staged Taylor-Galerkin scheme were developed in which second–order hyperbolic systems are derived which are equivalent to the equations of linear elastodynamics. It was observed that the governing operators naturally split into similar component parts which made application of the TG ideas straightforward.

Considerable time was spent on *a posteriori* error estimation for these types of schemes. These *a posteriori* estimates were developed for not only the time–dependent case but also for the elliptic systems obtained during each step of the Taylor-Galerkin approximation. The situation is this: rigorous mathematical theory for *a posteriori* error estimates for linear elliptic systems was developed and applied step–wise to the Taylor-Galerkin scheme. In the Taylor-Galerkin scheme, the elliptic step, of course, involves the time step so that the *a posteriori* estimate does include a description of this mesh parameter. A number of opportunities for measuring temporal error also present themselves. In particular, the usual use of predictor and a corrector in time allow for a fairly straightforward estimate of the temporal component of the approximation error. To date, a number of test problems have been run and results suggest that the total error in the two–dimensional elastodynamics problem can be kept under control and that fairly accurate error estimates can be obtained.

Finally, it is necessary to address the *hp*-adaptive strategy. This is an area in which considerable additional work reamins to be done. During the course of the project reported here, a number of so–called three–step schemes were explored in which criteria were established for producing first an h-refinement of a mesh and then a p-enrichment to control the error. Various versions of this strategy have been studied experimentally. The meshes obtained by these schemes are certainly not optimal, and some are quite far from optimal, but they can be implemented with great speed and thus the overall computational time of implementation often proves to be quite acceptable.

The status of these schemes is this: a number of papers on the mathematical ideas and the implementation have been published, a working research code for two–dimensional cases has been developed, and a number of test problems have been run. Further work remains to be done on error estimation, adaptive strategy, and on numerous details of implementation, such as the possibility of using domain decomposition and parallelization during the computational process. Mathematical issues deserving study include the study of stability of the TG schemes, *a priori* error estimation, proof of convergence of the *hp*-adaptive strategies, and further work on rigorous *a posteriori* estimates.

2.3 *Discontinuous hp Methods for Nonlinear Conservation Laws*

As noted earlier, much as been said in recent literature on the numerical solution of hyperbolic conservation laws with regard to the use of flux limiting methods and high–order approximations. This has led to the notions of TVD schemes, ENO schemes, etc., all of which seem to work very well for one–dimensional problems provided that no boundary conditions of significance are imposed. To extend these ideas to reasonable two– and three–dimensional cases involves some significant generalizations of the existing theory.

One generalization that was felt deserved some study was the notion of TVB (total variation bounded) algorithms developed Cockburn and Shu. While their work itself originally focused on one–dimensional cases, much of their theory is general and potentially extendable to higher dimensional cases.

As another thrust in the present research effort, the study of high–order *hp* schemes for discontinuous Galerkin approximations of nonlinear hyperbolic systems was undertaken. These were based on generalizations of the Cockburn-Shu TVB schemes, and employed high–order *hp* quadrilateral finite element approximations in two dimensions. The key to these types of methods is the construction of a special projection operator which maintains the TVB character of the numerical solution. During this project, an algorithm for producing such a projection was indeed developed and has been applied successfully to discontinuous *hp* approximations of hyperbolic conservation laws. The status of this work is that one paper on the subject has been published, another is in preparation. Several important details remain unresolved. These include the development of a useful adaptive strategy for these techniques, and a numerical strategy that truly exploits the spectral character of these types of approximations while using the *h*-adaptivity to control oscillations near shocks and contact discontinuities.

3 Summary of Publications and Presentations

The following papers and presentations were made as a result of the research done on this project.

Journal Articles:

1. Oden, J. T., Demkowicz, L., and Safjan, A., "Adaptive Finite Element Methods for Hyperbolic Systems with Applications to Transient Acoustics," *International Journal of Numerical Methods in Engineering*, Vol. 32, pp. 677–707, 1991.

2. Oden, J. T., and Demkowicz, L., "*hp*-Adaptive Finite Element Methods in Computational Fluid Dynamics," *Computer Methods in Applied Mechanics and Engineering*, Vol. 89, pp. 11–40, 1991.

3. Edwards, M. G., Oden, J. T., and Demkowicz, L., "An *hr*-Adaptive Second Order Approximate Riemann Solver for the Euler Equations in Two Dimensions," *SIAM Journal of Statistical and Scientific Computing* (in press).

4. Ainsworth, M., and Oden, J. T., "A Unified Approach to *A Posteriori* Error Estimation Using Element Residual Methods," *Numerische Mathematik* (in press).

5. Ainsworth, M., and Oden, J. T., "A Procedure for *A Posteriori* Error Estimation for *hp* Finite Element Methods," *Computer Methods in Applied Mechanics and Engineering* (in press).

6. Oden, J. T., Ainsworth, M., and Wu, W., "*A Posteriori* Error Estimation for *hp*-Approximations in Elastostatics," *Applied Numerical Mathematics* (in press).

Research Reports:

1. Bey, K. S., and Oden, J. T., "A Runge-Kutta Discontinuous Finite Element Methods for High Speed Flows," TICOM Report 91-04, Austin, 1991.

2. Ainsworth, M., and Oden, J. T., "A Unified Approach to *A Posteriori* Error Estimation Using Element Residual Methods," TICOM Report 91-03, Austin, Texas, 1991.

3. Oden, J. T., Ainsworth, M., and Wu, W., "*A Posteriori* Error Estimation for *hp*-Approximations in Elastostatics," TICOM Report 92-07, Austin, Texas, 1992.

4. Oden, J. T., "Notes on High-Order Flow Solvers for Nonlinear Hyperbolic Conservation Laws, TICOM Report 90-01, Austin, Texas, 1990.

5. Cockburn, B., and Shu, C-W, "Continuous Finite Element Methods for Nonlinear Conservation Laws: Preliminary Results," TICOM Report 89-09, Austin, Texas, 1989.

Conference Presentations and Proceedings:

1. "A Runge-Kutta Discontinuous Finite Element Method for High Speed Flows" (with K. Bey), AIAA 10th Computational Fluid Dynamics Conference, June 24–27, 1991, Honolulu, HI. Also published in Proceedings of that conference.

2. "*hp*-Adaptive Finite Element Methods in Transient Acoustics" (with A. Safjan), presented at ASME/WAM, December 1–5, 1991, Atlanta, GA.

3. "Smart Algorithms and Adaptive Methods for Compressible and Incompressible Flow: Optimization of the Computational Process," presented at Thinking Machines, Inc. Symposium on Very Large Scale Computing in the 21st Century, October 1–3, 1990, Boston, MA.

4. "Adaptivity and Smart Algorithms for Fluid–Structure Interaction," presented at the 28th Aerospace Sciences Meeting, AIAA, January 8–11, Reno, NV.

Book Contributions:

1. "Smart Algorithms and Adaptive Methods for Compressible and Incompressible Flow: Optimization of the Computational Process," *Very Large Scale Computation in the 21st Century*, ed. by Jill Mesirov, SIAM Publications, Chapter 7, 1990.

4 Participating Personnel

The following individuals made technical contributions to this project:

1. J. T. Oden, Principal Investigator

2. L. Demkowicz, Research Fellow

3. B. Cockburn, Research Fellow

4. C-W Shu, Research Fellow

5. K. S. Bey, Graduate Student

6. A. Safjan, Graduate Student

7. P. Geng, Graduate Student

APPENDIX

High-Order Taylor-Galerkin and Adaptive *hp*- Methods for 2nd order Hyperbolic Systems

In this Appendix a brief summary of some of the details of approach and numerical results of the hp–adaptive Taylor-Galerkin algorithms described in the text is given. This appendix is excepted from an article on the subject which is entitled "High–Order Taylor-Galerkin and Adaptive h–p Methods for Hyperbolic Systems" by A. Safjan and J. T. Oden.

1 INTRODUCTION

The use of high-order adaptive finite element methods for elliptic boundary-value problems in which the mesh size h and the local spectral order p of the approximation are varied in order to control the approximation error have been shown to produce exponential rates of convergence (e.g., [7, 8]). These methods treat the mesh variables h and p as arbitrary parameters, and, through a fairly elaborate data structure, distribute mesh sizes and orders nonuniformly over a mesh to control local errors, which are estimated using *a-posteriori* estimation techniques [7]. Thus, they represent optimal-control strategies which attempt to configure the mesh to optimize the computational process. Such strategies have

proved to be effective for several classes of problems, including problems in gas dynamics modeled by the Euler equations [1] and problems in compressible and incompressible flow (e.g., [7]).

For time-dependent problems, however, the use of high-order spatial approximations requires the use of a balanced temporal approximations that is high order as well.The search for robust high-order schemes that function efficiently on spatially-nonuniform meshes has been an elusive one, and few of the traditional schemes of high order (e.g., implicit Runge-Kutta methods) have proven to be effective for these types of approximations [9].

The so-called Taylor-Galerkin schemes represent generalizations of the Lax-Wendroff algorithm and have been used effectively for producing second- and third-order temporal approximations [5, 3]. However, no procedures for extending these techniques to temporal approximations of arbitrary order appear to be available.

In the present work, we present a new family of stable high order Taylor Galerkin (TG) methods for the numerical solutions of second-order hyperbolic systems. It is shown that for second order systems, a multi-stage process can be used that produces schemes of order $2s$ for s-stages, each of which involves the solution of a second-order system of elliptic equations. A detailed stability analysis is provided for the case of linear systems which establishes choices of parameters that result in unconditionally stable schemes.

An error estimation procedure is also presented which leads to estimates of both the spatial and temporal approximation error. In addition, an adaptive algorithm is developed which employs an *hp*-adaptive finite element method for controlling the spatial errors.

For focus, applications to linear elastodynamics problems in two space dimensions are described. The results of numerical experimnts on representative two-dimensional stress wave propagation problems are also given. The results indicate that the algorithms are capable of delivering high accuracy on meshes with very high order spatial approximations. Very little oscilations of solutions in the vicinity of wave fronts is observed, despite the very high-order approximations and minimal numerical dissipation.

2. Model 2nd order Hyperbolic System: Equations of Linear Elastodynamics

As a starting point , we consider equations of linear elasticity in the following form:

$$\begin{cases} div\boldsymbol{T}(\boldsymbol{u}) + \rho_0 \boldsymbol{b} = \rho_0 \partial_t^2 \boldsymbol{u} \\ \boldsymbol{T}(\boldsymbol{u}) = 2\mu\varepsilon(\boldsymbol{u}) + \lambda Tr(\varepsilon)\boldsymbol{I} \qquad \text{in } \Omega \\ 2\varepsilon(\boldsymbol{u}) = \nabla \boldsymbol{u} + \nabla \boldsymbol{u}^T \end{cases} \tag{2.1}$$

where :

Ω is a domain in $\mathbb{R}^N$, $N = 2, 3$

$\boldsymbol{u}$ = $\boldsymbol{u}(\boldsymbol{x}, t)$ is the displacement vector at particle $\boldsymbol{x} \in \Omega$ at time $t \geq 0$

$\boldsymbol{T}(\boldsymbol{u})$ = the stress tensor

$\varepsilon(\boldsymbol{u})$ = the strain tensor

$\boldsymbol{b}(\boldsymbol{x}, t)$ = the body force field

ρ_0 = mass density

μ, λ = Lamé coefficients

We reformulate equations (2.1) in terms of $\boldsymbol{u}$ only and arrive at

$$\rho_0 \partial_t^2 \boldsymbol{u} - \boldsymbol{D}^T \boldsymbol{C} \boldsymbol{D} \boldsymbol{u} = \rho_0 \boldsymbol{b} \tag{2.2}$$

where $\boldsymbol{D}$ is a generalized gradient operator :

$$\boldsymbol{D} \overset{\text{def}}{=} \begin{pmatrix} \partial_1 & 0 & 0 \\ 0 & \partial_2 & 0 \\ 0 & 0 & \partial_3 \\ 0 & \partial_3 & \partial_2 \\ \partial_3 & 0 & \partial_1 \\ \partial_2 & \partial_1 & 0 \end{pmatrix} \tag{2.3}$$

and $\boldsymbol{C}$ is a 6×6 symmetric positive definite matrix of elastic constants :

$$\boldsymbol{C} \overset{\text{def}}{=} \begin{pmatrix} C_{1111} & C_{1122} & C_{1133} & C_{1123} & C_{1131} & C_{1112} \\ \cdot & C_{2222} & C_{2233} & C_{2223} & C_{2231} & C_{2212} \\ \cdot & \cdot & C_{3333} & C_{3323} & C_{3331} & C_{3312} \\ \cdot & \cdot & \cdot & C_{2323} & C_{2331} & C_{2312} \\ \cdot & \cdot & \cdot & \cdot & C_{3131} & C_{3112} \\ \cdot & \cdot & \cdot & \cdot & \cdot & C_{1212} \end{pmatrix} \tag{2.3}$$

For isotropic material elasticities C_{ijkl} are given in term of Lamé constants λ and μ by

$$C_{ijkl} = \delta_{ij}\,\delta_{kl}\,\lambda + \mu(\,\delta_{ik}\,\delta_{jl} + \delta_{il}\,\delta_{jk}\,) \tag{2.4}$$

Equations (2.2) are to be solved in a domain $\Omega \subset \mathbb{R}^N$, $N = 2, 3$. Typically, two particular cases are of interest:

- *interior* problems when Ω is bounded
- *exterior* problems when Ω is a complement of a bounded set

The initial boundary value problem is further specified by introducing boundary conditions. We consider the following kinds of boundary conditions:

1. Kinematic boundary condition

$$u = \hat{u} \qquad \text{on} \quad \Gamma_u \tag{2.5}$$

where $\hat{u}$ is a prescribed displacement vector on the Γ_u – part of the boundary .

2. Traction boundary condition

$$T(u) \cdot n = t \qquad \text{on } \Gamma_t \tag{2.6}$$

where n is the unit outward normal to the boundary and t is a prescribed traction on the Γ_t – part of the boundary ($\partial\Omega = \overline{\Gamma_u \cup \Gamma_t}$, $\Gamma_u \cap \Gamma_t = \emptyset$).

The initial boundary value problem is completed by specifying initial conditions of the form

$$u = u_0 \text{ and } \partial_t u = v_0 \text{ at } t = 0 \tag{2.7}$$

In the case of homogeneous boundary conditions, the problem can be cast into the Hilbert space formulation as follows (see [4] for a detailed discussion).

We introduce

- The Hilbert space

$$\begin{aligned} H &= \left(L^2(\Omega)\right)^N \\ (u, v)_H &= (u, Mv)_{(L^2)^N} \end{aligned} \tag{2.8}$$

with the weighting matrix $M = (m_{kl})$

$$m_{kl} = \rho_0 \delta_{kl} \tag{2.9}$$

- Operator $\mathfrak{A} : H \supset D(\mathfrak{A}) \longrightarrow H$

$$\mathfrak{A}u \overset{\text{def}}{=} -M^{-1}D^T C D u \tag{2.10}$$

where $D(\mathfrak{A})$ is the domain of $\mathfrak{A}$ defined as

$$D(\mathfrak{A}) = \{ u \in H_0^1(\Omega) \mid D^T C D u \in H \} \tag{2.14}$$

for the Dirichlet boundary value problem, and

$$D(\mathfrak{A}) = \{ u \in H^1(\Omega) \mid C D u \in D_0^*(\Omega) \} \tag{2.15}$$

for the Neumann boundary value problem, where

$$D_0^*(\Omega) = \left\{ u \in (L^2(\Omega))^M \mid \exists w \in H(\Omega),\ \forall v \in H^1(\Omega),\ (u, Dv)_{(L^2)^M} = (w, v)_{(L^2)^N} \right\} \tag{2.16}$$

and $M = N(N+1)/2$. Note that the boundary condition on u is satisfied in the sense of the trace theorem, whereas the boundary condition on t is interpreted in the sense of the generalized Green's formula. For these reasons, the displacement boundary condition is classified as the Dirichlet boundary condition and the traction boundary condition as the Neumann boundary condition for operator $\mathfrak{A}$.

Within the Hilbert space formalism, the initial boundary value problem of linear elasticity can be reinterpreted as an abstract 2nd order Cauchy problem :

$$\begin{cases} \dfrac{d^2u}{dt^2} + \mathfrak{A}u = 0 & t > 0 \\ u = u_0 \,,\ \dfrac{du}{dt} = v_0 & t = 0 \end{cases} \tag{2.17}$$

An H – valued function of time $u = u(t)$

$$[0,\ \infty) \ni t \longrightarrow u(t) \in H \tag{2.18}$$

is called a weak solution of (2.17) if :

(i) u_0 and v_0 satisfy regularity assumption

$$u_0 , v_0 \in H \tag{2.19}$$

(ii) $u(t)$ satisfies regularity assumption

$$u \in C([0,\ \infty)\,;\, H) \tag{2.20}$$

(iii) $u(t)$ satisfies (2.21)

$$\int_0^\infty \int_\Omega u^T \left(\overline{\Phi_{,tt} + \mathfrak{A}\Phi} \right) dx\, dt + \left(u_0,\ \Phi_{,t}(0, \cdot) \right)_{(L^2)^N}$$

$$- \left(v_0, \Phi(0, \cdot) \right)_{(L^2)^N} = 0 \tag{2.21}$$

for every test function

$$\Phi \in C_0(R ; D(\mathcal{A})) \cap C^2(R ; H) \tag{2.22}$$

Notice that this definition admits, in particular, solutions in the d'Alembert sense.

We record now some fundamental results concerning operator $\mathcal{A}$ and the existence and uniqueness of weak solutions u. We restrict ourselves to the case of a bounded domain Ω.

1. Operator $\mathcal{A}$ is self-adjoint.

2. Operator $\mathcal{A}^{1/2}$ exists.

3. The spectrum of $\mathcal{A}$, $\sigma(\mathcal{A})$, consists of eigenvalues only. For the Dirichlet problem all the eigenvalues are positive

$$\begin{aligned} &\sigma(\mathcal{A}) = \{ \omega_1 , \omega_2 , \ldots \} \\ &0 < \omega_1 \le \omega_2 \le \ldots \le \omega_n \longrightarrow \infty \end{aligned} \tag{2.22}$$

and for the Neumann problem the eigenvalues are non-negative

$$\begin{aligned} &\sigma(\mathcal{A}) = \{ \omega_0, \omega_1 , \omega_2 , \ldots \} \\ &0 = \omega_0 < \omega_1 \le \omega_2 \le \ldots \le \omega_n \longrightarrow \infty \end{aligned} \tag{2.23}$$

All eigenvalues are of finite multiplicity and corresponding eigenspaces $\{u_n\}$ are orthogonal.

4. For the Neumann problem, the eigenspace corresponding to zero eigenvalue, i.e., the null space of operator $\mathcal{A}$, is spanned by constant vectors and by

$$\begin{pmatrix} 0 \\ x_3 \\ -x_2 \end{pmatrix} \qquad \begin{pmatrix} x_3 \\ 0 \\ -x_1 \end{pmatrix} \qquad \begin{pmatrix} x_2 \\ -x_1 \\ 0 \end{pmatrix} \tag{2.24}$$

5. Operator $\mathcal{A}$ admits a clasical spectral decomposition

$$\mathcal{A} = \sum_{n=n_0}^{\infty} \omega_n dP_n \tag{2.25}$$

$$I = \sum_{n=n_0}^{\infty} dP_n \tag{2.26}$$

where dP_n is the orthogonal projection on the eigenspace $\{u_n\}$ corresponding to ω_n

$$dP_n(\cdot) = (\cdot, u_n)u_n \tag{2.27}$$

and $n_0 = 1, 0$ for the Dirichlet and Neumann problems, respectively.

5. A weak solution u exists and is unique. Moreover, it is of the form

$$u(t) = cos\,(\mathcal{A}^{1/2}t)u_0 - \mathcal{A}^{-1/2} sin\,(\mathcal{A}^{1/2}t)v_0 \tag{2.28}$$

6. If the initial condition functions u_0 and v_0 satisfy an additional regularity assumption

$$u_0 \in D(\mathcal{A}^{1/2}), v_0 \in H \tag{2.29}$$

and the solution $u \in C^1([0, \infty); H) \cap C([0, \infty); D(\mathcal{A}^{1/2}))$, then the weak solution is also a solution with finite energy:

$$E(\cdot) \equiv \|u_{,t}\|_H^2 + \|\mathcal{A}^{1/2}u\|_H^2 \tag{2.30}$$

3 High-Order Taylor-Galerkin Methods

Given a bounded domain Ω in $\mathbb{R}^N$, $N = 2, 3$, we consider a system of conservation laws of the form

$$u_{,t} + F^k(\nabla u)_{,k} = 0 \quad x \in \Omega \quad t > 0 \quad k = 1, \ldots, N \tag{3.1}$$

where $u = u(x, t)$ is a column vector of M unknowns, F^k, $k = 1, \ldots, N$ are vector-valued functions of ∇u, commas denote the differentiation with respect to time t and spatial variables x_k and the usual summation convention holds.

This system of equations is accompanied by an initial condition,

$$u(x, 0) = u_0(x), \quad u_{,t}(x, 0) = v_0(x) \qquad x \in \Omega \tag{3.2}$$

and by appropriate boundary conditions.

By introducing velocity $v = u_{,t}$ as an auxiliary variable, equations (3.1) can be converted into the following first order system (in time):

$$\begin{cases} v_{,t} + F^k(\nabla u)_{,k} = 0 \\ u_{,t} - v = 0 \end{cases} \qquad x \in \Omega \quad t > 0 \tag{3.3}$$

Finally, (3.3) and (3.2) is cast in the form of an abstract Cauchy Problem

$$\begin{cases} U_{,t} + A\,U = 0 & t > 0 \\ U = U_0 & t = 0 \end{cases} \tag{3.4}$$

where

$$A \overset{\text{def}}{=} \begin{pmatrix} 0 & F^k(\nabla(\cdot))_{,k} \\ -I & 0 \end{pmatrix} \tag{3.5}$$

U is a group variable, $U = \begin{pmatrix} v \\ u \end{pmatrix}$, and U_0 specifies initial conditions, $U_0 = \begin{pmatrix} v_0 \\ u_0 \end{pmatrix}$.

3.1 Taylor-Galerkin Schemes for Nonlinear Systems

Given the solution $U^n = U(t_n)$ at time $t_n = n\Delta t$, we seek the next time step solution $U^{n+1} = U(t_n + \Delta t)$ in the following form

$$
\left[\begin{array}{lll}
Z_1 - \lambda\Delta t^2 Z_{1,tt} = U^n & + \mu_{10}\Delta t\, U^n_{,t} & + \nu_{10}\Delta t^2 U^n_{,tt} \\
Z_2 - \lambda\Delta t^2 Z_{2,tt} = U^n & + \mu_{20}\Delta t\, U^n_{,t} & + \nu_{20}\Delta t^2 U^n_{,tt} \\
 & + \mu_{21}\Delta t\, Z_{1,t} & + \nu_{21}\Delta t^2 Z_{1,tt} \\
\vdots & & \\
Z_s - \lambda\Delta t^2 Z_{s,tt} = U^n & + \mu_{s0}\Delta t\, U^n_{,t} & + \nu_{s0}\Delta t^2 U^n_{,tt} \\
 & + \mu_{s1}\Delta t\, Z_{1,t} & + \nu_{s1}\Delta t^2 Z_{1,tt} \\
 & + \ldots & \\
 & + \mu_{s,s-1}\Delta t\, Z_{s-1,t} & + \nu_{s,s-1}\Delta t^2 Z_{s-1,tt}
\end{array}\right. \qquad (3.6)
$$

where

$Z_i = U(t_n + c_i\Delta t)$, $i = 1, 2, \ldots, s-1$, are intermediate solutions called "internal approximations"

$Z_s = U(t_n + \Delta t) = U^{n+1}$ is the next time step solution (i.e., $c_s = 1$)

$\mu_{ij}, \nu_{ij}, \mu_{i0}, \nu_{i0}, c_i \in \mathbb{R}$, $i = 1, 2, \ldots, s$; $j = 1, 2, \ldots, i-1$

$\lambda \in \mathbb{R}_+$ is a stability parameter

s = number of stages

Coefficients μ_{ij}, ν_{ij}, μ_{i0}, ν_{i0}, c_i, are to be chosen so as to obtain the highest possible order of accuracy, subject to stability or other constraints. A free parameter λ is to be chosen from stability considerations.

It is convenient to rewrite (3.6) in the following compact form:

$$\begin{pmatrix} Z_1 \\ Z_2 \\ \cdot \\ \cdot \\ \cdot \\ Z_s \end{pmatrix} - \Delta t^2 \nu \otimes \begin{pmatrix} Z_{1,tt} \\ Z_{2,tt} \\ \cdot \\ \cdot \\ \cdot \\ Z_{s,tt} \end{pmatrix} - \Delta t\, \mu \otimes \begin{pmatrix} Z_{1,t} \\ Z_{2,t} \\ \cdot \\ \cdot \\ \cdot \\ Z_{s,t} \end{pmatrix} = \kappa \otimes \begin{pmatrix} U^n \\ \Delta t\ U^n_{,t} \\ \Delta t^2\ U^n_{,tt} \end{pmatrix} \qquad (3.7)$$

where

$\nu, \mu \in \mathbb{R}^{s \times s}$, $\kappa \in \mathbb{R}^{s \times 3}$

$$\nu = \begin{pmatrix} \lambda & 0 & 0 & 0 & 0 & 0 \\ \nu_{21} & \lambda & 0 & 0 & 0 & 0 \\ \nu_{31} & \nu_{32} & \lambda & 0 & 0 & 0 \\ \cdot & \cdot & \cdot & \cdot & \cdot & \cdot \\ \cdot & \cdot & \cdot & \cdot & \cdot & \cdot \\ \nu_{s1} & \nu_{s2} & \nu_{s3} & \cdot & \nu_{ss-1} & \lambda \end{pmatrix} \qquad c = (c_1\ c_2\ c_3 \cdot \cdot\ c_s)$$

$$\mu = \begin{pmatrix} 0 & 0 & 0 & 0 & 0 & 0 \\ \mu_{21} & 0 & 0 & 0 & 0 & 0 \\ \mu_{31} & \mu_{32} & 0 & 0 & 0 & 0 \\ \cdot & \cdot & \cdot & \cdot & \cdot & \cdot \\ \cdot & \cdot & \cdot & \cdot & \cdot & \cdot \\ \mu_{s1} & \mu_{s2} & \mu_{s3} & \cdot & \mu_{ss-1} & 0 \end{pmatrix} \qquad \kappa = \begin{pmatrix} 1 & \mu_{10} & \nu_{10} \\ 1 & \mu_{20} & \nu_{20} \\ 1 & \mu_{30} & \nu_{30} \\ \cdot & \cdot & \cdot \\ \cdot & \cdot & \cdot \\ 1 & \mu_{s0} & \nu_{s0} \end{pmatrix} \qquad (3.8)$$

Matrices ν, μ and κ together with vector c completely characterize difference scheme (3.6).

A distinct feature of (3.6) is that coefficient matrices ν and μ are lower triangular matrices which makes the resulting scheme semi-implicit (i.e, to compute Z_i it is necessary to know $Z_{i-1}, Z_{i-2}, ..., Z_1$, but it is not necessary to now Z_{i+1}). Moreover, all diagonal elements of ν are equal ($\nu_{ii} = \lambda$, i=1, 2, ..., s) and so are those of μ ($\mu_{ii} = 0$, i=1, 2, ..., s). This makes the operator defining the left-hand side of each stage of (3.6) identical for linear (or linearized) problems, and, hence, significantly reduces the cost of the method. A particular choice of zero diagonal elements of μ is made with an eye on a well-posedness of a typical one stage problem and a possible splitting of the operator defining the left hand side of each stage.

To make the i-th stage solution Z_i m-th order accurate, it is necessary to satisfy the order conditions for Z_i and to make the previus stage solutions $Z_{i-1}, Z_{i-2}, ..., Z_1$, to be at least of the order m-1. (Otherwise, some coefficients have to be set to zero, e.g., if Z_{i-1} is of the order m-2, then, necessarily $\mu_{i,i-1} = 0$). The order conditions for Z_i are obtained by expanding it in Taylor series at U^n :

$$Z_i = U^n + (c_i \Delta t)U^n_{,t} + \frac{1}{2!}(c_i \Delta t)^2 U^n_{,tt} + ... + \frac{1}{m!}(c_i \Delta t)^m \frac{\partial^m}{\partial t^m} U^n + O(\Delta t^{m+1}) \qquad (3.9)$$

plugging (3.9) into the left-hand side of the i-th stage equation

$$Z_i - \sum_{j=1}^{s} \left(\mu_{ij}\Delta t\, Z_{j,t} + \nu_{ij}\Delta t^2 Z_{j,tt} \right) = U^n + \kappa_{i2}\Delta t\, U^n_{,t} + \kappa_{i3}\Delta t^2 U^n_{,tt} \qquad (3.10)$$

and equating coefficients of powers of Δt to zero. This leads to the following system of nonlinear algebraic equations

$$c_i^k - k \sum_{j=1}^{s} c_j^{k-1}\mu_{ij} - k(k-1)\sum_{j=1}^{s} c_j^{k-2}\nu_{ij} = \begin{cases} \mu_{i0}, & i = 1 \\ 2\nu_{i0}, & i = 2 \\ 0, \text{ otherwise} \end{cases} \qquad (3.11)$$

$k = 1, 2, ..., m$

Equations (3.11) are referred to herein as the order conditions.

We now proceed to derive coefficients for some particular schemes. In the sequel we adopt the following notation: TG(s, m) = s-stage m-th order scheme.

2-stage schemes of order 4 (TG(2,4))

We make Z_1 and Z_2 to be $O(\Delta t^3)$ and $O(\Delta t^4)$, respectively, which leads to the following system of equations:

$$
\begin{aligned}
&\mu_{10} = c_1 \\
&2\nu_{10} = c_1^2 - 2\lambda \\
&6\lambda = c_1^2 \\
&\mu_{20} + \mu_{21} = 1 \\
&2(\nu_{20} + \nu_{21}) + 2\mu_{21} c_1 = 1 - 2\lambda \\
&6\nu_{21} c_1 + 3\mu_{21} c_1^2 = 1 - 6\lambda \\
&12\nu_{21} c_1^2 + 4\mu_{21} c_1^3 = 1 - 12\lambda
\end{aligned}
\tag{3.12}
$$

The solution of (3.12) reads:

$$
\begin{aligned}
c_1 &= \mu_{10} = (6\lambda)^{1/2} \\
\nu_{10} &= 2\lambda \\
\mu_{21} &= \frac{1 - 6\lambda}{6\lambda} - \frac{1}{2}\,\frac{1 - 12\lambda}{(6\lambda)^{3/2}} \\
\nu_{21} &= \frac{1}{4}\,\frac{1 - 12\lambda}{6\lambda} - \frac{1}{3}\,\frac{1 - 12\lambda}{(6\lambda)^{1/2}} \\
\mu_{20} &= 1 - \frac{1 - 6\lambda}{6\lambda} + \frac{1}{2}\,\frac{1 - 12\lambda}{(6\lambda)^{3/2}} \\
\nu_{20} &= \frac{1}{2} - \lambda + \frac{1}{4}\,\frac{1 - 12\lambda}{6\lambda} - \frac{2}{3}\,\frac{1 - 6\lambda}{(6\lambda)^{1/2}}
\end{aligned}
\tag{3.13}
$$

A different 4th order scheme can be obtained by discarding the 3rd equation of (3.12) (i.e., making Z_1 to be only $O(\Delta t^2)$) and by taking $\mu_{21} = 0$. The coefficients for this scheme are given below

$$
\begin{aligned}
c_1 &= \mu_{10} = \frac{1}{2}\,\frac{1 - 12\lambda}{1 - 6\lambda} \\
\nu_{10} &= \frac{1}{8}\left(\frac{1 - 12\lambda}{1 - 6\lambda}\right)^2 - \lambda \\
\mu_{21} &= 0
\end{aligned}
$$

$$\nu_{21} = \frac{1}{3}\,\frac{(1 - 6\lambda)^2}{1 - 12\lambda} \qquad (3.14)$$

$$\mu_{20} = 1$$

$$\nu_{20} = \frac{1}{6}\,\frac{1 - 18\lambda}{1 - 12\lambda}$$

■

3-stage scheme of order 5 (TG(3,5))

We make Z_1, Z_2 and Z_3 to be $O(\Delta t^3)$, $O(\Delta t^4)$ and $O(\Delta t^5)$, respectively, which leads to the following system of equations:

$$\begin{aligned}
&\mu_{10} = c_1 \\
&2\nu_{10} = c_1^2 - 2\lambda \\
&6\lambda = c_1^2 \\
&\mu_{20} + \mu_{21} = c_2 \\
&2(\nu_{20} + \nu_{21}) + 2\mu_{21}c_1 = c_2^2 - 2\lambda \\
&6\nu_{21}c_1 + 3\mu_{21}c_1^2 = c_2^3 - 6\lambda c_2 \\
&12\nu_{21}c_1^2 + 4\mu_{21}c_1^3 = c_2^4 - 12\lambda c_2^2 \\
&\mu_{30} + \mu_{32} = 1 \\
&2(\nu_{30} + \nu_{31} + \nu_{32} + \mu_{32}) = 1 - 2\lambda \\
&6(\nu_{31} + \nu_{32}c_2) + 3\mu_{32}c_2^2 = 1 - 6\lambda \\
&12(\nu_{31} + \nu_{32}c_2^2) + 4\mu_{32}c_2^3 = 1 - 12\lambda \\
&20(\nu_{31} + \nu_{32}c_2^3) + 5\mu_{32}c_2^4 = 1 - 20\lambda \\
&\mu_{21} = 0
\end{aligned} \qquad (3.15)$$

For stability purpose we require additionaly that

$$\nu_{32}(\nu_{21}\nu_{10} - \nu_{20}\lambda) = 0 \qquad (3.16)$$

A solution to (3.15) and (3.16) is given below:

$$c_1 = \mu_{10} = (6\lambda)^{1/2}$$

$$\nu_{10} = 2\lambda$$

$$
\begin{aligned}
c_2 &= \frac{1}{30}\,(28 \pm 8) \\
\mu_{21} &= c_1^{-3}\,[\, c_1 c_2^3 - \tfrac{1}{2}\, c_2^4 - 6\lambda(c_1 c_2 - c_2^2)\,] \\
\nu_{21} &= c_1^{-2}\,[\tfrac{1}{4}\, c_2^4 - \tfrac{1}{3}\, c_1 c_2^3 - \lambda(3c_2^2 - 2c_1 c_2)\,] \\
\mu_{20} &= c_2 - \mu_{21} \\
\nu_{20} &= \tfrac{1}{2}\, c_2^2 - \lambda - \nu_{21} - \mu_{21} c_1 \\
\mu_{32} &= (6c_2^2 - 4c_2^3)^{-1} \\
\nu_{32} &= 0 \\
\mu_{31} &= 0 \\
\nu_{31} &= \tfrac{1}{6} - \lambda - \tfrac{1}{2}\, \mu_{32} c_2^2 \\
\mu_{30} &= 1 - \mu_{32} \\
\nu_{30} &= \tfrac{1}{2} - \lambda - \nu_{31} - \mu_{32}
\end{aligned}
\qquad (3.17)
$$

■

3-stage imbedded scheme of order 4 (TG(3,4))

To allow for an error control, we construct a method in which a 1-stage 2nd order scheme is imbedded in a 2-stage 3rd order scheme which, in turn, is imbedded in a 3-stage 4th order scheme. (We symbolically write TG(1, 2) "$\subset$" TG(2, 3) "$\subset$" TG(3, 4)). Toward this end, we make Z_1, Z_2 and Z_3 to be $O(\Delta t^2)$, $O(\Delta t^3)$ and $O(\Delta t^4)$, respectively, and we set $c_1 = c_2 = 1$. Thus, each stage is an approximation to the solution U at time $t_n + \Delta t$ and the difference $||Z_i - Z_{i-1}||$ defines a relative error for Z_{i-1}. Resulting order conditions are listed below:

$$
\begin{aligned}
&\mu_{10} = 1 \\
&2\nu_{10} = 1 - 2\lambda \\
&\mu_{20} + \mu_{21} = 1 \\
&2(\nu_{20} + \nu_{21}) + 2\mu_{21} = 1 - 2\lambda \\
&6\nu_{21} + 3\mu_{21} = 1 - 6\lambda \\
&\mu_{30} + \mu_{32} = 1 \\
&2(\nu_{30} + \nu_{31} + \nu_{32} + \mu_{32}) = 1 - 2\lambda \\
&6(\nu_{31} + \nu_{32} c_2) + 3\mu_{32} = 1 - 6\lambda \\
&12(\nu_{31} + \nu_{32}) + 4\mu_{32} = 1 - 12\lambda \\
&\mu_{31} = 0
\end{aligned}
\qquad (3.18)
$$

For stability purpose we require additionaly that

$$\begin{aligned} &\nu_{21}\nu_{t0} - \nu_{20}\lambda = 0 \\ &\nu_{32}(\nu_{21}\mu_{t0} - \mu_{21}\nu_{10} - \mu_{20}\lambda) = 0 \end{aligned} \tag{3.19}$$

A solution to (3.18) and (3.19) is given below:

$$\begin{aligned} \mu_{10} &= c_1 = 1 \\ \nu_{10} &= \tfrac{1}{2} - \lambda \\ c_2 &= 1 \\ \nu_{20} &= \tfrac{3}{4}\,\frac{(\tfrac{1}{2} - \lambda)(-\tfrac{1}{18} + \lambda)}{\tfrac{1}{8} - \lambda} \\ \nu_{21} &= \tfrac{3}{4}\,\frac{\lambda(-\tfrac{1}{18} + \lambda)}{\tfrac{1}{8} - \lambda} \\ \mu_{21} &= \tfrac{1}{3} - 2\lambda - \tfrac{3}{2}\,\frac{\lambda(-\tfrac{1}{18} + \lambda)}{\tfrac{1}{8} - \lambda} \\ \mu_{20} &= -\tfrac{2}{3} + 2\lambda + \tfrac{3}{2}\,\frac{\lambda(-\tfrac{1}{18} + \lambda)}{\tfrac{1}{8} - \lambda} \\ \mu_{32} &= \tfrac{1}{2} \\ \nu_{32} &= 0 \\ \mu_{31} &= 0 \\ \nu_{31} &= -\tfrac{1}{12} - \lambda \\ \mu_{30} &= 0 \\ \mu_{30} &= \tfrac{1}{12} \end{aligned} \tag{3.20}$$

■

Next, using the original equations (3.1) - (3.5), we calculate the time derivatives in terms of spatial derivatives as follows:

$$\begin{aligned} U_{,t} &= -A\,U \\ &= -\begin{pmatrix} F^k(\nabla u)_{,k} \\ -v \end{pmatrix} \end{aligned} \tag{3.21}$$

$$
\begin{aligned}
U_{,tt} &= -(AU)_{,t} \\
&= -\begin{pmatrix} (R^{kl}(\nabla u)v_{,l})_{,k} \\ F^{k}(\nabla u)_{,k} \end{pmatrix}
\end{aligned}
\tag{3.22}
$$

where $R^{kl} = \dfrac{\partial F^k}{\partial u_{,l}}$ are the Jacobian matrices corresponding to fluxes F^k. In deriving (3.22) we used the following relations:

$$
\begin{aligned}
v_{,tt} &= -(F^k(\nabla u)_{,k})_{,t} \\
&= -(F^k(\nabla u)_{,t})_{,k} \\
&= -(\frac{\partial F^k}{\partial u_{,l}} u_{,lt})_{,k} \\
&= -(R^{kl}(\nabla u)\, v_{,l})_{,k}
\end{aligned}
\tag{3.23}
$$

Also, it is important to notice that $U_{,tt}$ can be expressed in terms of spatial derivatives of u and v of the order at most 2, which can be effectively handeled by C^0 continuous finite elements.

Next, replacing the time derivatives in (3.7) by formulas (3.21) and (3.22), and denoting $Z_i = \begin{pmatrix} v_i \\ u_i \end{pmatrix}$ and $U^n = \begin{pmatrix} v^n \\ u^n \end{pmatrix}$, we arrive at the following system of equations

$$
\left[
\begin{aligned}
v_i &- \sum_{j=1}^{s} \left(\mu_{ij}\Delta t\, [-F^k(\nabla u_j)_{,k}] + \nu_{ij}\Delta t^2 [-(R^{kl}(\nabla u_j)\, v_{j,l})_{,k}] \right) \\
&= v^n + \kappa_{i2}\Delta t\, [-F^k(\nabla u^n)_{,k}] + \kappa_{i3}\Delta t^2 [-(R^{kl}(\nabla u^n)\, v^n{}_{,l})_{,k}] \\
u_i &- \sum_{j=1}^{s} \left(\mu_{ij}\Delta t\, [v_j] + \nu_{ij}\Delta t^2 [-F^k(\nabla u_j)_{,k}] \right) \\
&= u^n + \kappa_{i2}\Delta t\, [v^n] + \kappa_{i3}\Delta t^2 [-F^k(\nabla u^n)_{,k}] \\
& \qquad i = 1, 2, \ldots, s
\end{aligned}
\right.
\tag{3.24}
$$

where the indices i and j are used to denote a particular stage, the indices k and l refere to the axis of a Cartesian coordinate system, comma denotes partial differentiation, and the summation convention for k and l holds.

Finally, multiplying (3.13) by vector-valued test function $W = \begin{pmatrix} w_v \\ w_u \end{pmatrix}$, integrating over Ω and integrating by parts, we arrive at the variational formulation of the form:

Find v_i and u_i, $i = 1, 2, ..., s$, such that

$$
\begin{aligned}
&\int_\Omega w_v^T v_i \, dx \\
&- \sum_{j=1}^{s} \mu_{ij}\Delta t \left[\int_\Omega w_{v,k}^T F^k(\nabla u_j)\, dx - \int_{\partial\Omega} w_v^T F^k(\nabla u_j) n_k \, ds \right] \\
&- \sum_{j=1}^{s} \nu_{ij}\Delta t^2 \left[\int_\Omega w_{v,k}^T \left(R^{kl}(\nabla u_j)\, v_{j,l} \right) dx - \int_{\partial\Omega} w_v^T \left(R^{kl}(\nabla u_j)\, v_{j,l} \right) n_k \, ds \right] \\
&= \int_\Omega w_v^T v^n \, dx \\
&- \kappa_{i2}\Delta t \left[\int_\Omega w_{v,k}^T F^k(\nabla u^n)\, dx - \int_{\partial\Omega} w_v^T F^k(\nabla u^n) n_k \, ds \right] \\
&- \kappa_{i3}\Delta t^2 \left[\int_\Omega w_{v,k}^T \left(R^{kl}(\nabla u^n)\, v^n{}_{,l} \right) dx - \int_{\partial\Omega} w_v^T \left(R^{kl}(\nabla u^n)\, v^n{}_{,l} \right) n_k \, ds \right]
\end{aligned}
\tag{3.25}
$$

$$
\begin{aligned}
&\int_\Omega w_u^T u_i \, dx \\
&- \sum_{j=1}^{s} \mu_{ij}\Delta t \int_\Omega w_u^T v_j \, dx \\
&- \sum_{j=1}^{s} \nu_{ij}\Delta t^2 \left[\int_\Omega w_{u,k}^T F^k(\nabla u_j) dx - \int_{\partial\Omega} w_u^T F^k(\nabla u_j) n_k \, ds \right] \\
&= \int_\Omega w_u^T u^n \, dx \\
&- \kappa_{i2}\Delta t \int_\Omega w_u^T v^n \, dx \\
&- \kappa_{i3}\Delta t^2 \left[\int_\Omega w_{u,k}^T F^k(\nabla u^n)\, dx - \int_{\partial\Omega} w_u^T F^k(\nabla u^n) n_k \, ds \right]
\end{aligned}
$$

for all admissible test functions w_v and w_u.

where $n = (n_k)$ is the unit outward normal. Weak form (3.25) is the basis for FE approximations.

3.2 Taylor-Galerkin Schemes for Linear Systems

We now give an alternative derivation of TG schemes which is valid for linear systems of conservation laws with constant coefficients addmiting spectral decomposition of underlying spatial operator.

Given the solution $U^n = U(t_n)$ at time $t_n = n\Delta t$, we seek the next time step solution $U^{n+1} = U(t_n + \Delta t)$ in the following form

$$\underbrace{\left[(I - \lambda\Delta t^2\partial^2/\partial t^2) \ldots (I - \lambda\Delta t^2\partial^2/\partial t^2)\right]}_{s \text{ times}} U^{n+1}$$

$$= \left[I + \chi_1(\lambda)\Delta t\partial/\partial t + \chi_2(\lambda)\Delta t^2\partial^2/\partial t^2 + \ldots + \chi_{2s}(\lambda)\Delta t^{2s}\partial^{2s}/\partial t^{2s}\right]U^n + O(\Delta t^{m+1}) \quad (3.26)$$

where

$\chi_j(\lambda) \in \mathbb{R}$, $j = 1, 2, \ldots, 2s$
$\chi_j(\lambda) \equiv 0$, $j = m + 1, m + 2, \ldots, 2s$
$\lambda \in \mathbb{R}_+$
s = number of stages
$m \le 2s$ is the order of the highest derivative at the right-hand-side of (3.26).

Coefficients $\chi_j(\lambda)$ are to be chosen so as to obtain the highest possible order of accuracy, subject to stability or other constraints. As previously, a free parameter λ is to be chosen from stability considerations.

The coefficients $\chi_j(\lambda)$ are determined by expanding U^{n+1} at the left-hand side of (3.26) in a Taylor series about U^n and equating coefficients of powers of Δt to zero. Accordingly, identity (3.27)

$$\underbrace{\left[(I - \lambda\Delta t^2\partial^2/\partial t^2) \ldots (I - \lambda\Delta t^2\partial^2/\partial t^2)\right]}_{s \text{ times}}\left[I + \Delta t\partial/\partial t + \frac{1}{2!}\Delta t^2\partial^2/\partial t^2 + \ldots + \frac{1}{(2s)!}\Delta t^{2s}\partial^{2s}/\partial t^{2s}\right]U^n$$

$$= \left[I + \chi_1(\lambda)\Delta t\partial/\partial t + \chi_2(\lambda)\Delta t^2\partial^2/\partial t^2 + \ldots + \chi_{2s}(\lambda)\Delta t^{2s}\partial^{2s}/\partial t^{2s}\right]U^n + O(\Delta t^{m+1}) \quad (3.27)$$

leads to the following relations for $\chi_j(\lambda)$

$$
\begin{aligned}
\chi_1(\lambda) &= 1 \\
\chi_2(\lambda) &= \frac{1}{2!} - \binom{s}{1}\lambda \\
\chi_3(\lambda) &= \frac{t}{3!} - \binom{s}{1}\lambda \\
\chi_4(\lambda) &= \frac{t}{4!} - \frac{t}{2!}\binom{s}{1}\lambda + \binom{s}{2}\lambda^2 \\
\chi_5(\lambda) &= \frac{t}{5!} - \frac{t}{3!}\binom{s}{1}\lambda + \binom{s}{2}\lambda^2 \\
\chi_6(\lambda) &= \frac{1}{6!} - \frac{t}{4!}\binom{s}{1}\lambda + \frac{t}{2!}\binom{s}{2}\lambda^2 - \binom{s}{3}\lambda^3 \\
\chi_7(\lambda) &= \frac{1}{7!} - \frac{t}{5!}\binom{s}{1}\lambda + \frac{t}{2!}\binom{s}{2}\lambda^2 - \binom{s}{3}\lambda^3 \\
&\text{etc.}
\end{aligned}
\tag{3.28}
$$

where $\binom{s}{k} = \frac{s!}{k!(s-k)!}$ is the Newton binominal symbol.

Constructed in this way, an s-stage scheme is of the order $m \leq 2s$. Furthermore, for particular values of λ it will be of the order $m+1$, and, in fact, this is the highest attainable order of accuracy. Typically we choose $m = 2s$, i.e., an s-stage scheme of the order $2s$ (or $2s + 1$). On the other hand, the choice $m < 2s$, when some of the coefficients χ_j are *a priori* specified to be zero, may be advantageous from the stability point of view, e.g., by setting $\chi_{2s} \equiv \chi_{2s-1} \equiv 0$, the resulting s-stage scheme will be of the order $2s - 2$ (or, at most $2s - 1$).

Remark: the scheme with $m < 2s$, e.g., $m = 2s - 1$, where $\chi_{2s} \equiv 0$, should not be confused with the scheme with $m = 2s$ and λ being so chosen that $\chi_{2s} = 0$. The former is of the order $2s - 1$ while the letter is of the order $2s$. It is only for this particular value of λ that both schemes are identical. ■

EXAMPLE 3.1

The 3-stage scheme of the order 6 is of the form:

$$
\begin{aligned}
\left[I - \lambda\Delta t^2\partial^2/\partial t^2\right]^3 U^{n+1} = \Big[I &\\
&+ \Delta t\, \partial/\partial t \\
&+ \left(\frac{1}{2} - 3\lambda\right)\Delta t^2\, \partial^2/\partial t^2 \\
&+ \left(\frac{1}{6} - 3\lambda\right)\Delta t^3\, \partial^3/\partial t^3
\end{aligned}
$$

$$+ \left(\frac{1}{24} - \frac{3}{2}\lambda + 3\lambda^2\right)\Delta t^4\,\partial^4/\partial t^4$$
$$+ \left(\frac{1}{120} - \frac{1}{2}\lambda + 3\lambda^2\right)\Delta t^5\,\partial^5/\partial t^5$$
$$+ \left(\frac{1}{720} - \frac{1}{8}\lambda + \frac{3}{2}\lambda^2 - \lambda^3\right)\Delta t^6\,\partial^6/\partial t^6\Big]U^n \qquad (3.29)$$

with the local truncation error E_t satisfies

$$\left[I - \lambda\Delta t^2\partial^2/\partial t^2\right]^3 E_t = \Big[\underbrace{\left(\frac{1}{5040} - \frac{1}{40}\lambda + \frac{1}{2}\lambda^2 - \lambda^3\right)\Delta t^7\,\partial^7/\partial t^7}_{e_t(\lambda)}\Big]U^n + O(\Delta t^8) \qquad (3.30)$$

Setting $\lambda \approx 1.41218087134444$ yields $\chi_6 = 0$ but the resulting scheme is still of the order 6. By choosing λ to be a zero of $e_t(\lambda)$ (e.g., $\lambda \approx 0.444797521031781$), formula (3.29) has order 7.

The 3-stage scheme of the 4th order is of the form:

$$\left[I - \lambda\Delta t^2\partial^2/\partial t^2\right]^3 U^{n+1} = \Big[I$$
$$+ \Delta t\,\partial/\partial t$$
$$+ \left(\frac{1}{2} - 3\lambda\right)\Delta t^2\,\partial^2/\partial t^2$$
$$+ \left(\frac{1}{6} - 3\lambda\right)\Delta t^3\,\partial^3/\partial t^3$$
$$+ \left(\frac{1}{24} - \frac{3}{2}\lambda + 3\lambda^2\right)\Delta t^4\,\partial^4/\partial t^4\Big]U^n \qquad (3.31)$$

■

In order to implement formula (3.27) efficiently, it is necessary to factorize the right-hand-side operator into the product of "quadratics" as follows:

$$\left(I + \chi_1(\lambda)\Delta t\partial/\partial t + \chi_2(\lambda)\Delta t^2\partial^2/\partial t^2 + \ldots + \chi_{2s}(\lambda)\Delta t^{2s}\partial^{2s}/\partial t^{2s}\right)$$
$$= \underbrace{\left(I + \mu_1(\lambda)\Delta t\partial/\partial t + \nu_1(\lambda)\Delta t^2\partial^2/\partial t^2\right)\ldots\left(I + \mu_s(\lambda)\Delta t\partial/\partial t + \nu_s(\lambda)\Delta t^2\partial^2/\partial t^2\right)}_{s\text{ times}} \qquad (3.32)$$

Indentity (3.32) leads to the following system of nonlinear algebraic equations for μ_j and ν_j, $j = 1, 2, \ldots, s$:

$$
\begin{aligned}
&\mu_1 + \mu_2 + \ldots + \mu_s = 1 \\
&\nu_1 + \nu_2 + \ldots + \nu_s + \mu_1\mu_2 + \ldots + \mu_{s-1}\mu_s = \chi_2(\lambda) \\
&\cdot \\
&\cdot \\
&\cdot \\
&\nu_1\nu_2 \ldots \nu_s = \chi_{2s}(\lambda)
\end{aligned}
\tag{3.33}
$$

Factorization (3.33) exists and is unique. The coefficients of the factorization can be found numerically for a given value of parameter λ and are given in an Appendix.

Next, we use relations (3.21) and (3.22) to express time derivatives in term of spatial derivatives. For linear systems with constant coefficients, these equations take a particulary simple form:

$$
\begin{aligned}
U_{,t} &= -AU \\
U_{,tt} &= A^2U
\end{aligned}
\tag{3.34}
$$

Replacing the time derivatives in the left-hand side of (3.27) and the right-hand side of (3.29) by formulas (3.34) and introducing auxiliary stages Y_i, we arrive at the following system of equations

$$
\left[
\begin{aligned}
&Y_1 - \lambda\Delta t^2A^2Y_1 = U^n - \mu_1\Delta t\,AU^n + \nu_1\Delta t^2A^2U^n \\
&Y_2 - \lambda\Delta t^2A^2Y_2 = Y_1 - \mu_2\Delta t\,AY_1 + \nu_2\Delta t^2A^2Y_1 \\
&\cdot \\
&\cdot \qquad s \text{ times} \\
&\cdot \\
&U^{n+1} - \lambda\Delta t^2A^2U^{n+1} = Y_{s-1} - \mu_s\Delta t\,AY_{s-1} + \nu_s\Delta t^2A^2Y_{s-1}
\end{aligned}
\right.
\tag{3.35}
$$

In deriving (3.35) we used the fact that the operators $\left[I - \lambda\Delta t^2A^2\right]^{-1}$ and $\left[I - \mu_j\Delta t\,A + \nu_j\Delta t^2A^2\right]$ commute. (In general, $[f(A)\circ g(A)](U) = \sum_{n=n_0}^{\infty} f(\omega_n)g(\omega_n)dP_n(U) = [g(A)\circ f(A)](U)$, where $f(A)$ is a bounded operator, ω_n are the eigenvalues of A and dP_n are the associated eigenprojections; see also Section 2).

As can be seen, (3.35) is a sequence of s linear elliptic-like PDE's with the same left-hand side operator. Moreover, since operator A^2 has zero off-diagonal terms :

$$A^2 = \begin{pmatrix} -F^k(\nabla(\cdot))_{,k} & 0 \\ 0 & -F^k(\nabla(\cdot))_{,k} \end{pmatrix} \tag{3.36}$$

a typical "one stage problem" is splitted into v-equations and u-equations, which can be solved independently and in parallel (the presence of A at the left-hand side of (3.35) would have destroyed this property). In addition, the diagonal terms of A^2 are identical which means that the operators defining the left-hand side of each stage of (3.35) are identical for both v- and u-equations (and for all stages).

Finally, multiplying (3.35) by vector-valued test function W, integrating over Ω and integrating by parts, and denoting $Y_0 \equiv U^n$ and $Y_s \equiv U^{n+1}$, we arrive at the variational formulation of the form:

Given $Y_0 \in X$

Find $Y_i = \begin{pmatrix} v_i \\ u_i \end{pmatrix} \in X$, $i = 1, 2, ..., s$, such that

$$\begin{aligned} & a(w_v, v_i) - \lambda\Delta t^2[b(w_v, v_i) - b_\Gamma(w_v, v_i)] \\ = \; & a(w_v, v_{i-1}) + \mu_i \Delta t[b(w_v, u_{i-1}) - b_\Gamma(w_v, u_{i-1})] \\ + \; & \nu_i \Delta t^2[b(w_v, v_{i-1}) - b_\Gamma(w_v, v_{i-1})] \end{aligned}$$

$$\begin{aligned} & a(w_u, u_i) - \lambda\Delta t^2[b(w_u, u_i) - b_\Gamma(w_u, u_i)] \\ = \; & a(w_u, u_{i-1}) - \mu_i \Delta t\, a(w_u, v_{i-1}) \\ + \; & \nu_i \Delta t^2[b(w_u, u_{i-1}) - b_\Gamma(w_u, u_{i-1})] \end{aligned} \tag{3.37}$$

for all admissible test functions $W = \begin{pmatrix} w_v \\ w_u \end{pmatrix} \in X$

Here :

$$\begin{aligned} a(w, u) &= \int_\Omega w^T u \, dx \\ b(w, u) &= \int_\Omega w^T_{,k} R^{kl} u_{,l} \, dx \\ b_\Gamma(w, u) &= \int_{\partial\Omega} w^T n_k R^{kl} u \, ds \end{aligned} \tag{3.38}$$

Jacobian fluxes $\boldsymbol{R}^{kl} = \dfrac{\partial \boldsymbol{F}^k}{\partial \boldsymbol{u}_{,l}}$ are now constant matrices, and n_k is the unit outward normal.

Replacing X in (3.37) with a finite dimensional subspace X_h of X, we arrive at the fully discretized problem.

$$
\left[\begin{array}{l}
\text{Given } Y_{h,0} \in X_h \\
\text{Find } Y_{h,i} = \begin{pmatrix} v_{h,i} \\ u_{h,i} \end{pmatrix} \in X_h \ , i = 1, 2, \ldots, s, \ \text{such that} \\
\\
\quad a(w_v , v_{h,i}) - \lambda \Delta t^2 [b(w_v , v_{h,i}) - b_\Gamma(w_v , v_{h,i})] \\
= \ a(w_v , v_{h,i-1}) + \mu_i \Delta t [b(w_v , u_{h,i-1}) - b_\Gamma(w_v , u_{h,i-1})] \\
+ \ \nu_i \Delta t^2 [b(w_v , v_{h,i-1}) - b_\Gamma(w_v , v_{h,i-1})] \\
\\
\quad a(w_u , u_{h,i}) - \lambda \Delta t^2 [b(w_u , u_{h,i}) - b_\Gamma(w_u , u_{h,i})] \\
= \ a(w_u , u_{h,i-1}) - \mu_i \Delta t \, a(w_u , v_{h,i-1}) \\
+ \ \nu_i \Delta t^2 [b(w_u , u_{h,i-1}) - b_\Gamma(w_u , u_{h,i-1})] \\
\\
\text{for all admissible test functions } W = \begin{pmatrix} w_v \\ w_u \end{pmatrix} \in X_h
\end{array}\right. \tag{3.39}
$$

Formula (3.39) is referred to as an s-stage, high-order Taylor-Galerkin (TG) method.

4 A Linear Stability Analysis

We shall now restrict ouerselves to the special case of the eqautions of linear elastodynamics. Thus, we consider the problem of the form

$$
\begin{cases}
\dfrac{d^2 \boldsymbol{u}}{dt^2} + \mathfrak{A} \boldsymbol{u} = \boldsymbol{0} & t > 0 \\
\\
\boldsymbol{u} = \boldsymbol{u}_0 \ , \ \dfrac{d\boldsymbol{u}}{dt} = \boldsymbol{v}_0 & t = 0
\end{cases} \tag{4.1}
$$

where the operator $\mathcal{A}$ is defined by eqns (2.10) - (2.16). It is convenient to convert (4.1) into the 1st order system of the following form

$$\begin{cases} U_{,t} + iA\,U = 0 & t > 0 \\ U = U_0 & t = 0 \end{cases} \tag{4.2}$$

where

$$AU \overset{\text{def}}{=} -i \begin{pmatrix} 0 & \mathcal{A} \\ -I & 0 \end{pmatrix} U \tag{4.3}$$

U is a group variable, $U = \begin{pmatrix} v \\ u \end{pmatrix}$, U_0 specifies initial conditions, $U_0 = \begin{pmatrix} v_0 \\ u_0 \end{pmatrix}$, and i is the imaginary unit. The form of (4.3) is similar to (3.4) except the multiplier i, which is introduced to make the operator A self-adjoint.

The multi-stage Taylor-Galerkin method for solving (4.2) reduces to a sequence of s linear variational boundary-value problems of the form

Given $U^n \in X$
Find $Y_1, Y_2, \ldots, Y_{s-1}, U^{n+1} \in X$ such that

$$A(W, Y_1) + \lambda \Delta t^2 B(W, Y_1) = A(W, U^n) + \mu_1 \Delta t C(W, U^n) - \nu_1 \Delta t^2 B(W, U^n)$$

$$A(W, Y_2) + \lambda \Delta t^2 B(W, Y_2) = A(W, Y_1) + \mu_2 \Delta t C(W, Y_1) - \nu_2 \Delta t^2 B(W, Y_1)$$

$$\vdots \quad s \text{ times}$$

$$A(W, U^{n+1}) + \lambda \Delta t^2 B(W, U^{n+1}) = A(W, Y_{s-1}) + \mu_s \Delta t C(W, Y_{s-1}) - \nu_s \Delta t^2 B(W, Y_{s-1}) \tag{4.4}$$

for all admissible test functions $W \in X$

where $X = X_v \times X_u = H \times D(\mathcal{A})$, the bilinear (sesqulinear) forms A, B and C are defined by

$$
\begin{aligned}
A, B, C &: (X_v \times X_u) \times (X_v \times X_u) \longrightarrow C, \\
A(W, U) &= (U, W)_{H \times H} \\
B(W, U) &= (AU, AW)_{H \times H} \\
C(W, U) &= -i(U, AW)_{H \times H}
\end{aligned}
\tag{4.5}
$$

and the inner product $(\cdot, \cdot)_{H \times H}$ is defined by

$$
\begin{aligned}
(U, W)_{H \times H} &= ([v, u], [w_v, w_u])_{H \times H} \\
&= (v, w_v)_H + (u, w_u)_H
\end{aligned}
\tag{4.6}
$$

Each stage of (4.4) defines a linear operator T_j from $X_1 = X \cap Rg(T_j)$ into itself:

$$
\begin{aligned}
T_j &: X_1 \longrightarrow X_1 \\
Z_j &= T_j Z_{j-1}
\end{aligned}
\tag{4.7}
$$

and the composition

$$
T = T_s \circ T_{s-1} \circ \ldots \circ T_1 \tag{4.8}
$$

defines a transient operator T taking an approximate solution U^n at time level t_n into U^{n+1}

$$
\begin{aligned}
T &: X_1 \longrightarrow X_1 \\
U^{n+1} &= TU^n
\end{aligned}
\tag{4.9}
$$

It should be noted that bilinear forms forms A and B are symmetric (Hermitian)

$$
\begin{aligned}
\overline{A(W, U)} &= A(U, W) \\
\overline{B(W, U)} &= B(U, W)
\end{aligned}
\tag{4.10}
$$

and bilinear form C is skew-symmetric (skew-Hermitian)

$$\begin{aligned} \overline{C(W,U)} &= -\,i(U,AW)_{H\times H} \\ &= -\,i(AU,W)_{H\times H} \\ &= -\,\overline{i\,(U,AW)}_{H\times H} \\ &= \overline{i(U,AW)}_{H\times H} \\ &= -\,C(U,W) \end{aligned} \tag{4.11}$$

Moreover, the bilinear form appearing at the left-hand side of (4.4) satisfies the inf-sup stability condition

$$\sup_{W} \left| A(W,U) + \lambda\Delta t^2 B(W,U) \right| \geq (U,U)_{H\times H} + \lambda\Delta t^2 (AU,AU)_{H\times H} \tag{4.12}$$

and defines a natural, energy norm for problem (4.4). Condition (4.12) implies also that the variational problem (4.4) posesses a unique solution U^{n+1} and guarantees the usual convergence properties for variational boundary-value problems.

To investigate stability properties of (4.4), we need to estimate the eigenvalues of transient operator T, or, equivalently, the eigenvalues of the the following eigenproblem

Find an eigenpair $(\Omega, 0 \neq U \in X)$
and $Y_1, Y_2, \ldots, Y_{s-1} \in X$ such that

$$A(W,Y_1) + \lambda\Delta t^2 B(W,Y_1) = A(W,U) + \mu_1\Delta t C(W,U) - \nu_1\Delta t^2 B(W,U)$$

$$A(W,Y_2) + \lambda\Delta t^2 B(W,Y_2)$$

$$= A(W, Y_1) + \mu_2 \Delta t C(W, Y_1) - \nu_2 \Delta t^2 B(W, Y_1) \tag{4.13}$$

.

. s times

.

$$\Omega\left[A(W, U) + \lambda \Delta t^2 B(W, U)\right]$$
$$= A(W, Y_{s-1}) + \mu_s \Delta t C(W, Y_{s-1}) - \nu_s \Delta t^2 B(W, Y_{s-1})$$

for all admissible test functions $W \in X$

Toward this end we notice that the underlying operator A is self-adjoint (in the complex sense) and has a pure point spectrum

$$\sigma(A) = \{0, \omega_1, \omega_{-1}, \omega_2, \omega_{-2}, \ldots\}$$
$$0 < \omega_1 \leq \omega_2 \leq \ldots \leq \omega_n \longrightarrow \infty, \ \omega_n \in \mathbb{R}_+ \tag{4.14}$$

with corresponding orthonormal eigenfunctions $\{U_n\}$ such that

$$A = \sum_{n=-\infty}^{\infty} \omega_n dP_n \tag{4.15}$$

$$I = dP_0 + \sum_{n=-\infty}^{\infty} dP_n \tag{4.16}$$

$$A(U_m, U_n) = \delta_{mn} \tag{4.17}$$

where $dP_n(\cdot) = A(\cdot, U_n)U_n$, dP_0 is the projector onto $N(A)$, $\omega_{-n} \equiv -\omega_n$ and $U_{-n} \equiv -\overline{U_n}$. By taking

$$U = dP_0(U) + \sum_{n=-\infty}^{\infty} dP_n(U) \tag{4.18}$$

$$Z_j = dP_0(Z_j) + \sum_{n=-\infty}^{\infty} dP_n(Z_j) \tag{4.19}$$

$$W = U_n \notin N(A) \tag{4.20}$$

eigenproblem (4.13) can be reduced to the following form:

$$\left[\begin{array}{l}
\text{Find an eigenpair } (\Omega_n, 0 \neq U \in X) \\
\text{and } Y_1, Y_2, \ldots, Y_{s-1} \in D(A) \quad \text{such that} \\
\\
A(U_n, Y_1) + \lambda\Delta t^2\omega_n^2 A(U_n, Y_1) \\
= A(U_n, U) - i\mu_1\Delta t\omega_n A(U_n, U) - \nu_1\Delta t^2\omega_n^2 A(U_n, U) \\
\\
A(U_n, Y_2) + \lambda\Delta t^2\omega_n^2 A(U_n, Y_2) \\
= A(U_n, Y_1) - i\mu_2\Delta t\omega_n A(U_n, Y_1) - \nu_2\Delta t^2\omega_n^2 A(U_n, Y_1) \\
\quad \vdots \quad s \text{ times} \\
\Omega_n \left[A(U_n, U) + \lambda\Delta t^2\omega_n^2 A(U_n, U)\right] \\
= A(U_n, Y_{s-1}) - i\mu_s\Delta t\omega_n A(U_n, Y_{s-1}) - \nu_s\Delta t^2\omega_n^2 A(U_n, Y_{s-1}) \\
\\
\text{for } U_n \in X
\end{array}\right. \tag{4.21}$$

From (4.21), we can obtain Ω_n,

$$\Omega_n = \prod_{j=1}^{s} \frac{1 - \nu_j(\lambda)\Delta t^2\omega_n^2 - i\mu_j(\lambda)\Delta t\,\omega_n}{1 + \lambda\Delta t^2\omega_n^2} \tag{4.22}$$

and its modulus

$$|\Omega_n|^2 = \prod_{j=1}^{s} \frac{(1 - \nu_j(\lambda)\Delta t^2\omega_n^2)^2 + (\mu_j(\lambda)\Delta t\,\omega_n)^2}{(1 + \lambda\Delta t^2\omega_n^2)^2} \tag{4.23}$$

By choosing $U = W \in N(A)$ it is easily seen that the corresponding eigenvalue of T, Ω_0, is equal to unity:

$$\Omega_0 = 1 \tag{4.24}$$

Similarly, the eigenvalues of the j-th stage eigenvalue problem :

$$\left[\begin{array}{l} \text{Find an eigenpair } (\Omega_{j,n},\ 0 \neq \boldsymbol{Z} \in \boldsymbol{X}\ ) \text{ such that} \\ \\ \Omega_{j,n}\left[A(\boldsymbol{W},\boldsymbol{Z}) + \lambda\Delta t^2 B(\boldsymbol{W},\boldsymbol{Z})\right] \\ \quad = A(\boldsymbol{W},\boldsymbol{Z}) + \mu_j\Delta t C(\boldsymbol{W},\boldsymbol{Z}) - \nu_j\Delta t^2 B(\boldsymbol{W},\boldsymbol{Z}) \\ \\ \text{for all admissible test functions } \boldsymbol{W} \in \boldsymbol{X} \end{array}\right. \tag{4.25}$$

read

$$\begin{aligned} \Omega_{j,n} &= \frac{1 - \nu_j(\lambda)\Delta t^2\omega_n^2 - i\mu_j(\lambda)\Delta t\ \omega_n}{1 + \lambda\Delta t^2\omega_n^2} \\ \\ \Omega_{j,0} &= 1 \end{aligned} \tag{4.26}$$

and, therefore (4.22) and (4.24) can be written as

$$\Omega_n = \prod_{j=1}^{s} \Omega_{j,n} \qquad n = 0,\ 1,\ \ldots \tag{4.27}$$

In other words, the eigenvalues of the transient operator $\boldsymbol{T}$ are products of the eigenvalues of the component operators $\boldsymbol{T}_j$.

To show unconditional stability of TG methods, we need to show existence of a λ such that

$$\begin{aligned} &|\Omega_n| \leq 1, \qquad n = 1,\ 2,\ \ldots \\ \\ &\forall\ \Delta t \in \mathbb{R}_+ \end{aligned} \tag{4.28}$$

Thus, in order to find a λ producing unconditionally stable Taylor-Galerkin method, we need to solve the following problem:

$$\left[\begin{array}{l} \text{Find } \lambda \in \mathbb{R}_+ \text{ such that} \\ \\ \prod_{j=1}^{s} \dfrac{(1 - \nu_j(\lambda)\Delta t^2\omega_n^2)^2 + (\mu_j(\lambda)\Delta t\ \omega_n)^2}{(1 + \lambda\Delta t^2\omega_n^2)^2} \leq 1 \end{array}\right.$$

$$
\left.
\begin{aligned}
&\mu_1 + \mu_2 + \ldots + \mu_s = 1 \\
&\nu_1 + \nu_2 + \ldots + \nu_s + \mu_1\mu_2 + \ldots + \mu_{s-1}\mu_s = c_2(\lambda) \\
&\quad \vdots \\
&\nu_1\nu_2 \ldots \nu_s = c_{2s}(\lambda) \\
&\text{for all } \Delta t^2\omega_n^2 \in \mathbb{R}_+
\end{aligned}
\right\} \tag{4.29}
$$

Unfortunately, (4.29) can be solved analytically for $s = 1$ only. In this case, it reduces to finding λ such that

$$
\frac{\left(1 - (\frac{1}{2} - \lambda)\Delta t^2\omega_n^2\right)^2 + \Delta t^2\omega_n^2}{\left(1 + \lambda\Delta t^2\omega_n^2\right)^2} \leq 1 \tag{4.30}
$$

which is satisfied for all Δt provided $\lambda \geq \frac{1}{4}$. (This result was proven in an alternative way by Demkowicz *et al.* in [1].) For $s > 1$ we compute μ_j and ν_j for a given λ and verify stability criterion (4.30). The results of numerical computation of the ranges of λ which satisfy (4.29) are summarized in Tables 4.1 and 4.2. In addition, Figs. 1-7 show the variation of $|\Omega_n|$ as a function of $\Delta t^2\omega_n^2$ for λ's lying at the boundary of stability regions listed in Tables 4.1 and 4.2.

Table 4.1

s	m	λ
1	2	$[\frac{1}{4}, \infty)$
2	4	[0.47048, ∞)
3	6	[0.695, ∞)
4	8	[0.91943, ∞)
5	10	[1.15, ∞)

Table 4.2

s	m	λ
3	4	$[0.22, \infty)$
4	6	$[0.29, \infty)$
5	8	$[0.38, \infty)$

It is interesting to check whether the s-stage methods of order $2s+1$, i.e., the methods of the highest attainable order of accuracy, are unconditionally stable. Table 4.3 gives the largest values of λ producing s-stage methods of the order $2s+1$. Unfortunately, all those λ's are not in the range of unconditional stability, and, therefore, the s-stage $(2s+1)$th order methods can be at most conditionally stable.

Table 4.3

s	m	λ
1	2	$\frac{1}{6}$
2	4	$\frac{1}{6}+\frac{1}{2}\sqrt{\frac{21}{270}}$
3	6	0.444797521031781
4	8	0.583260771000355
5	10	0.721627161040466

Next we check stability properties of the s-stage $2s$-th order methods with λ so chosen that coefficient $c_{2s} = 0$. Table 4.4 lists the smallest of such λ's and Figs. 8 - 11 show the corresponding variations of eigenvalues $|\Omega_n|$ as a function of $\Delta t^2 \omega_n^2$. As expected, all those λ's produce unconditionally stable Taylor-Galerkin methods.

Table 4.4

s	m	λ
1	2	$\frac{1}{2}$
2	4	0.956435464587639

3	6	1.41218087134444
4	8	1.86773692752801
5	10	2.32321418507049

Moreover, this class of methods has the property that the eigenvalues Ω_n tend to zero as Δt goes to infinity

$$\lim_{\Delta t \to \infty} |\Omega_n| = 0 \tag{4.31}$$

This is easily seen, since from (4.23) we have

$$\lim_{\Delta t \to \infty} |\Omega_n| = \frac{|\nu_1 \nu_2 \ldots \nu_s|}{\lambda^s} \tag{4.32}$$

and one of the ν_j is equal to zero. In fact, all the methods with $m < 2s$ will have property (4.32).

Equation (4.32) suggests also a criterion of selection of λ for methods with $m = 2s$. Namely, of all the λ's guaranteeing unconditional stability we choose the one for which $|\nu_1 \nu_2 \ldots \nu_s|/\lambda^s$ is the largest, i.e., we choose the λ which will produce the method with least possible numerical dissipation. These optimal values of λ as well as corresponding asymptotic values of $|\Omega_n|$ are given in Table 4.5. As can be seen, all the methods but $s = 1$ are dissipative. Note also that the optimal λ's lie at the boundary of stability regions listed in Table 4.1.

Table 4.5

s	m	λ	$\lvert\nu_1 \nu_2 \ldots \nu_s\rvert/\lambda^s$
1	2	$\frac{1}{4}$	1
2	4	0.47048	0.937
3	6	0.695	0.904
4	8	0.91943	0.887
5	10	1.15	0.868

Figure 12 illustrates the decomposition of the eigenvalue of the transient operator $\boldsymbol{T}$ into the product of the eigenvalues of the component operators $\boldsymbol{T}_j$ for the 4-stage 8th order TG method (compare eqn (4.27)). As can be seen, the moduli of eigenvalues of $\boldsymbol{T}_j$ are bounded but they are not necessarilly less than unity for *all* the component operators. (This property also holds for other unconditionally stable schemes). In general we have

$$|\Omega_{j,n}| \leq C_j \quad , \qquad j = 1,2, \ldots, s \tag{4.33}$$

where

$$C_j = \operatorname*{ess\,sup}_{0 \leq \Delta t^2 \omega_n^2 < \infty} |\Omega_{j,n}| \tag{4.34}$$

usually $C_j = \max\{ 1, |\nu_j|/\lambda \}$.

Thusfar we investigated stability properties of TG methods for X_1 being infinite-dimensional and we showed the existence of ranges of the stability parameter λ for which the spectral radius of $\boldsymbol{T}$, $r(\boldsymbol{T})$, is less than or eqal to unity. To show unconditional stability of TG methods for finite dimensions, i.e., when $\boldsymbol{T}$ is restricted to X_h ($X_h \subset X_1$, dim $X_h < \infty$), we will show that the spectral radius of $\boldsymbol{T}$ satisfies the following maximum principle:

$$\sup_{\substack{U \in X_1 \\ U \neq 0}} \frac{B_1(\boldsymbol{T}U \, , \, \boldsymbol{T}U)}{B_1(U \, , \, U)} = r^2(\boldsymbol{T}) \tag{4.35}$$

where

$$B_1(U, U) = A(U, U) + \lambda \Delta t^2 B(U, U) \tag{4.36}$$

is the bilinear form appearing at the left-hand side of (4.4), and

$$r(\boldsymbol{T}) = \sup_{\Omega_m \in \sigma(T)} |\Omega_m| \tag{4.37}$$

Indeed,

$$B_1(U, U) =$$

$$= B_1\Big(dP_0(U) + \sum_{m=-\infty}^{\infty} dP_m(U)\,,\, dP_0(U) + \sum_{n=-\infty}^{\infty} dP_n(U)\Big)$$

$$= B_1\Big(dP_0(U) + \sum_{m=-\infty}^{\infty} A(U, U_m)U_m\,,\, dP_0(U) + \sum_{n=-\infty}^{\infty} A(U, U_n)U_n\Big)$$

$$= A\Big(dP_0(U), dP_0(U)\Big) + A\Big(\sum_{m=-\infty}^{\infty} A(U, U_m)U_m\,,\, \sum_{n=-\infty}^{\infty} A(U, U_n)U_n\Big)$$

$$+ \lambda\Delta t^2 A\Big(\sum_{m=-\infty}^{\infty} \omega_m A(U, U_m)U_m\,,\, \sum_{n=-\infty}^{\infty} \omega_n A(U, U_n)U_n\Big)$$

$$= A\Big(dP_0(U)\,,\, dP_0(U)\Big) + \sum_{n=-\infty}^{\infty} |A(U, U_n)|^2\Big(1 + \lambda\Delta t^2|\omega_n|^2\Big) \qquad (4.38)$$

and

$$B_1(TU, TU) =$$

$$= B_1\Big(T\,(dP_0(U) + \sum_{m=-\infty}^{\infty} dP_m(U))\,,\, T\,(dP_0(U) + \sum_{n=-\infty}^{\infty} dP_n(U))\Big)$$

$$= B_1\Big(dP_0(U) + \sum_{m=-\infty}^{\infty} \Omega_m A(U, U_m)U_m\,,\, dP_0(U) + \sum_{n=-\infty}^{\infty} \Omega_n A(U, U_n)U_n\Big)$$

$$= A\Big(dP_0(U)\,,\, dP_0(U)\Big) + A\Big(\sum_{m=-\infty}^{\infty} \Omega_m A(U, U_m)U_m\,,\, \sum_{n=-\infty}^{\infty} \Omega_n A(U, U_n)U_n\Big)$$

$$+ \lambda\Delta t^2 A\Big(\sum_{m=-\infty}^{\infty} \Omega_m\omega_m A(U, U_m)U_m\,,\, \sum_{n=-\infty}^{\infty} \Omega_n\omega_n A(U, U_n)U_n\Big)$$

$$= A\big(dP_0(U)\,,\, dP_0(U)\big) + \sum_{n=-\infty}^{\infty} |\Omega_n|^2\, |A(U, U_n)|^2\big(1 + \lambda\Delta t^2|\omega_n|^2\big)$$

$$\leq A\big(dP_0(U)\,,\, dP_0(U)\big) + \sup|\Omega_m|^2 \sum_{n=-\infty}^{\infty} |A(U, U_n)|^2\big(1 + \lambda\Delta t^2|\omega_n|^2\big)$$

$$\leq \max\big\{1, \sup|\Omega_m|^2\big\}\Big[A\big(dP_0(U)\,,\, dP_0(U)\big) + \sum_{n=-\infty}^{\infty} |A(U, U_n)|^2\big(1 + \lambda\Delta t^2|\omega_n|^2\big)\Big]$$

$$= \max\big\{|\Omega_0|^2, \sup|\Omega_m|^2\big\}\, B_1(U, U)$$

$$= r^2(T)\, B_1(U, U) \tag{4.39}$$

Thus,

$$\sup_{\substack{U\in X_1\\ U\neq 0}} \frac{B_1(TU\,,\, TU)}{B_1(U\,,\, U)} \leq r^2(T) \tag{4.40}$$

Conversely,

$$|\Omega_n|^2 = \frac{B_1(TU_n\,,\, TU_n)}{B_1(U_n\,,\, U_n)} \leq \sup_{\substack{U\in X_1\\ U\neq 0}} \frac{B_1(TU\,,\, TU)}{B_1(U\,,\, U)} \tag{4.41}$$

from which (4.35) follows.

Consider now the finite dimensional counterpart of eigenvalue problem (4.13):

$$\left[\begin{array}{l} \text{Find an eigenpair } (\Omega_h, 0 \neq U_h \in X_h) \\ \text{and } Z_{h,1}, Z_{h,2}, \ldots, Z_{h,s-1} \in X_h \text{ such that} \\ \\ A(W, Z_{h,1}) + \lambda\Delta t^2 B(W, Z_{h,1}) \\ = A(W, U_h) + \mu_1\Delta t C(W, U_h) - \nu_1\Delta t^2 B(W, U_h) \end{array}\right.$$

$$
\begin{aligned}
&A(W, Z_{h,2}) + \lambda\Delta t^2 B(W, Z_{h,2}) \\
&= A(W, Z_{h,1}) + \mu_2 \Delta t C(W, Z_{h,1}) - \nu_2 \Delta t^2 B(W, Z_{h,1}) \qquad (4.42) \\
&\quad \vdots \quad s \text{ times} \\
&\Omega_h \left[A(W, U_h) + \lambda\Delta t^2 B(W, U_h) \right] \\
&= A(W, Z_{h,s-1}) + \mu_s \Delta t C(W, Z_{h,s-1}) - \nu_s \Delta t^2 B(W, Z_{h,s-1})
\end{aligned}
$$

for all admissible test functions $W \in X_h$

Since

$$
\begin{aligned}
\max|\Omega_h|^2 &\leq \sup_{\substack{U \in X_h \\ U \neq 0}} \frac{B_1(TU, TU)}{B_1(U, U)} \\
&\leq \sup_{\substack{U \in X_1 \\ U \neq 0}} \frac{B_1(TU, TU)}{B_1(U, U)} \qquad (4.43) \\
&= r^2(T)
\end{aligned}
$$

unconditional stability of the TG scheme for infinite dimensional levels (i.e., $r^2(T) \leq 1 \; \forall \; \Delta t \in \mathbb{R}_+$) implies its unconditional stability at finite dimensional levels, independently of the approximation used with respect to space variables (any finite element mesh).

5. Adaptivity (Linear Problems)

5.1 Error Estimation for High-Order TG Methods

As a starting point, we consider the estimation of the spatial approximation error commited at a typical *stage*. The j-th stage problem reads

Given $Z_{h,p;j-1} \in X_{h,p}$ find $Z_{h,p;j} \in X_{h,p}$ such that

$$B_1(W, Z_{h,p;j}) = L_j(W, Z_{h,p;j-1}) \tag{5.1}$$

for all admissible test functions $W \in X_{h,p}$

where

$$\begin{aligned} B_1(W, U) &= A(W, U) + \lambda \Delta t^2 B(W, U) \\ L_j(W, U) &= A(W, U) + \mu_j \Delta t C(W, U) - \nu_j \Delta t^2 B(W, U) \end{aligned} \tag{5.2}$$

$X_{h,p} \subset X_1$, $\dim X_{h,p} < \infty$ and indices h and p refer to the use of arbitrary h-p finite element meshes, with locally varying mesh size h and spectral order p.

Assuming that there is no error in $Z_{h,p;j-1}$, we consider the enriched space $X_{h,p+1}$ corresponding to the same mesh but with local order of approximation uniformly increased by one and we define the relative error as

$$E_j^{(1)} = Z_{h,p+1;j} - Z_{h,p;j} \tag{5.3}$$

where $Z_{h,p+1;j}$ is the enriched space solution.

We estimate $\|E_j^{(1)}\|_E$ using the element residual method in the form [5]

$$\|E_j^{(1)}\|_E = \sup_{W \in X_{h,p+1}} \frac{|B_1(W, Z_{h,p;j}) - L_j(W, Z_{h,p;j-1})|}{\|W\|_E}$$

$$= \|Z_{h,p+1;j} - Z_{h,p;j}\|_E \tag{5.4}$$

$$\leq \left(\sum_K \eta_{K,j}^2 \right)^{1/2}$$

where

- $\|\cdot\|_E$ is the global energy norm defined as

$$\|U\|_E = B_1(U, U)^{1/2} \tag{5.5}$$

- $\eta_{K,j}$ is the element error indicator function evaluated as

$$\eta_{K,j} = B_{1,K}(\phi_{K,j}, \phi_{K,j})^{1/2} \tag{5.6}$$

with $B_{1,K}$ the element contribution to the (global) bilinear form B_1 and the $\phi_{K,j}$ the element indicator function which is the solution to the local problem

$$\left[\begin{array}{l} \text{Find } \phi_{K,j} \in X^0_{h,p+1}(K) \text{ such that} \\ B_{1,K}(W, \phi_{K,j}) = R_j(W) \;\forall\; W \in X^0_{h,p+1}(K) \end{array}\right. \tag{5.7}$$

where R_j is an appropriate residual corresponding to element K and $X^0_{h,p+1}(K)$ is the kernel of the h-p interpolation operator defined on the element enriched space $X_{h,p+1}(K)$.

For all details we refer to [5].

Next we consider the error $E^{(2)}_j$ which is caused by the error in the previous stage solution $Z_{h,p;j-1}$ and enters (5.1) through the right-hand side. Formally $E^{(2)}_j$ is computed as

$$E^{(2)}_j = T_{h,p+1;j}\, E_{j-1} \tag{5.8}$$

where $T_{h,p+1;j}$ is the operator taking the previous stage solution $Z_{h,p+1;j-1}$ into $Z_{h,p+1;j}$

$$\begin{aligned} &T_{h,p+1;j} : X_{h,p+1} \longrightarrow X_{h,p+1} \\ &Z_{h,p+1;j} = T_{h,p+1;j}\, Z_{h,p+1;j-1} \end{aligned} \tag{5.9}$$

and E_{j-1} is the error in $Z_{h,\,p+1;\,j-1}$:

$$E_{j-1} = E_{j-1}^{(1)} + T_{h,\,p+1;\,j-1}\,E_{j-2}^{(1)} + T_{h,\,p+1;\,j-1} \circ T_{h,\,p+1;\,j-2}\,E_{j-3}^{(1)}$$
$$+ \ldots + T_{h,\,p+1;\,j-1} \circ T_{h,\,p+1;\,j-2} \circ \ldots \circ T_{h,\,p+1;\,2}\,E_1^{(1)} \tag{5.10}$$

Notice that E_{j-1} is the *accumulated* error up to stage j-1.

We have the following estimate:

$$\|E_j^{(2)}\|_E^2 = \|T_{h,\,p+1;\,j}\,E_{j-1}\|_E^2$$

$$\leq \|T_{h,\,p+1;\,j}\|_E^2 \;\; \|E_{j-1}\|_E^2$$

$$= \sup_{\substack{U \in X_{h,p+1} \\ U \neq 0}} \frac{B_1(T_jU\,,\,T_jU)}{B_1(U\,,\,U)} \;\; \|E_{j-1}\|_E^2$$

$$\leq \sup_{\substack{U \in X_1 \\ U \neq 0}} \frac{B_1(T_jU\,,\,T_jU)}{B_1(U\,,\,U)} \;\; \|E_{j-1}\|_E^2$$

$$= r^2(T_j)\,\|E_{j-1}\|_E^2$$

$$\leq C_j^2 \;\; \|E_{j-1}\|_E^2 \tag{5.11}$$

where $r(T_j)$ is the spectral radius of T_j and C_j are the constants defined by (4.34). In deriving (5.11) we used the following maximum principle

$$\sup_{\substack{U \in X_1 \\ U \neq 0}} \frac{B_1(T_jU\,,\,T_jU)}{B_1(U\,,\,U)} = r^2(T_j) \tag{5.12}$$

which can be proved in exactly the same way as the maximum principle (4.35).

Thus, the spatial approximation error accumulated up to the j-th stage is given by the following recurrence relation

$$\begin{aligned} \|E_j\|_E &\le \|E_j^{(1)}\|_E + \|E_j^{(2)}\|_E \\ &\le \|E_j^{(1)}\|_E + C_j \|E_{j-1}\|_E \end{aligned} \tag{5.13}$$

By using (5.13) at each stage, we can estimate the spatial approximation error commited at a typical time step $U_{h,p}^n \longrightarrow U_{h,p}^{n+1}$. Accordingly,

$$\begin{aligned} \|E_s\|_E &\le \|E_s^{(1)}\|_E + C_s \|E_{s-1}\|_E \\ \|E_{s-1}\|_E &\le \|E_{s-1}^{(1)}\|_E + C_{s-1} \|E_{s-2}\|_E \\ &\vdots \\ \|E_1\|_E &= \|E_1^{(1)}\|_E \end{aligned} \tag{5.14}$$

and, therefore,

$$\begin{aligned} &\|E_\sigma^n\|_E \equiv \|E_s\|_E \\ &\le C_s \left(C_{s-1} \left(C_{s-2} \ldots C_2 \|E_1^{(1)}\|_E + \|E_2^{(1)}\|_E \right) + \|E_3^{(1)}\|_E \right) + \ldots + \|E_{s-1}^{(1)}\|_E \Big) + \|E_s^{(1)}\|_E \end{aligned} \tag{5.15}$$

where it is assumed that there is no error in the previous step solution $U_{h,p}^n$. It can also be shown that $\|E_\sigma^n\|_E$ is a bound for the relative spatial approximation error commited at a typical time step:

$$\|E_\sigma^n\|_E \le \|U_{h,p+1}^{n+1} - U_{h,p}^{n+1}\|_E \tag{5.16}$$

where

$$\begin{aligned} U_{h,p}^{n+1} &= T_{h,p} U_{h,p}^n \\ U_{h,p+1}^{n+1} &= T_{h,p+1} U_{h,p}^n \end{aligned} \tag{5.17}$$

and $T_{h,p}$ and $T_{h,p+1}$ are restrictions of transient operator T, eqn (4.6), to $X_{h,p}$ and

$X_{h,p+1}$, respectively.

To account for the total error commited at a typical time step, it is also necessary to consider the temporal approximation error. We estimate the relative temporal approximation error as follows:

$$\|E_\tau^n\|_E = \|\tilde{U}_{h,p}^{n+1} - U_{h,p}^{n+1}\|_E \tag{5.18}$$

where $U_{h,p}^{n+1}$ is the solution obtained by using an s-stage m-th order TG scheme which is referred to herein as the basic solution scheme and $\tilde{U}_{h,p}^{n+1}$ is the solution obtained by using the $(s+1)$-stage $(m+2)$th order scheme (with the same stability parameter λ and the same time step Δt) which is referred to as the auxiliary solution scheme. Notice that the definition of auxiliary scheme is unique. Since the bilinear form defining the left-hand side of the basic method is the same as that defining the left-hand side of the auxiliary method (since λ and Δt are unchanged), the computation of $\tilde{U}_{h,p}^{n+1}$ and, hence, $\|E_\tau^n\|_E$ is economically feasible.

Thusfar we estimated the approximation error $\|E^{(1),n}\|_E$ commited at a typical time step and consisting of spatial approximation error and temporal approximation error :

$$\|E^{(1),n}\|_E = \|E_\sigma^n\|_E + \|E_\tau^n\|_E \tag{5.19}$$

To obtain the error for the whole evolution process, it is necessary to consider the error $\|E^{(2),n}\|_E$ which is introduced by the error in the previous time step solution $U_{h,p}^n$. Formally,

$$E^{(2),n} = T_{h,p+1} E^{n-1} \tag{5.20}$$

where $T_{h,p+1}$ is the transient operator taking the previous time step solution $U_{h,p+1}^n$ into $U_{h,p+1}^{n+1}$ and E^{n-1} is the error in $U_{h,p}^n$. (More precisly, E^{n-1} is the error accumulated up to the $(n-1)$th time step).

We have the following estimate:

$$\|E^{(2),n}\|_E^2 = \|T_{h,p+1} E^{n-1}\|_E^2$$

$$\leq \|T_{h,p+1}\|_E^2 \|E^{n-1}\|_E^2$$

$$= \sup_{\substack{U \in X_{h,p+1} \\ U \neq 0}} \frac{B_1(TU, TU)}{B_1(U, U)} \|E^{n-1}\|_E^2 \tag{5.21}$$

$$\leq \sup_{\substack{U \in X_1 \\ U \neq 0}} \frac{B_1(TU, TU)}{B_1(U, U)} \|E^{n-1}\|_E^2$$

$$= r^2(T) \|E^{n-1}\|_E^2$$

$$\leq \|E^{n-1}\|_E^2$$

where it is assumed that $r(T) \leq 1$.
Thus, the approximation error accumulated up to the n-th time step is given by the following recurrence relation

$$\begin{aligned} \|E^n\|_E &\leq \|E^{(1),n}\|_E + \|E^{(2),n}\|_E \\ &\leq \|E^{(1),n}\|_E + \|E^{n-1}\|_E \end{aligned} \tag{5.22}$$

Inequality (5.22) provides a basis for the control of the quality of results for the whole evolution problem.

5.2 Adaptive Strategy and Computational Considerations

We neglect the temporal approximation error (inasmuch as we use high-order schemes); we use a constant time step Δt and employ a simple strategy based on equidistribution of spatial approximatin error for each time step. The equidistribution

strategy means simply that a number of elements with the largest error indicators are refined. The use of a constant Δt is permissible because of the unconditional stability of TG schemes.

Formally the algorithm is as follows:

Step 1 Read in data (geometry, initial conditions, etc.).
Specify time step Δt, number of time steps NSTEP and the target error for the whole evolution problem η_t.

For each time step $U^n_{h,p} \longrightarrow U^{n+1}_{h,p}$:

Step 2 Specify the target error for "one time step problem" $\eta_{\Delta t}$, e.g., $\eta_{\Delta t} = \frac{\eta_t}{\text{NSTEP}}$

Step 3 Solve for $U^{n+1}_{h,p}$, save the internal approximations $Z_{h,p;j}$, $j = 1, 2, \ldots s\text{-}1$. Use a direct solver or an iterative solver using $U^n_{h,p}$ and the previous time step internal approximations as starting vectors.

Error estimation

Step 5 For each element K determine error indicators $\eta_{K,j}$ via (5.6)

Step 6 Determine the global error commited at this time step:

$$\|E^{(1),n}\|_E \approx \|E^n_\sigma\|_E$$

where $\|E^n_\sigma\|_E$ is estimated via inequality (5.15).

Step 7 Check the error. If $\|E^{(1),n}\|_E \leq \eta_{\Delta t}$, then go to Step 13.

Step 8 For each element K determine error indicators for mesh refinements η_K. Identify the largest admissible error indicator η_{ad}.

Step 9 Create a list of elements such that $\eta_K > \eta_{ad}$.

Step 10 Check the number of elements on the list. If it is too small (zero in particular), decrease η_{ad} and return to Step 9.

Step 11 Refine elements K from the list created at Step 9.
Project $U^n_{h,p}$, $Z_{h,p;j}$, $j = 1, 2, \ldots s\text{-}1$, and $U^{n+1}_{h,p}$ onto enriched space.

Step 12 Solve for $U^{n+1}_{h,p}$ using iterative solver and coarse mesh solutions $U^n_{h,p}$, $Z_{h,p;j}$, $j = 1, 2, \ldots s\text{-}1$, and $U^{n+1}_{h,p}$ as starting vectors. Save the fine mesh solutions.
Set "fine" = "coarse" and return to Step 5.

Step 13 For each element L, determine error indicators for mesh unrefinements ξ_L.
Identify the largest admissible error indicator ξ_{ad}.

Step 14 Create a list of elements L such that

- $\eta_L < 0.01\eta_{ad}$
- $\xi_L < \xi_{ad}$

Step 15 Unrefine all elements L from the list created at Step 14.
Project $U^n_{h,p}$, $Z_{h,p;j}$, $j = 1, 2, \ldots s\text{-}1$, and $U^{n+1}_{h,p}$ onto unenriched space.

Step 16 Set $U^n_{h,p} = U^{n+1}_{h,p}$ and go to Step 2.

The element indicator for mesh unrefinements ξ_L is defined to be averaged "physical" energy (cf. (2.30))

$$\xi_L^2 = \frac{E_L(U^{n+1}_{h,-}, U^{n+1}_{h,p})}{\text{meas}(\Omega_L)} \tag{5.23}$$

with E_L the element contribution to the global energy E and $\text{meas}(\Omega_L)$ the area of element L.

Element error indicators for mesh refinements η_K for typical time step are chosen in such a way that

$$\|E_\sigma^n\|_E \leq \left(\sum_K \eta_K^2 \right)^{1/2} \tag{5.24}$$

Accordingly, η_K are computed as:

$$\begin{aligned} \eta_K^2 &= \eta_{K,2}^2 + C_2^2 \eta_{K,1}^2 \\ &+ 2C_2 E_1^{(1)} \eta_{K,2} \end{aligned} \tag{5.25}$$

for 2-stage scheme,

$$\begin{aligned} \eta_K^2 &= \eta_{K,3}^2 + C_3^2 \eta_{K,2}^2 + C_3^2 C_2^2 \eta_{K,1}^2 \\ &+ 2(C_3 E_2^{(1)} + C_3 C_2 E_1^{(1)}) \eta_{K,3} \\ &+ 2C_3^2 C_2 E_1^{(1)} \eta_{K,2} \end{aligned} \tag{5.26}$$

for 3-stage scheme, and

$$\begin{aligned} \eta_K^2 &= \eta_{K,4}^2 + C_4^2 \eta_{K,3}^2 + C_4^2 C_3^2 \eta_{K,2}^2 + C_4^2 C_3^2 C_2^2 \eta_{K,1}^2 \\ &+ 2(C_4 E_3^{(1)} + C_4 C_3 E_2^{(1)} + C_4 C_3 C_2 E_1^{(1)}) \eta_{K,4} \\ &+ 2(C_4^2 C_3 E_2^{(1)} + C_4^2 C_3 C_2 E_1^{(1)}) \eta_{K,3} \\ &+ 2C_4^2 C_3^2 C_2 E_1^{(1)} \eta_{K,2} \end{aligned} \tag{5.27}$$

for 4-stage scheme.

The solution strategy for the "one-stage problem" deserves special attention. Since the formal operator equivalent to the bilinear form B_1 has zero off-diagonal terms, velocity equations and displacement equations can be solved independently and in parallel (the coupling between velocity and displacements is only through the right-hand side).

Finally, we emphasize the need of using an *iterative* linear equation solver in the adaptivity loop (cf. Step 12). Notice that the matrix defining the left-hand side of the resulting algebraic problem is symmetric and positive definite which is the most popular case in the theory of iterative solvers. Notice also that the total computational effort involved in the adaptivity loop is governed by the total number of iterations required to solve the resulting system of linear equations on different meshes rather that by the total number of mesh adaptations.

6 Numerical Example

Stress wave propagation in an elastic panel with a cut-off (2D)

As an example we chose the problem of wave propagation in an elastic panel with a cut-off (Fig.13). A plane progressive transient wave is normally incident on a traction-free rectangular cut-off and gives rise to complicated pattern of stress field caused by the interference of incident, reflected and diffracted waves, and by singularities at the corners.

The problem was solved for the following data:

- Lamé coefficients, $\mu = 0.25\ Pa$, $\lambda = 0.5\ Pa$
- Mass density, $\rho_0 = 1\ kg/m^3$
- Initial conditions :

$$\begin{cases} x\text{-velocity, } v_x(x, y, 0) = f(x)[H(x - 1) - H(x - \frac{3}{2})] \\ y\text{-velocity, } v_y(x, y, 0) = 0 \\ x\text{-displacement, } u_x(x, y, 0) = F(x) \\ y\text{-displacement, } u_y(x, y, 0) = 0 \end{cases} \tag{6.1}$$

where $f(x) = -1 + 32(\frac{5}{4} - x)^2 - 256(\frac{5}{4} - x)^4$ and $F(x)$ = anti-derivative of $f(x)$.

The problem was solved by using a 2-stage 4th order Taylor-Galerkin method with stability parameter $\lambda = 0.47125$ and constant time step $\Delta t = 0.0078125\ s$. No local p-

refinements were used in this example, as the p capabilities of the code were used only to specify an initial order of approximation ($p = 4$ in the example).

Figure 14 shows the initial finite element mesh and Figs. 15 and 16 show the initial condition functions in the form of 3D plots (x-velocity and x-displacement, respectively). Figure 17 presents the adapted finite element mesh at time $t = 0.25\ s$ and Figs. 18 - 23 present the corresponding distributions of velocity components (v_x and v_y) and displacements (u_x and u_y). Displacement vector, as the most interesting, is shown in the form of both the 3D plots and contour maps; velocity components are presented in the form of 3D plots only. As can be seen, a doubling of the amplitude of x-velocity occures at the part of the left face of the cut-off which is in perfect agreement with the plane wave solution (the wavefiel is locally plane at this region of space-time). Also, sharp gradients of v_y and u_y in the vicinity of point A($x = 1.5\ m, y = 0.5\ m$) can be noticed. Similarly, Fig. 24 presents the finite element mesh at time $t = 0.5\ s$ and Figs. 25 - 30 present corresponding distributions of v_x, v_y, u_x and u_y.

Figures 31 - 33 show the finite element mesh at time $t = 0.75\ s$ and Figs. 34 - 40 show the corresponding solution (v_x, v_y, u_x and u_y). Figure 32 presents a zoom of the finite element mesh in the vicinity of corner A. A total number of 19 mesh refinements was needed to capture the singularity at A. Thus, the CFL number, ν:

$$\nu = \max_K \frac{\Delta t\, p_K \max\{|\lambda_{K,x}|, |\lambda_{K,y}|\}}{h_K} \tag{6.2}$$

is of the order of 10^3. This would place a severe limitation on the time-step size for any conditionally stable scheme. Here h_K is the element size, p_K the corresponding order of approximation, and $\lambda_{K,x}$, $\lambda_{K,y}$ are the maximum values of eigenvalues for Jacobian matrices $\boldsymbol{R}^{kl}$. Similarly, Fig. 33 presents a zoom of the finite element mesh in the vicinity of point B($x = 1.75\ m, y = 0.5\ m$).

Figures 40 - 42 show the distribution of the components of stress tensor T_{xx}, T_{yy} and T_{xy}, in the form of 3D plots. A very strong singularity in stresses at the corner points A and B are observed. Finally, Fig. 43 shows the history of the error bound (5.22) for the whole evolution problem, and Fig. 44 shows the number of mesh adaptations as a function of time.

References

1. Demkowicz, L., Oden, J. T., Rachowicz, W., and Hardy, O., "An *h-p* Taylor-Galerkin Finite Element Method for Compressible Euler Equations," *Comp. Meth. in Appl. Mech. and Engrg.*, Vol. 88, pp. 363-396, 1991.

2. Demkowicz, L., Oden, J. T., Rachowicz, W., and Hardy, O., "Toward a Universal *h-p* Adaptive Finite Element Strategy. Part 1: Constrained Approximation and Data Structure," *Comp. Meth. in Appl. Mech. and Engrg.*, Vol. 77, pp. 79-112, 1989.

3. Donea, J., "A Taylor-Galerkin Method for Convective Transport Problems," *Int.J. Numer. Meth. Eng.*, Vol. 20, pp. 101-120, 1984.

4. Leis, R., **Initial Boundary Value Problems in Mathematical Physics**, John Wiley and Sons, New York, 1986.

5. Oden, J. T., "Formulation and Application of Certain Primal and Mixed Finite Element Models of Finite Deformations of Elastic Bodies," **Computing Methods in Applied Sciences and Engineering**, Ed. R. Glowinski and J. L. Lions, Springer, 1974.

6. Oden, J. T., Demkowicz, L., Rachowicz, W., and Westermann, T. A., "*A Posteriori* Error Analysis in Finite Elements: The Element Residual Method for Symmetrizable Problems with Applications to Compressible Euler and Navier-Stokes Equations," **Reliability in Computational Mechanics**, Edited by J. T. Oden, and *Comp. Meth. in Appl. Mech. and Engrg.*, Vol. 82, pp. 183-203, 1990.

7. Oden, J. T., Demkowicz, L., Rachowicz, W., and Westermann, T. A., "Toward a Universal *h-p* Adaptive Finite Element Strategy. Part 2: *A Posteriori* Error Estimation," *Comp. Meth. in Appl. Mech. and Engrg.*, Vol. 77, pp. 113-180, 1989.

8. Rachowicz, W., Oden, J. T., and Demkowicz, L., "Toward a Universal *h-p* Adaptive Finite Element Strategy. Part 3: Design of *h-p* Meshes," *Comp. Meth. in Appl. Mech. and Engrg.*, Vol. 77, pp. 181-212, 1989.

9. Safjan, A., Demkowicz, L., and Oden, J. T., "Adaptive Finite Element Methods for Hyperbolic Systems with Application to Transient Acoustics," *International Journal for Numerical Methods in Engineering* , Vol. 32, pp. 677-707, 1991.

APPENDIX: Coefficients for TG Schemes

Listed in Table A1 are coefficients μ_j and ν_j of factorization (3.32) for various schemes and various values of stability parameter λ.

Table A1

s	m	λ	μ_j	ν_j
2	4	0.47125	-0.429094784839126	-0.378098940635512
			1.42909478483913	0.548816059850774
		0.956435464587639	-1.24942270597577	0.
			2.24942270597577	1.39760887500830
3	6	0.695	1.49387844844708	0.646649962127165
			1.49654973431122	0.455862817625521
			-1.99042818275830	1.02905635860739
		1.41218087134444	1.59760032454113	0.
			2.26129033257844	1.55344122448889
			-2.85889065711958	2.12952443875392
	4	0.22	1.20431944918114	0.423802122065587
			0.487902005145560	0.
			-0.692221454326699	0.
4	8	0.92	1.51162577127872	0.699029877978738
			-0.834510555244671	-0.525519943835058
			-2.07038751330515	1.17729970655410
			2.39327229727110	1.46702890097419
		1.86773692752800	2.24345154354026	1.63319393127839
			-1.80258065404047	0.
			-2.95806878678511	2.41911998051307
			3.51719789728532	3.17835029737392

	6	0.29	1.40623086480151 -1.45772045255471 0. 1.05148958775320	0.492263592133862 0.562362275582733 0. 0.389406390318465
5	10	1.15	1.82704798577991 -2.74777882789812 -2.09945299083185 2.49966934516921 1.52051448778085	0.581806316107477 1.91908830024251 1.27190423205347 1.66880094503773 0.736603622974089
		2.32321418507049	2.22324138974647 -3.93321086941255 -2.98201123343815 3.63234175933788 2.05963895376635	1.68098156751573 3.93536053161087 2.58923026751565 3.54903685460515 0.
	8	0.38	0.641021237097618 -0.905360775899868 -1.47520238954498 1.70120453471140 1.03833739363583	0. 0. 0.625291329822029 0.751557791280019 0.412675810404174

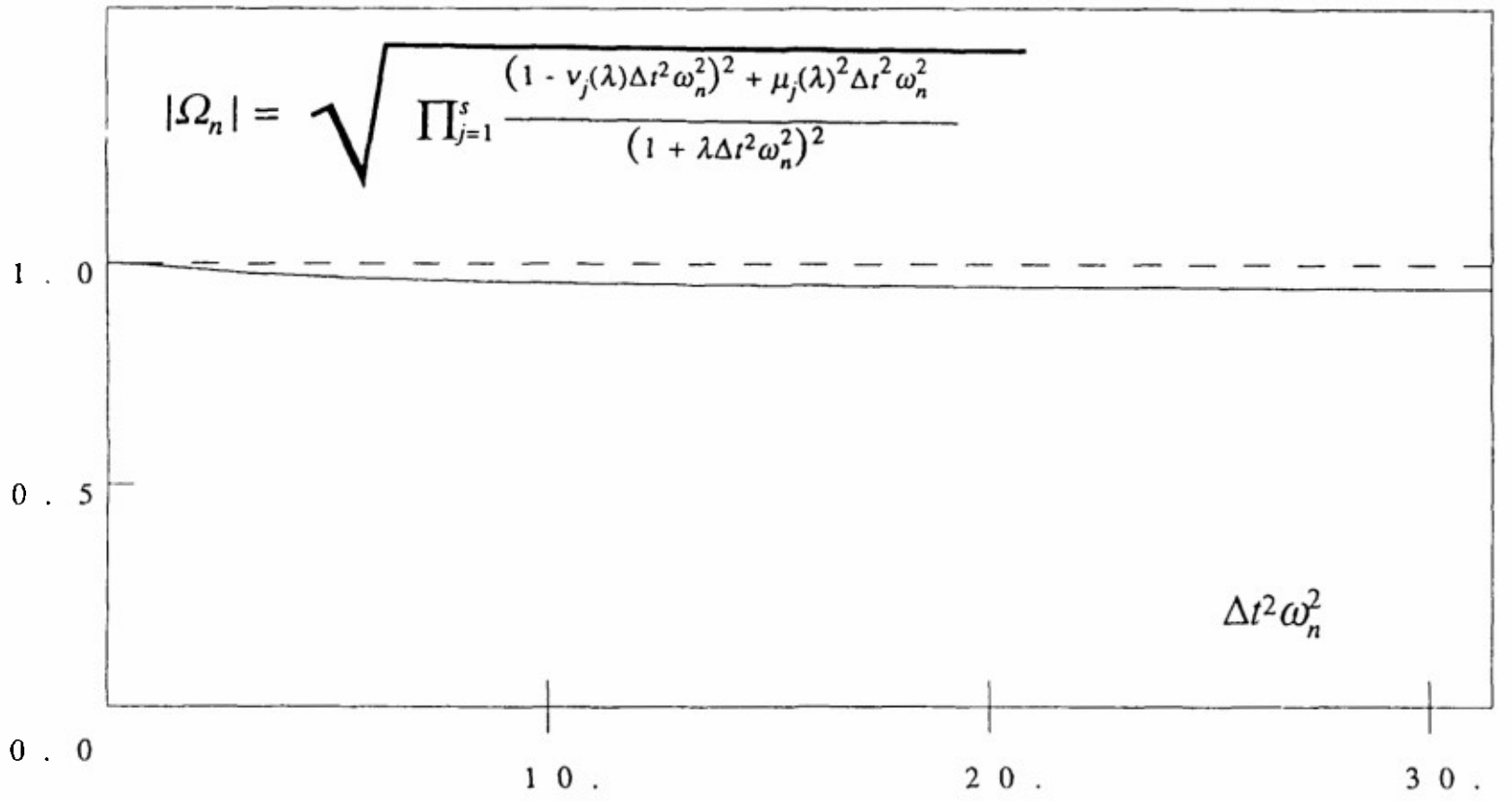

Fig. 1 Eigenvalues of transient operator $\boldsymbol{T}$, $s = 2$, $m = 4$, $\lambda = 0.47048$.

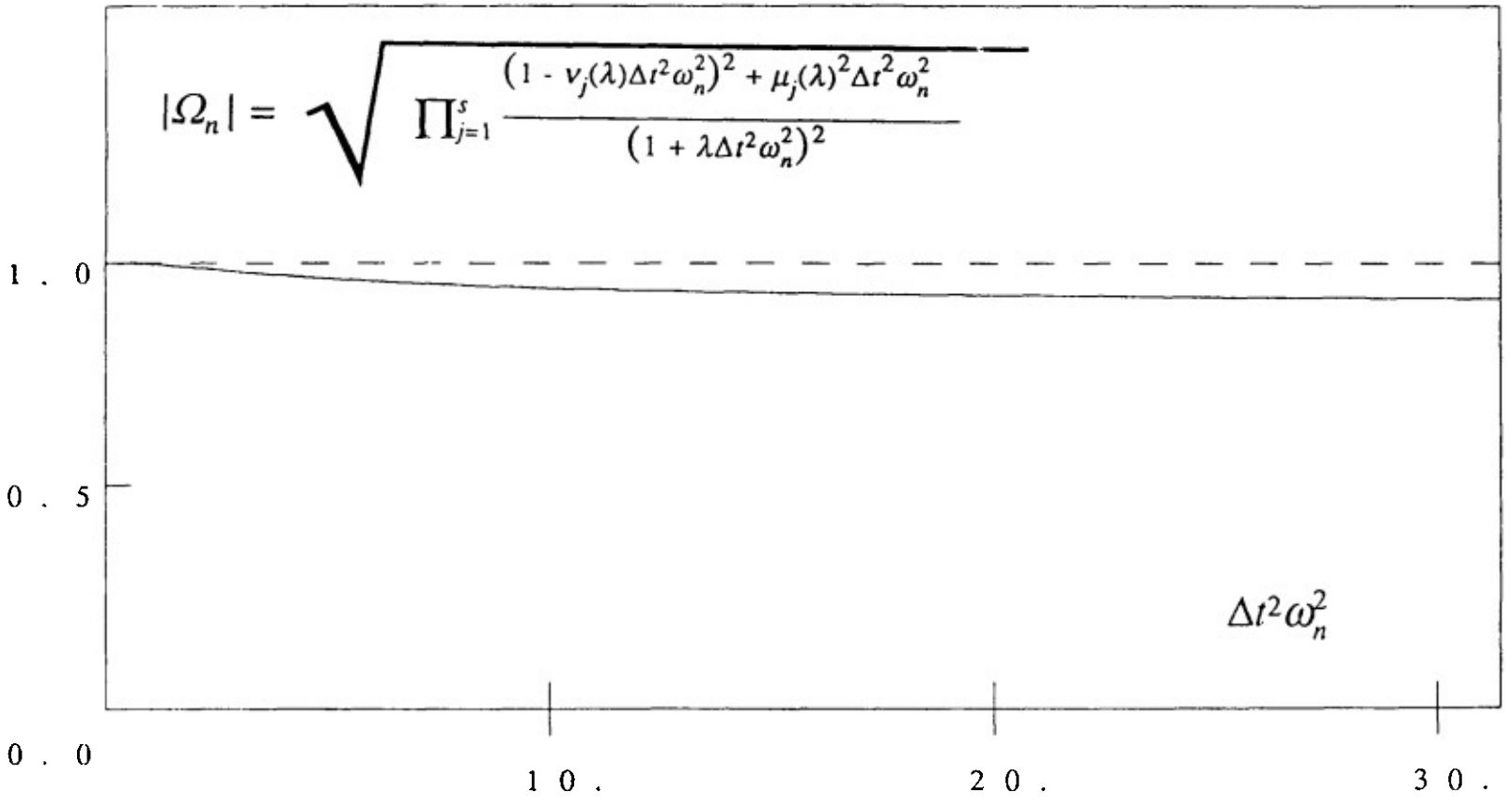

Fig. 2 Eigenvalues of transient operator $\boldsymbol{T}$, $s = 3$, $m = 6$, $\lambda = 0.695$.

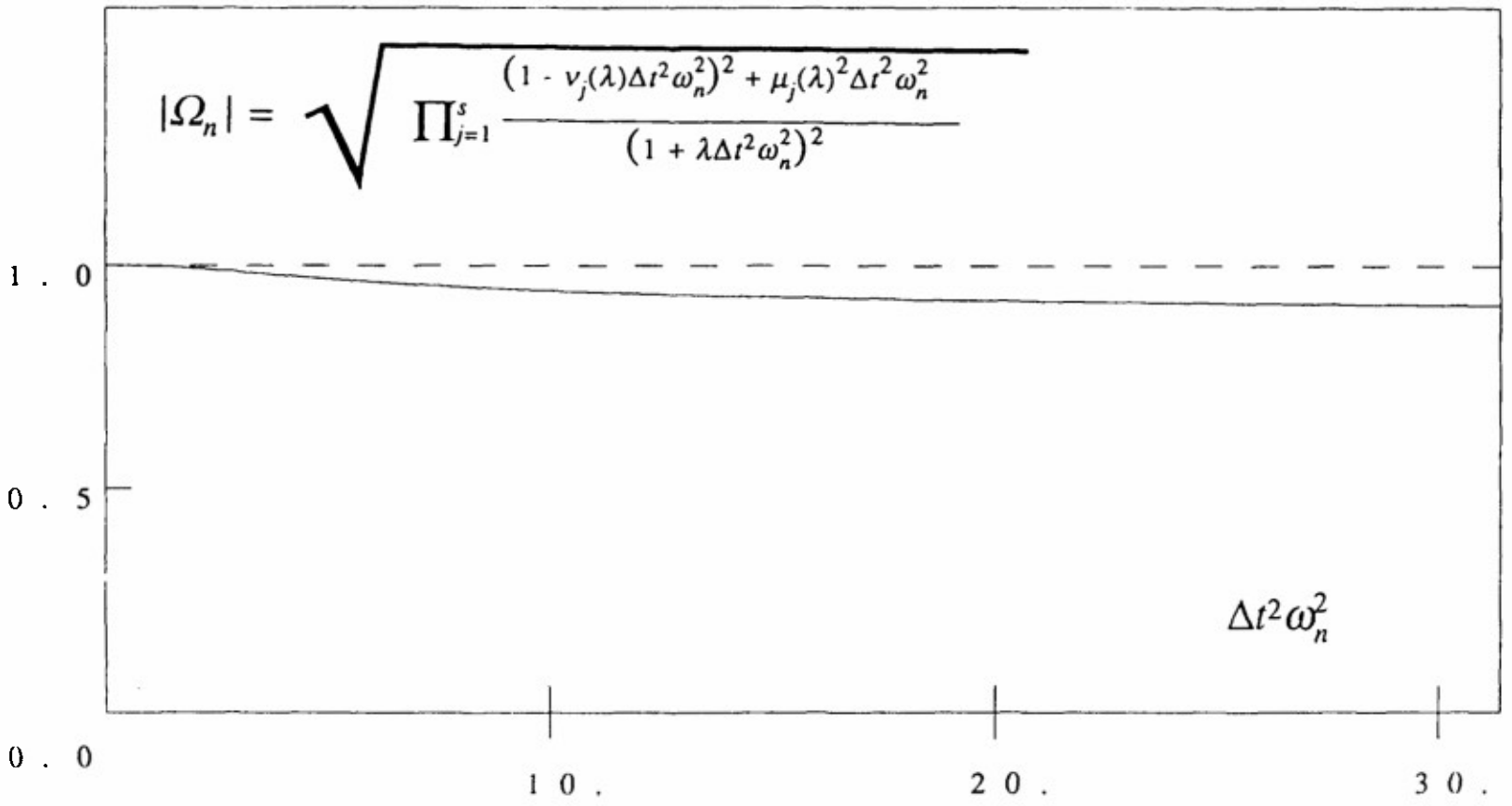

Fig. 3 Eigenvalues of transient operator T, $s = 4$, $m = 8$, $\lambda = 0.91943$.

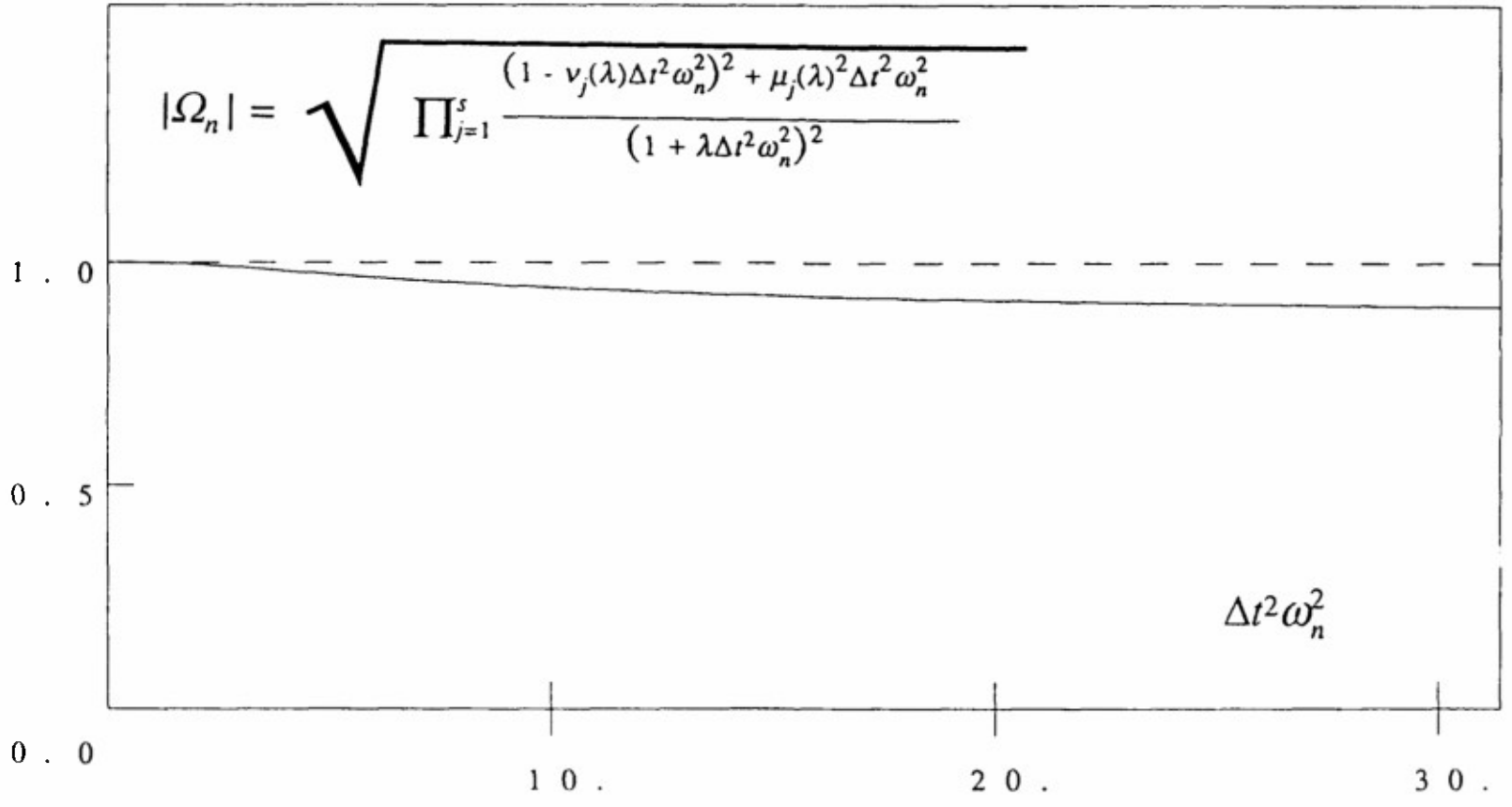

Fig. 4 Eigenvalues of transient operator T, $s = 5$, $m = 10$, $\lambda = 1.15$.

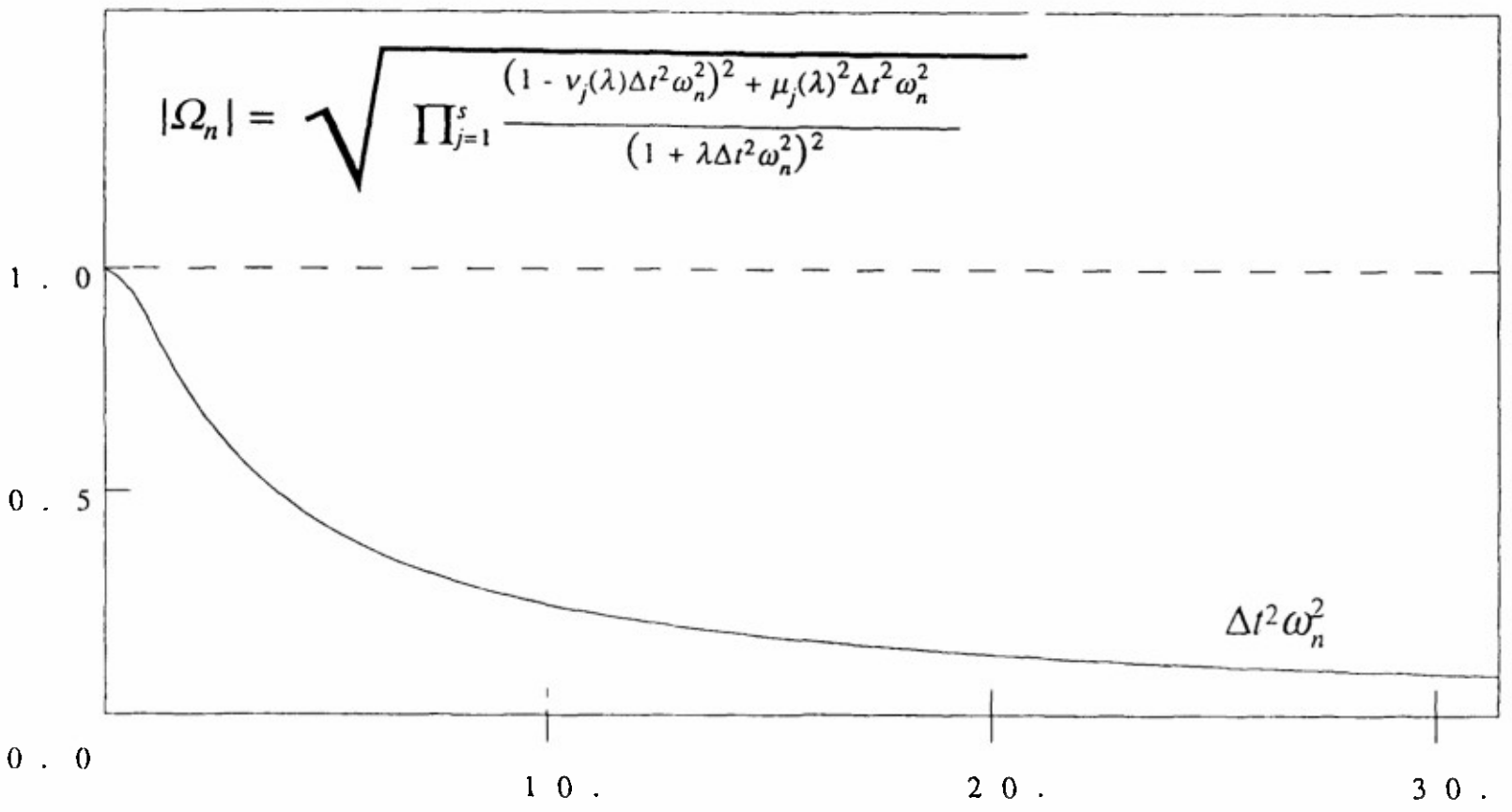

Fig. 5 Eigenvalues of transient operator T, $s = 3$, $m = 4$, $\lambda = 0.22$.

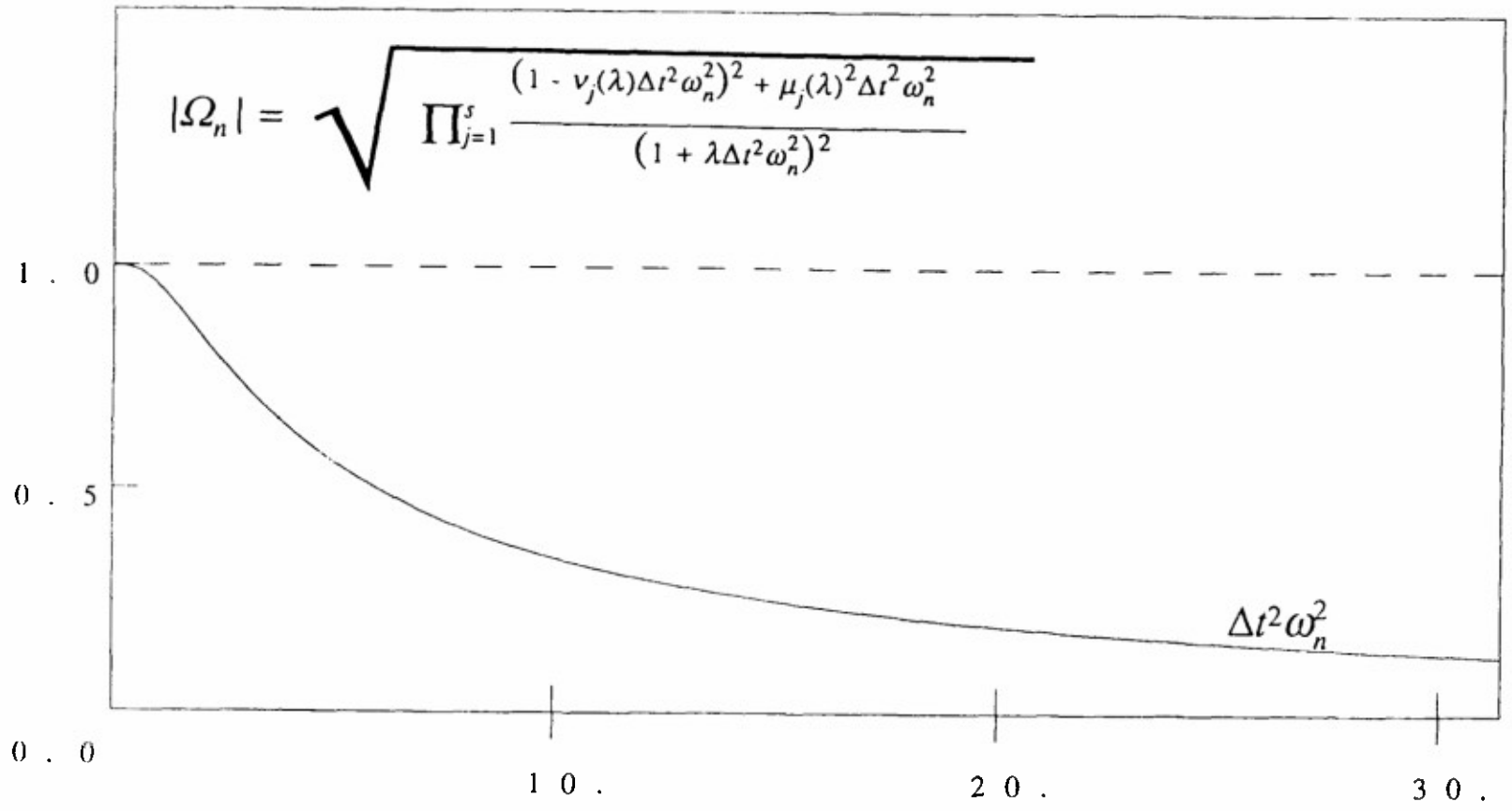

Fig. 6 Eigenvalues of transient operator T, $s = 4$, $m = 6$, $\lambda = 0.29$.

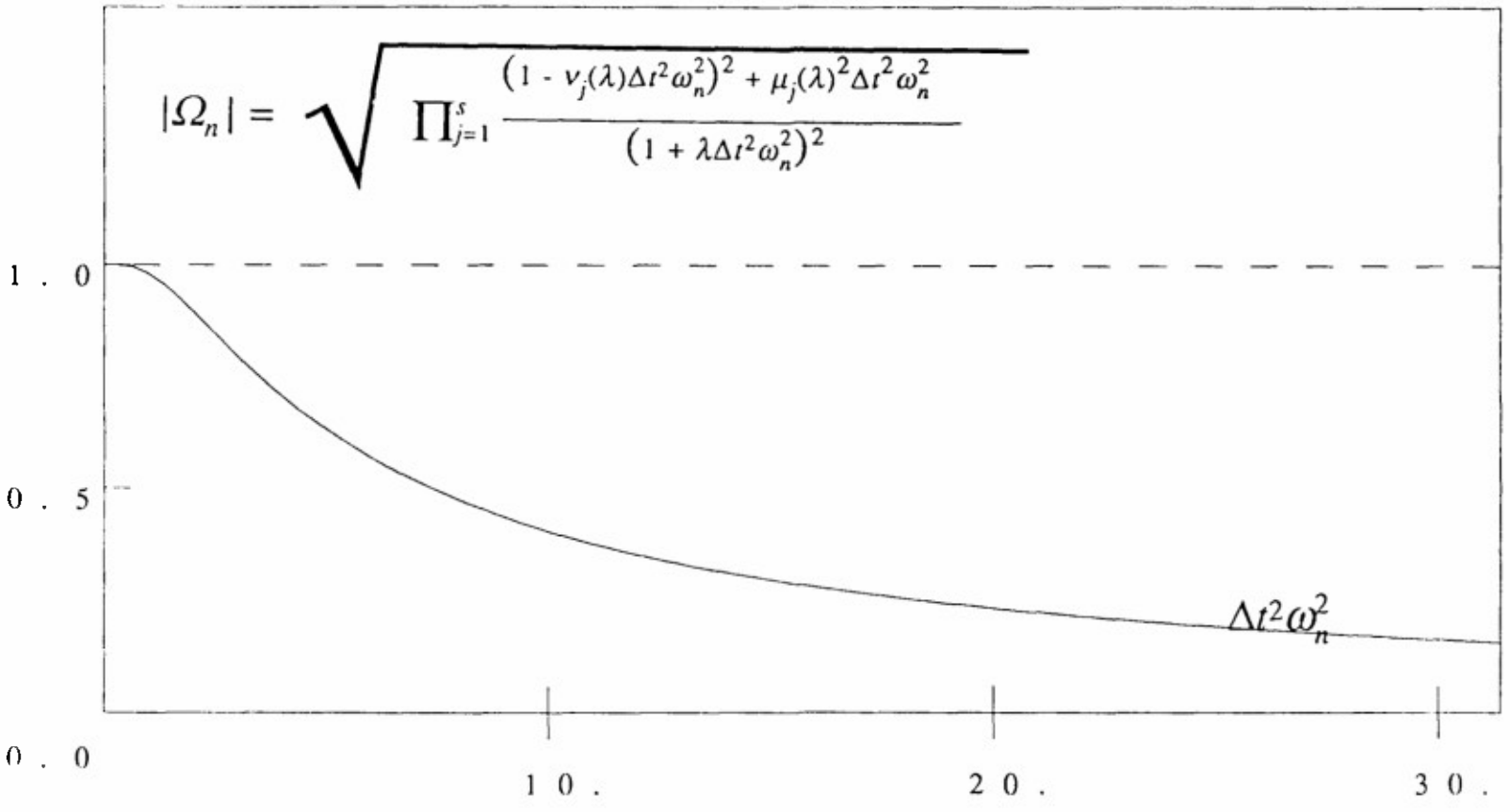

Fig. 7 Eigenvalues of transient operator $\boldsymbol{T}$, $s = 5$, $m = 8$, $\lambda = 0.38$.

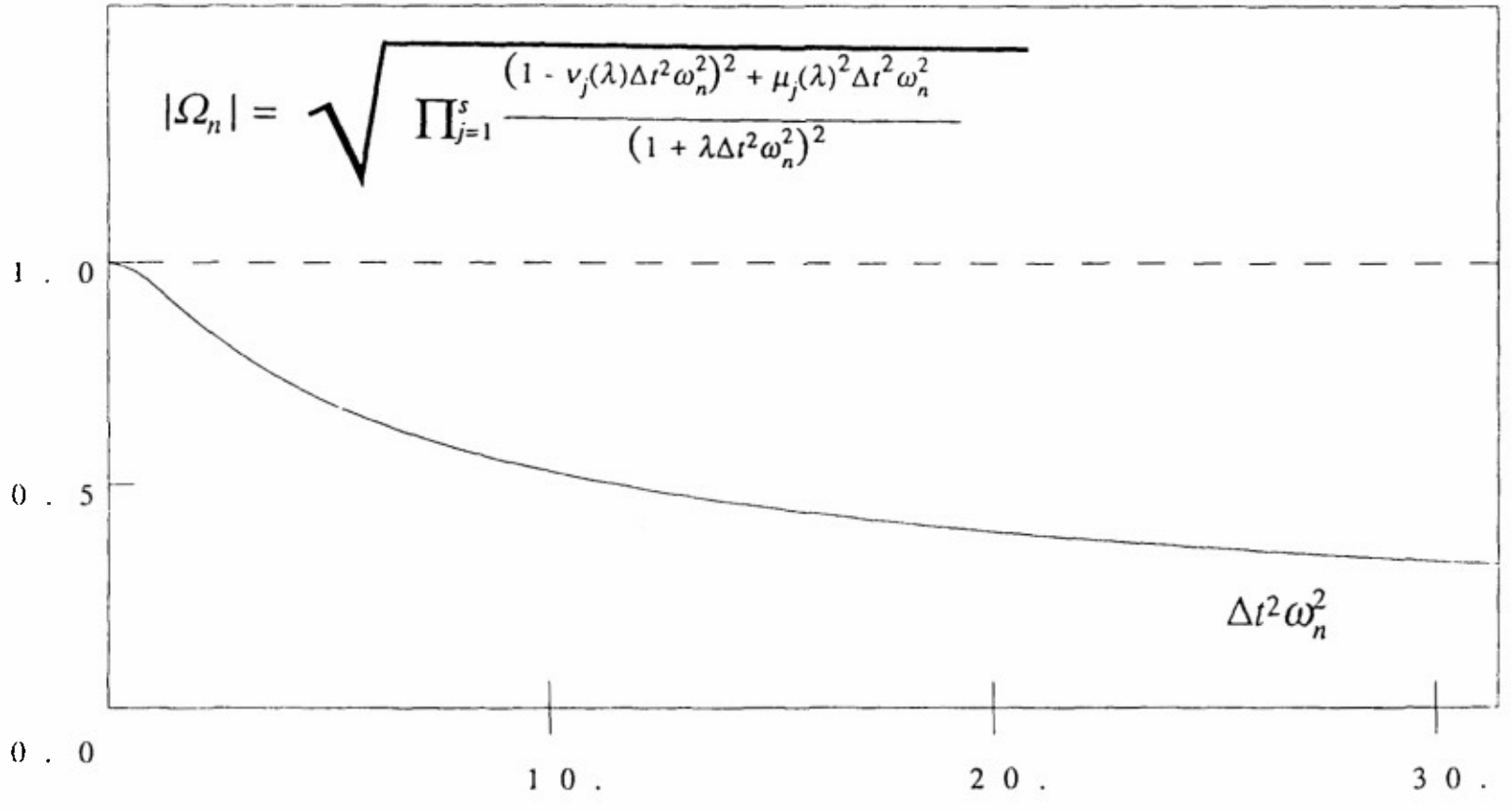

Fig. 8 Eigenvalues of transient operator T, $s = 2$, $m = 4$, $\lambda = 0.95644$.

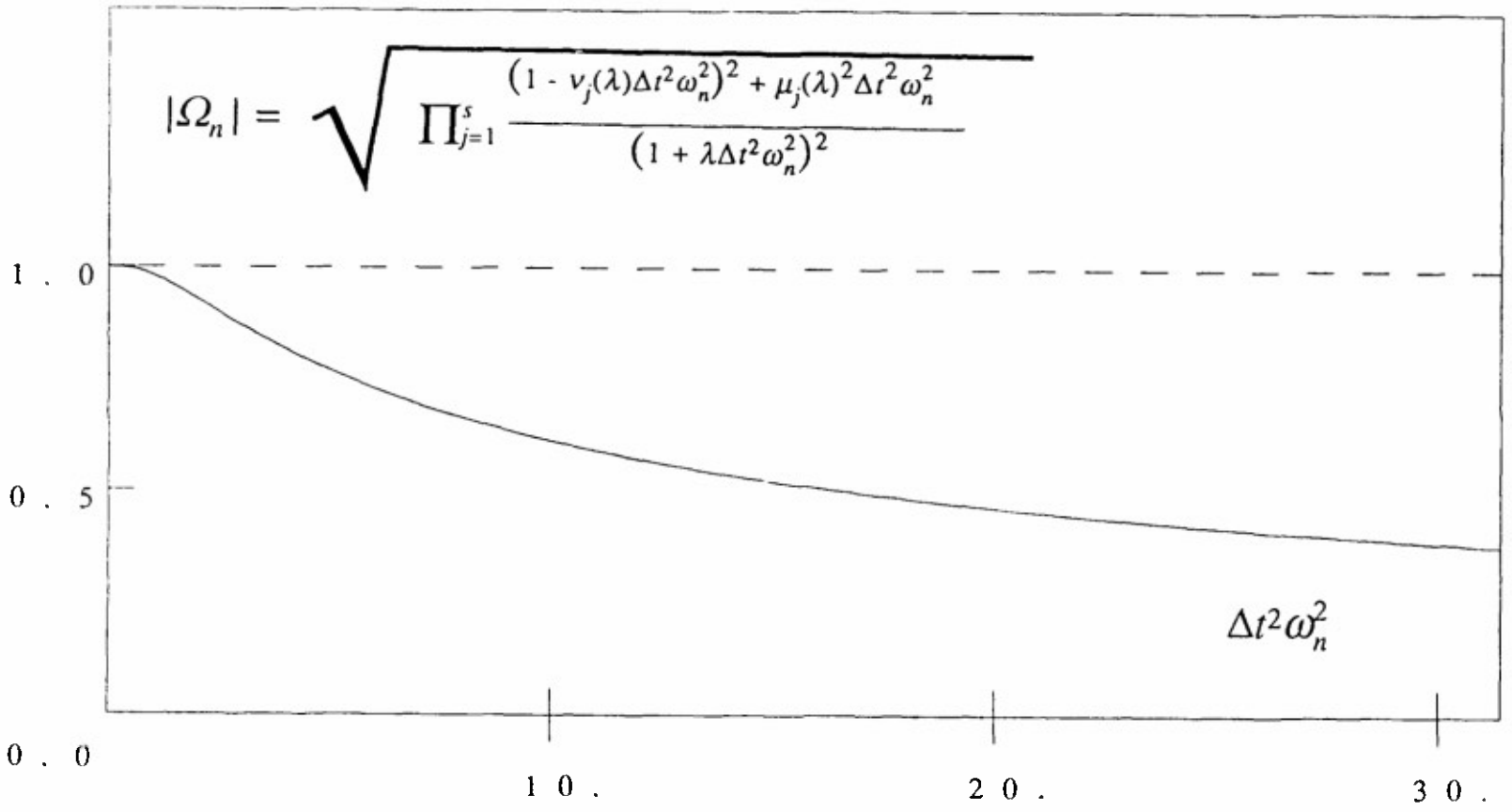

Fig. 9 Eigenvalues of transient operator T, $s = 3$, $m = 6$, $\lambda = 1.41218$.

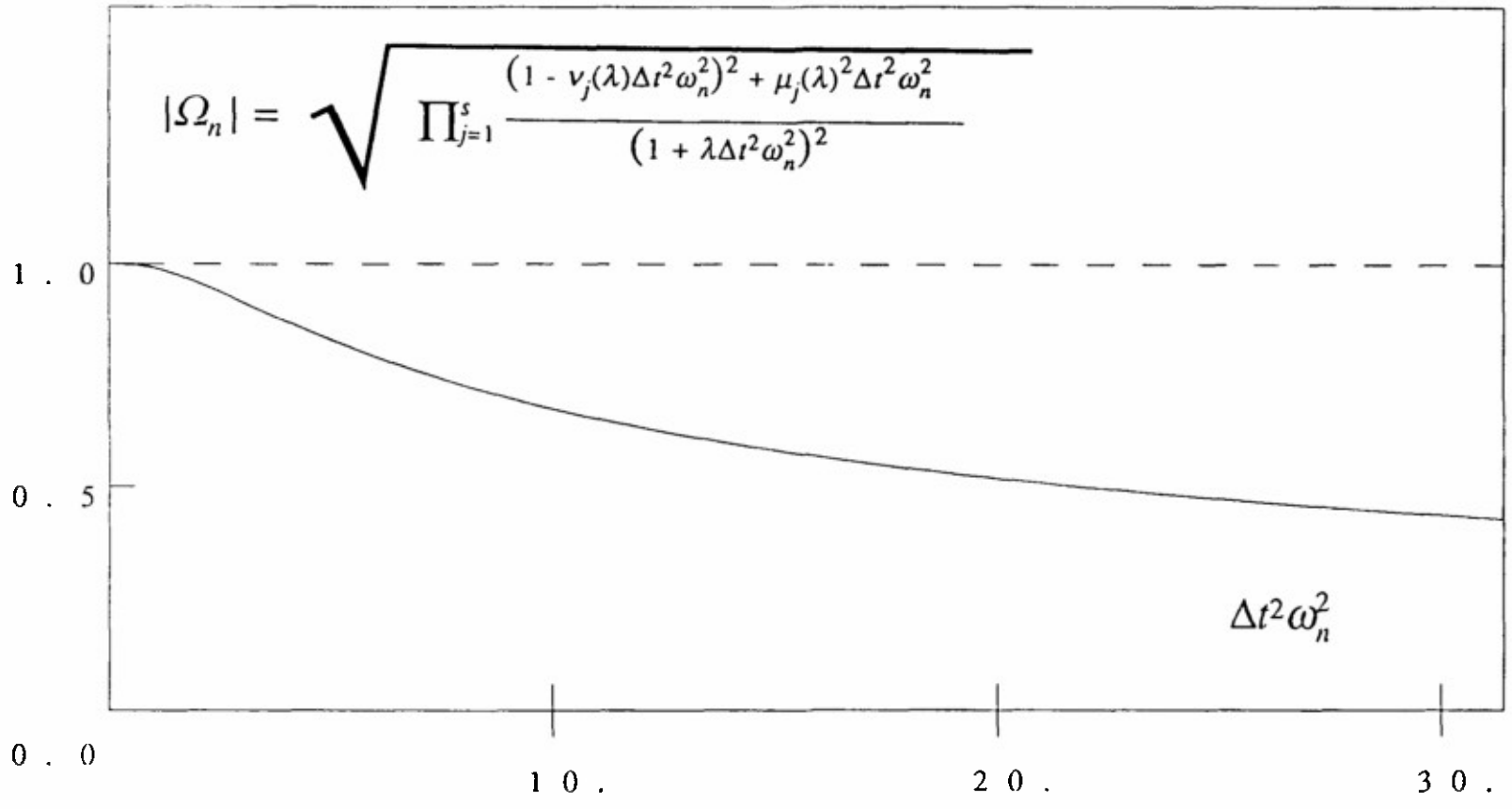

Fig. 10 Eigenvalues of transient operator T, $s = 4$, $m = 8$, $\lambda = 1.86774$.

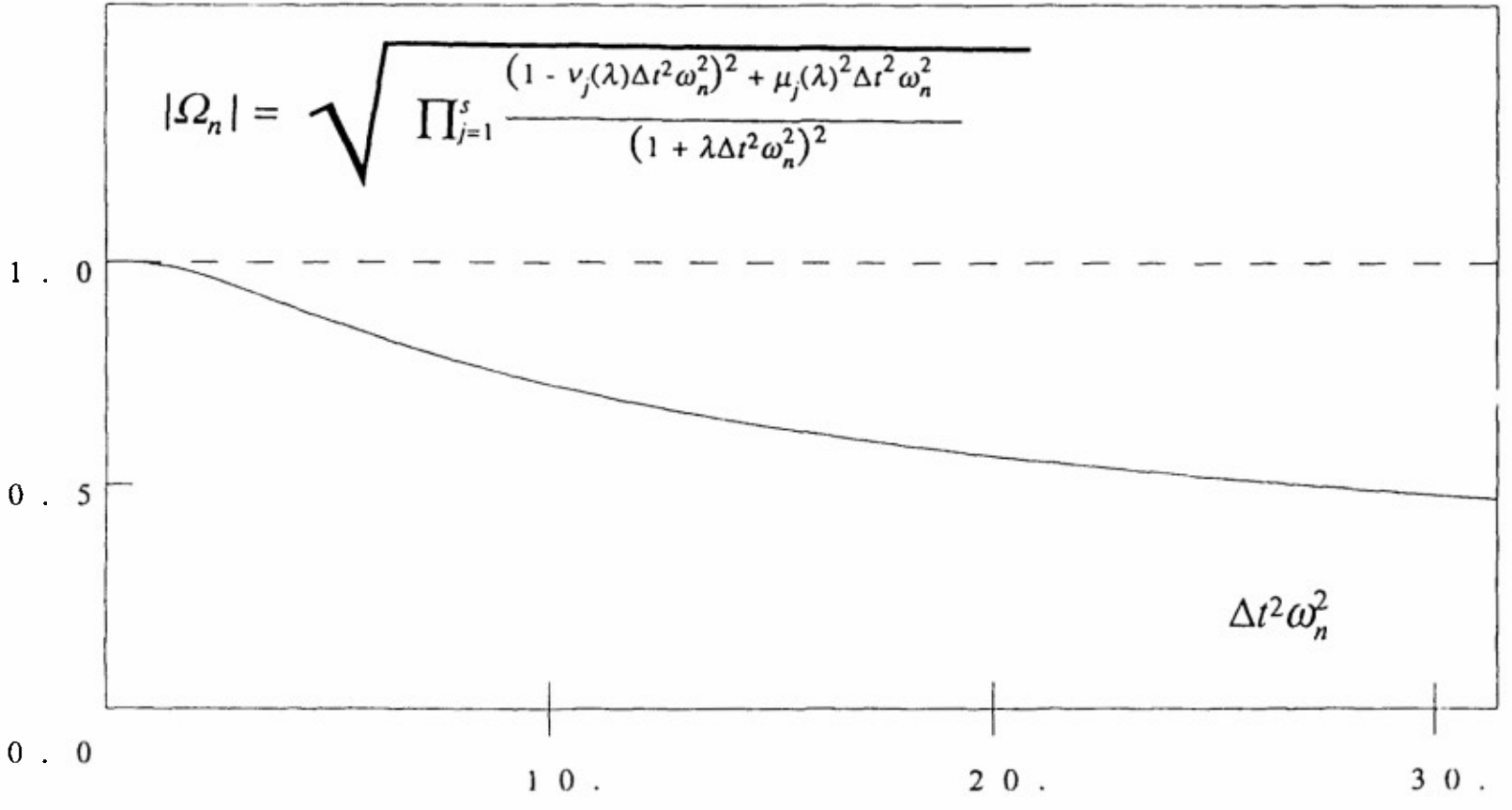

Fig. 11 Eigenvalues of transient operator T, $s = 5$, $m = 10$, $\lambda = 2.32321$.

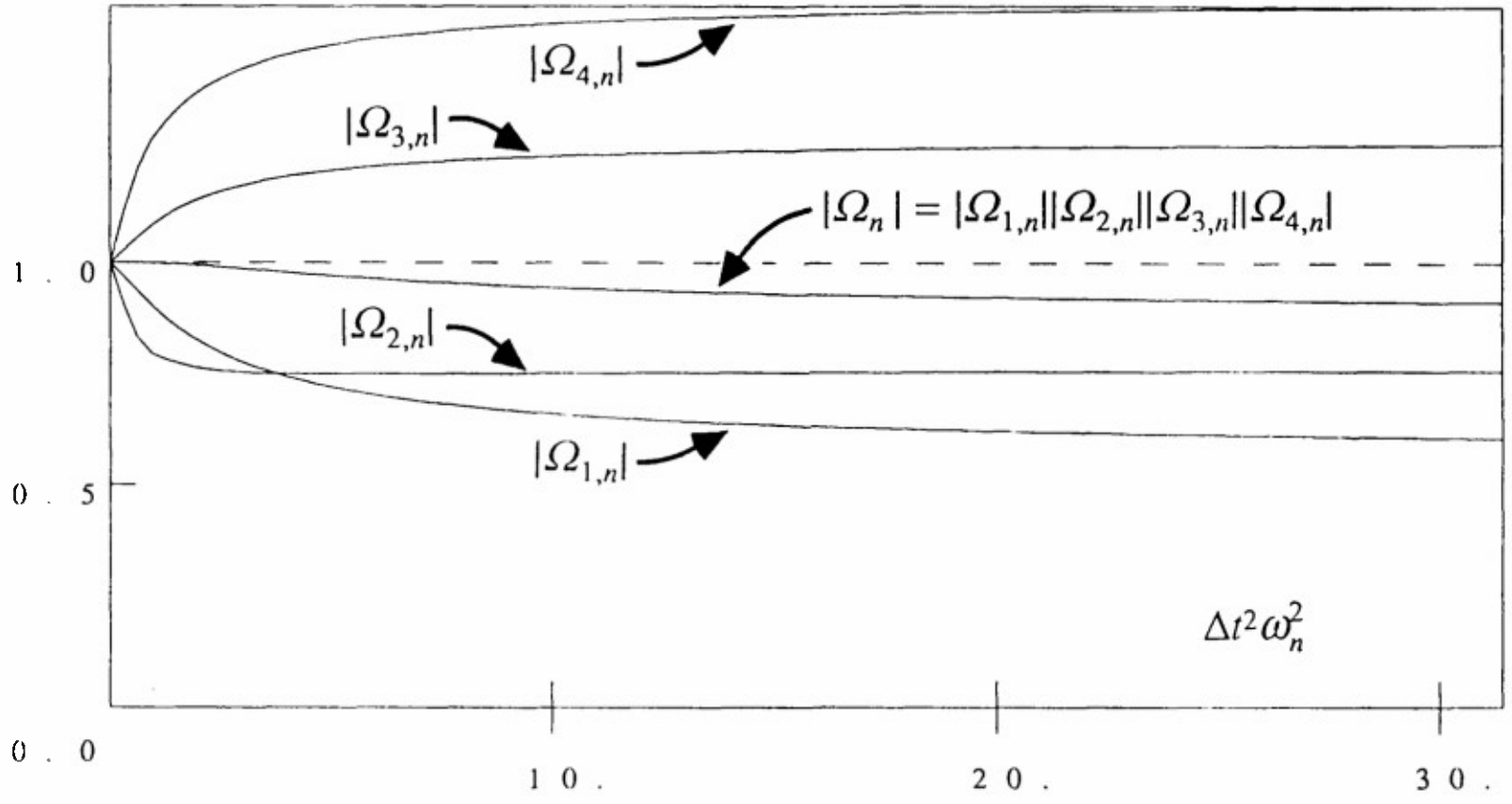

Fig. 12 Decomposition of eigenvalues of transient operator T into the product of eigenvalues of composite operators T_j, $s = 4$, $m = 8$, $\lambda = 0.91943$.

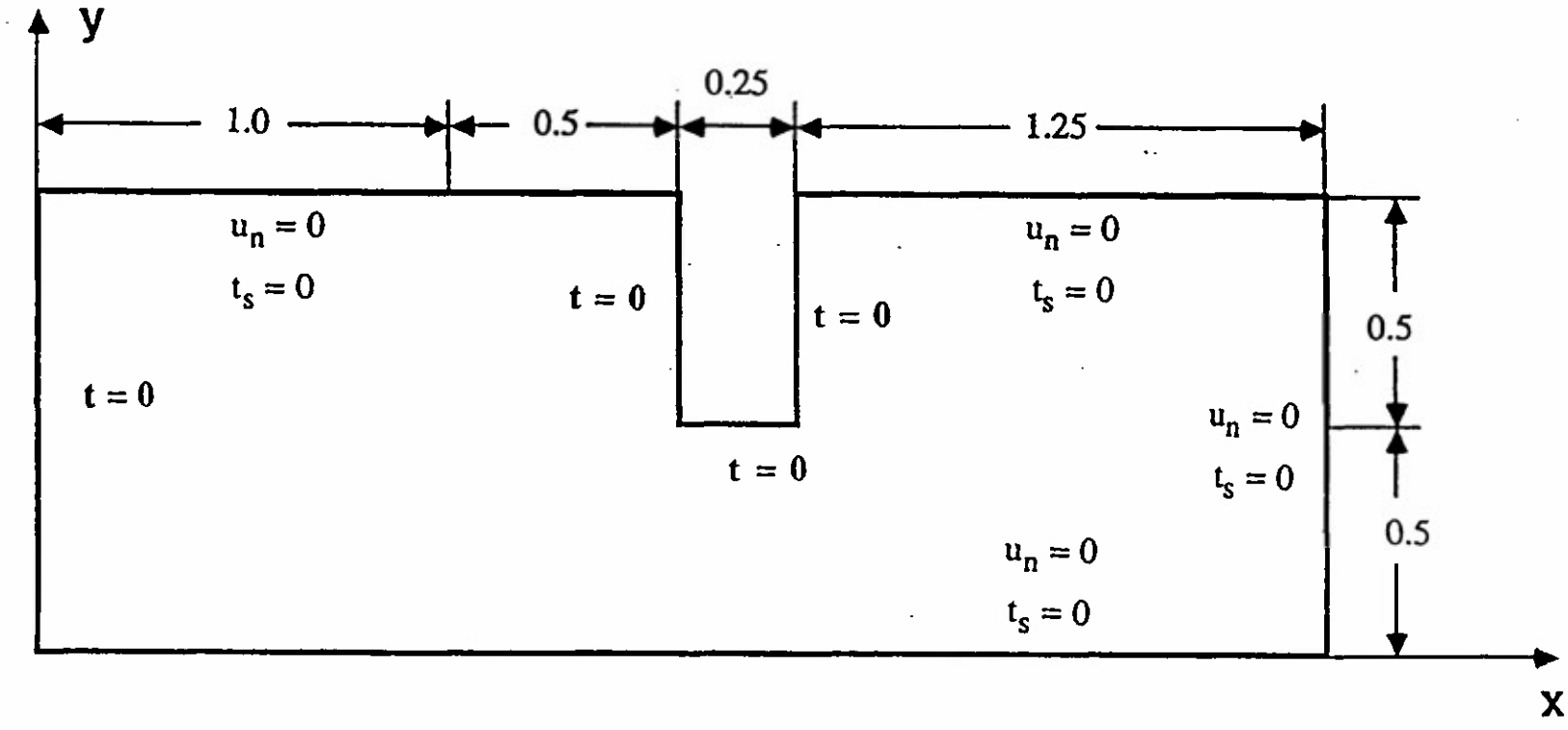

Fig. 13 Wave propagation in an elastic panel. Problem definition.

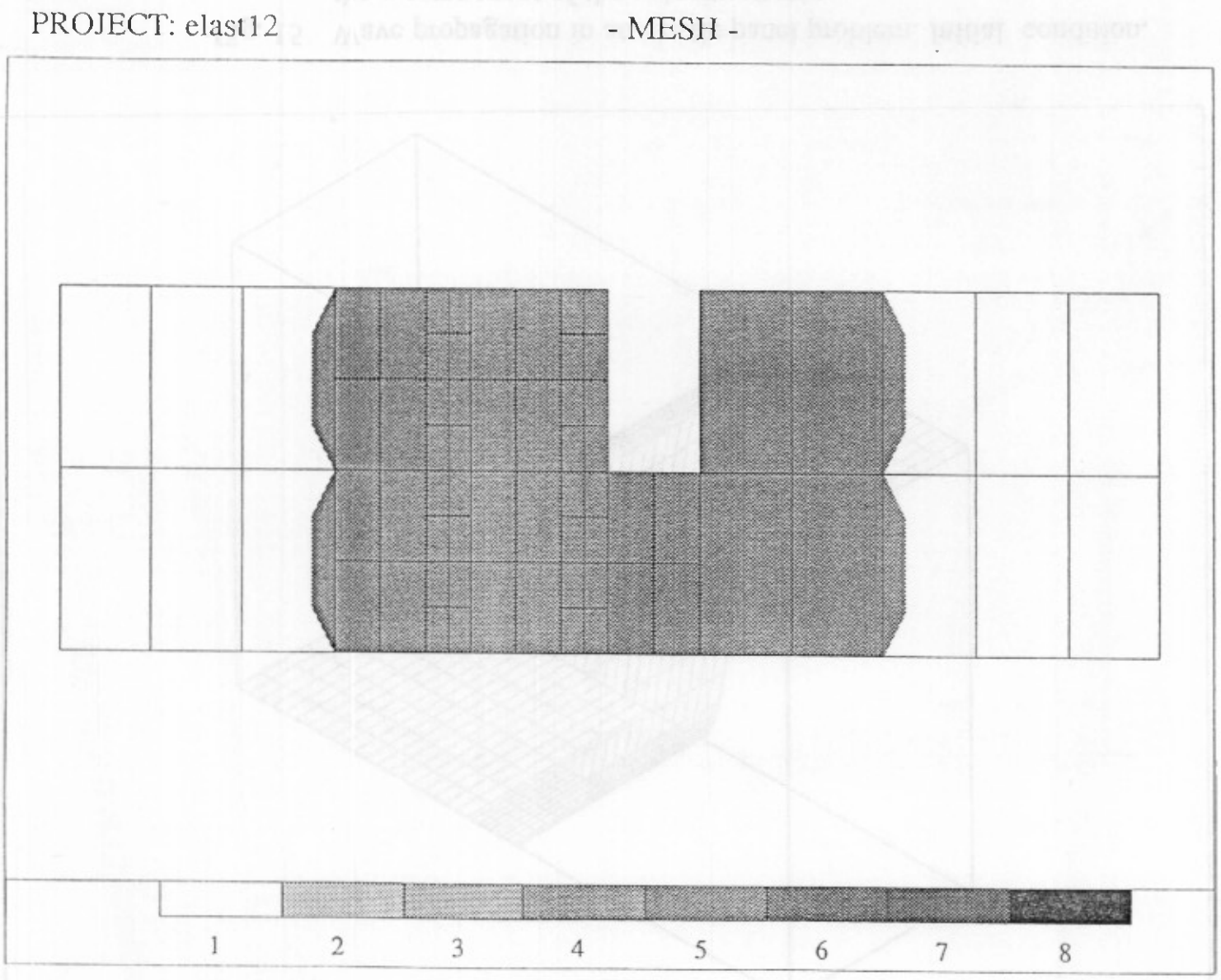

Fig. 14 Wave propagation in an elastic panel problem. Initial FE mesh.

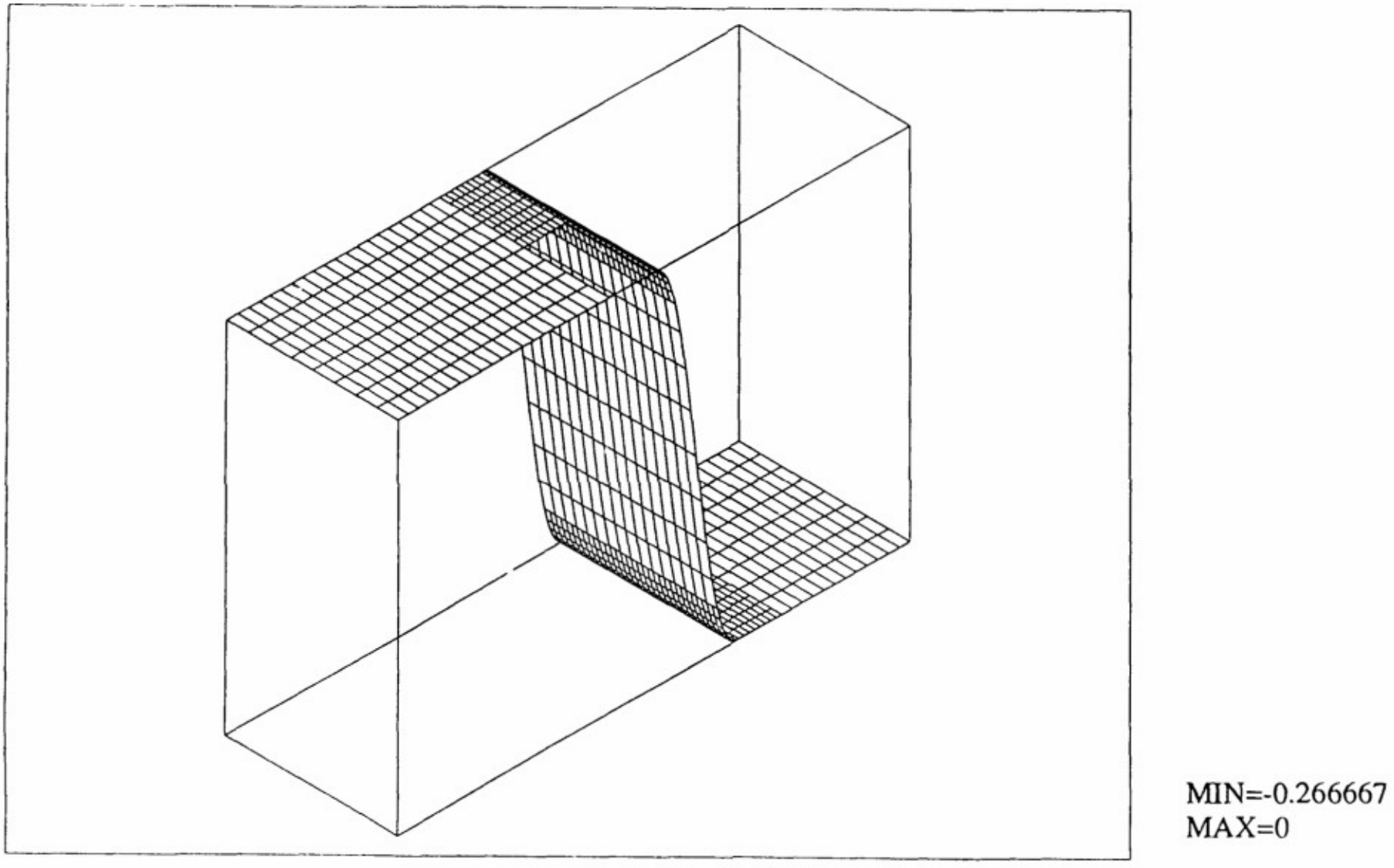

Fig. 15 Wave propagation in an elastic panel problem. Initial condition, the x component of the velocity vector.

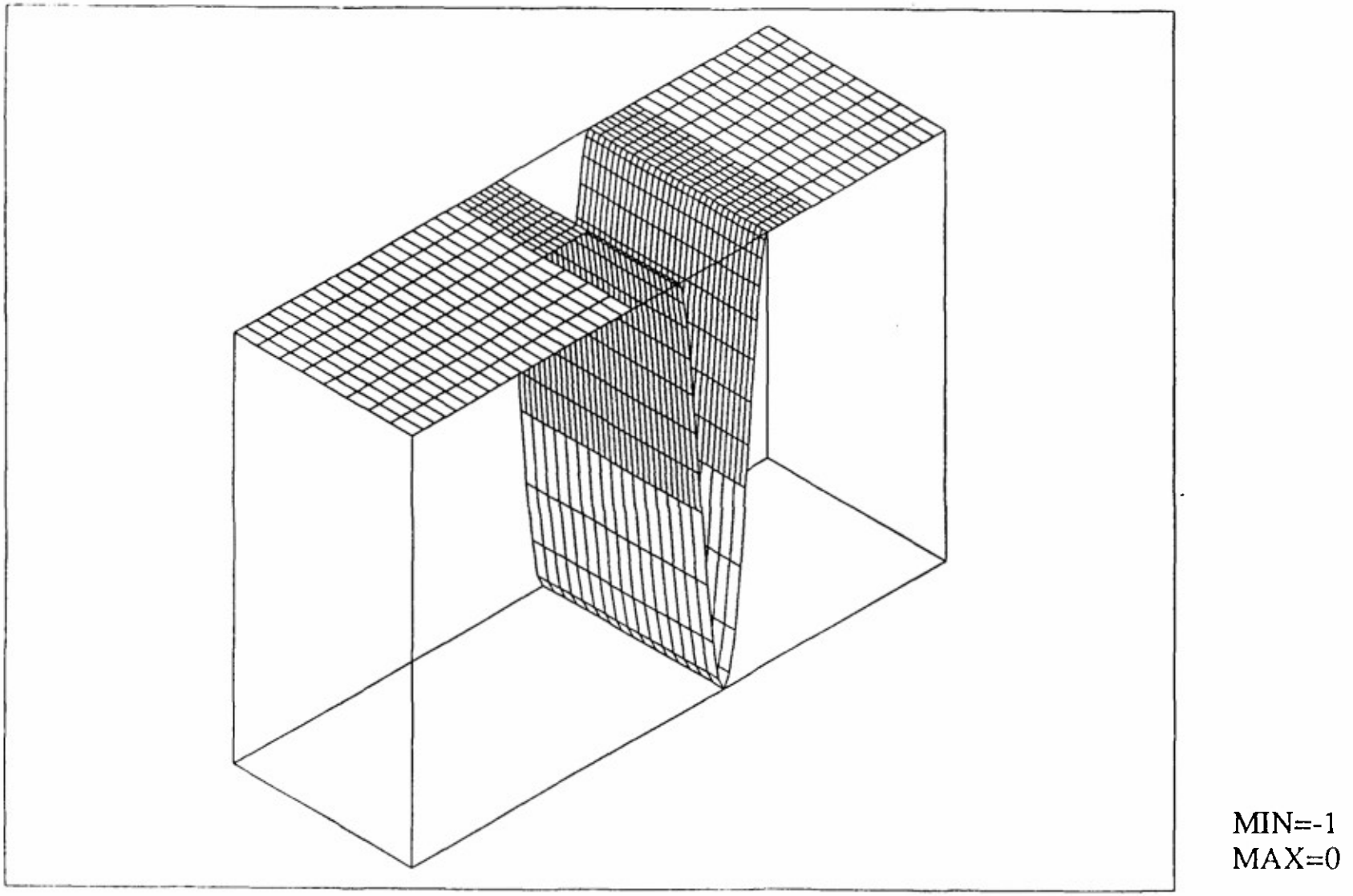

Fig. 16 Wave propagation in an elastic panel problem. Initial condition, the x component of the displacement vector.

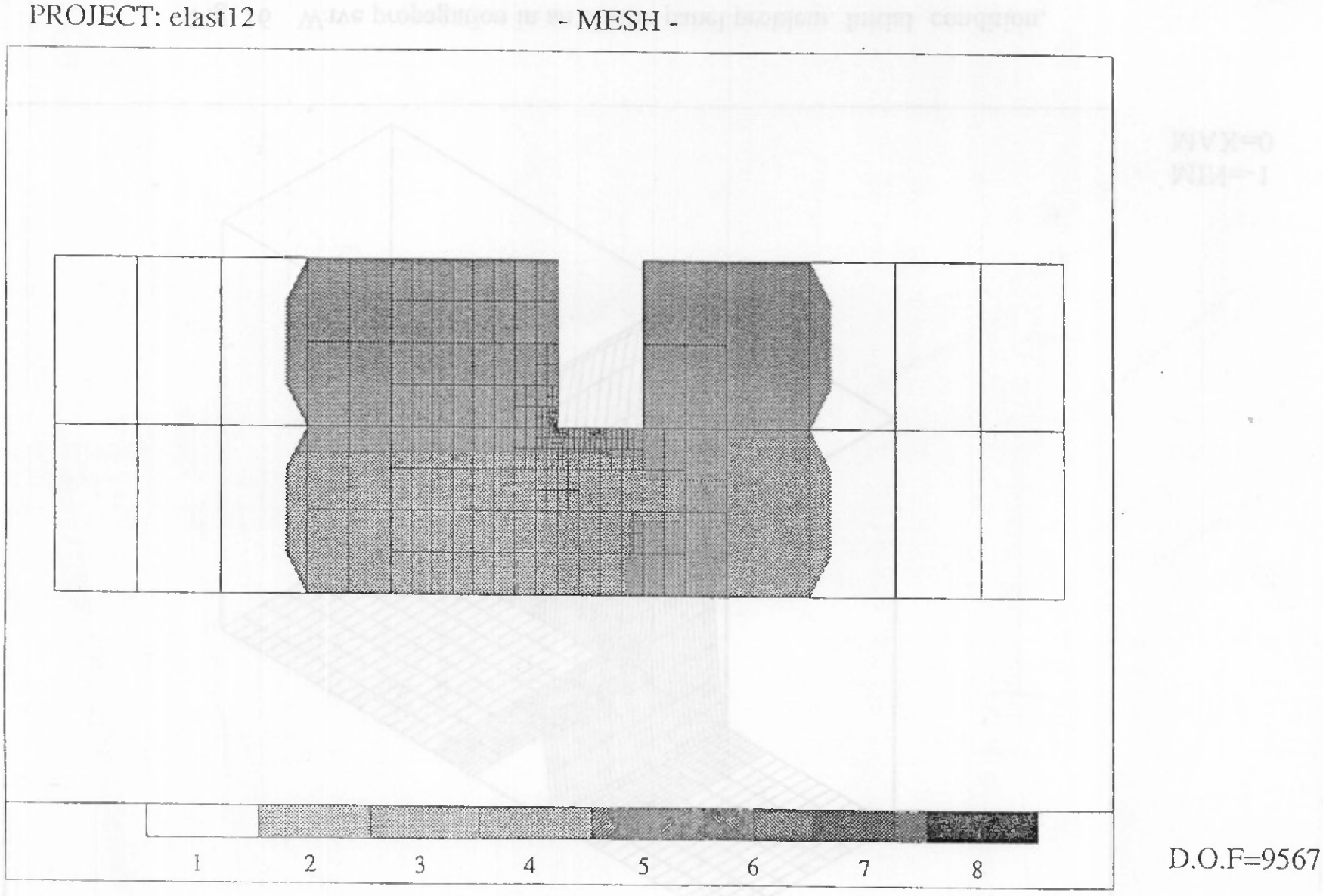

Fig. 17 Wave propagation in an elastic panel problem. An h adaptive finite element mesh at time $t = 0.25$ s.

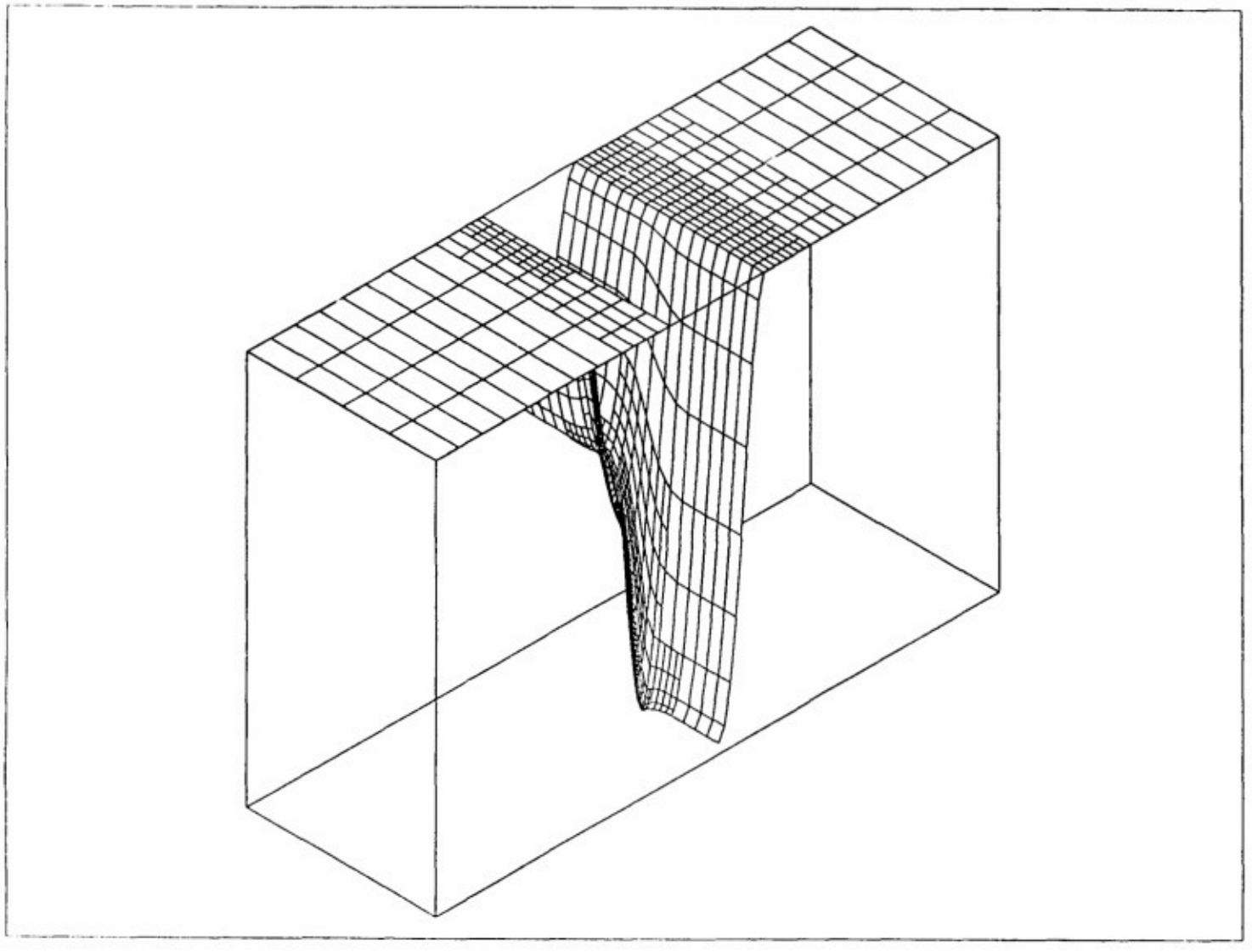

Fig. 18 Wave propagation in an elastic panel problem. The x component of the velocity vector at time $t = 0.25$ s.

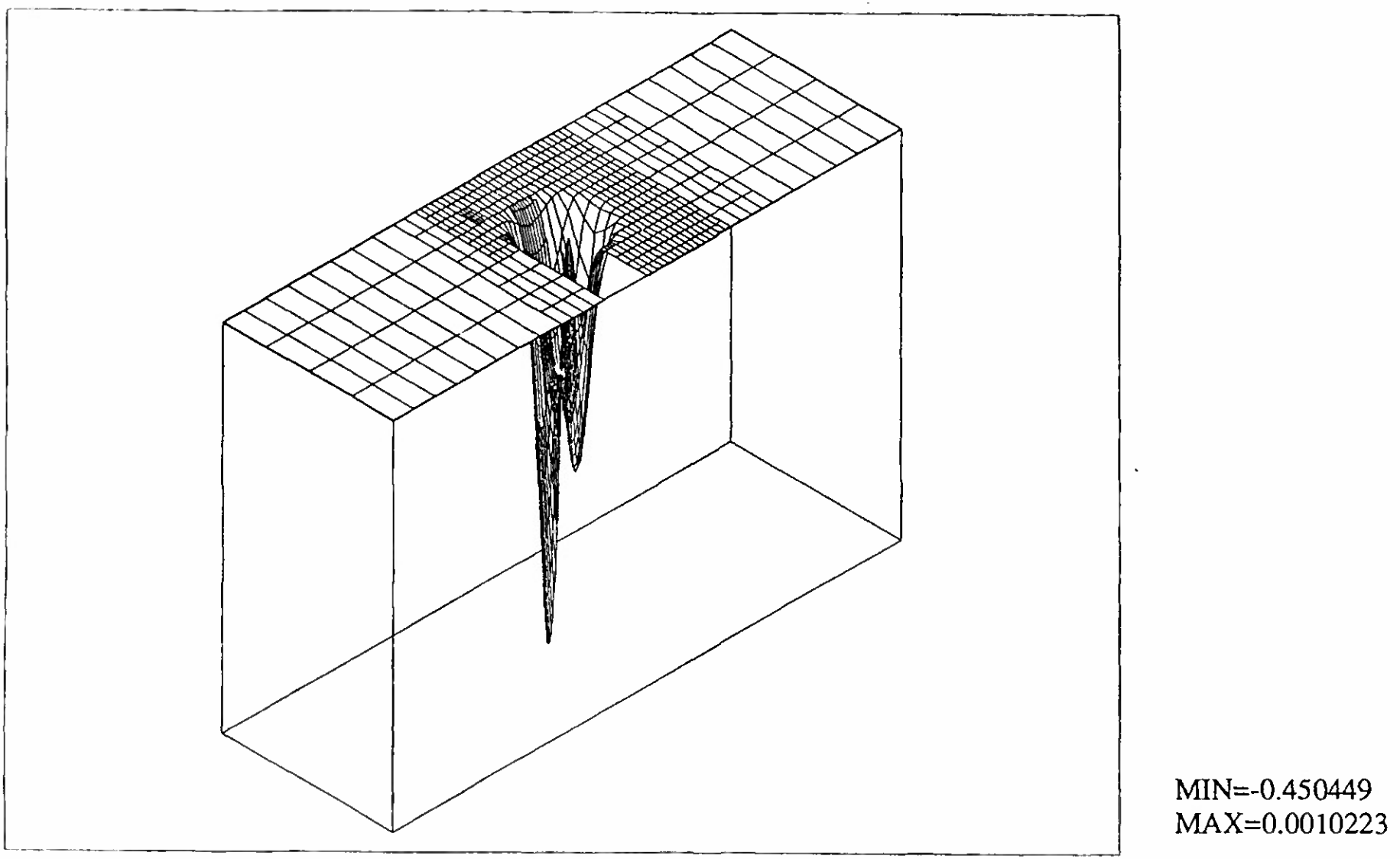

Fig. 19 Wave propagation in an elastic panel problem. The y component of the velocity vector at time $t = 0.25$ s.

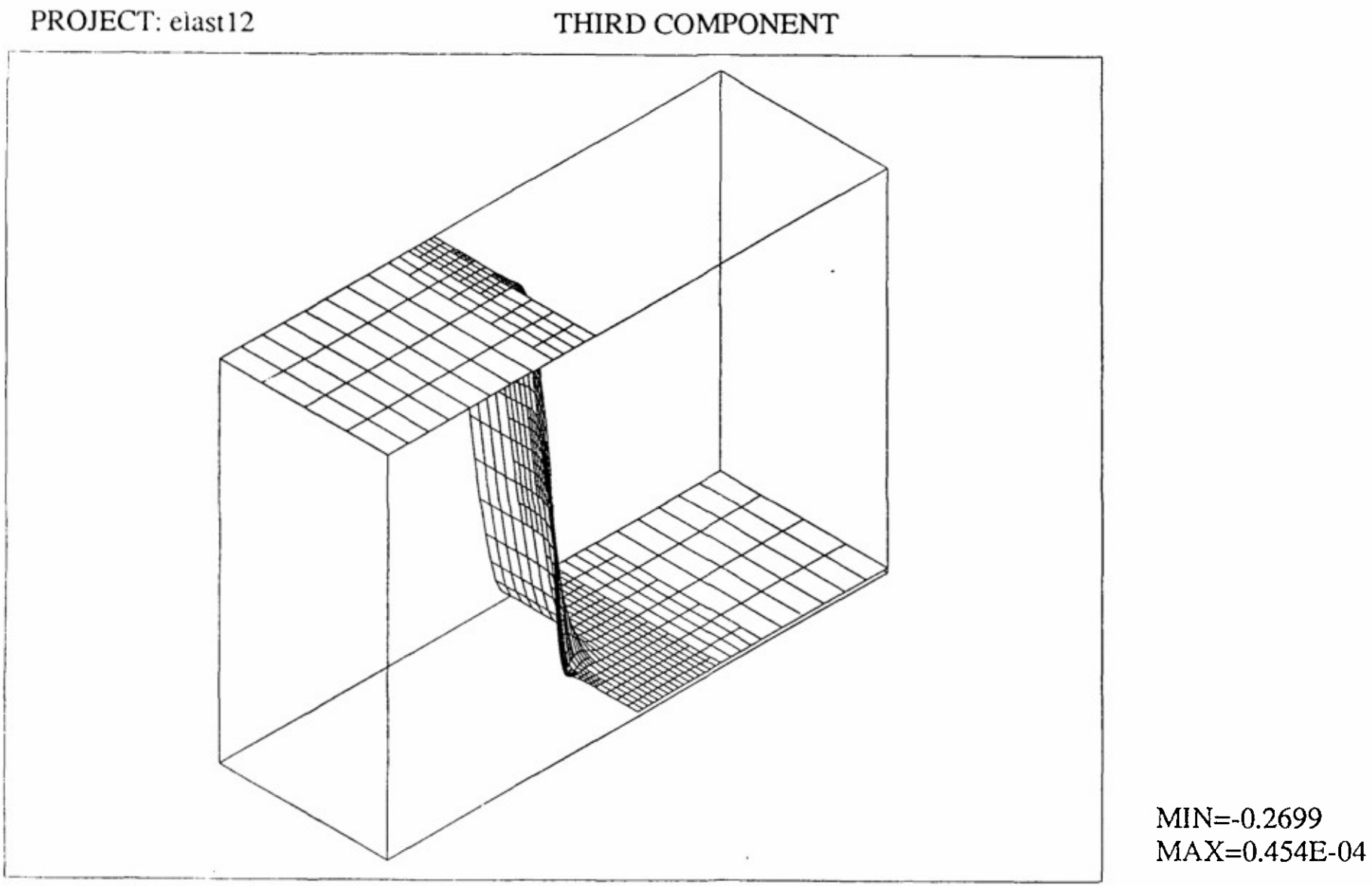

Fig. 20 Wave propagation in an elastic panel problem. The x component of the displacement vector at time $t = 0.25$ s.

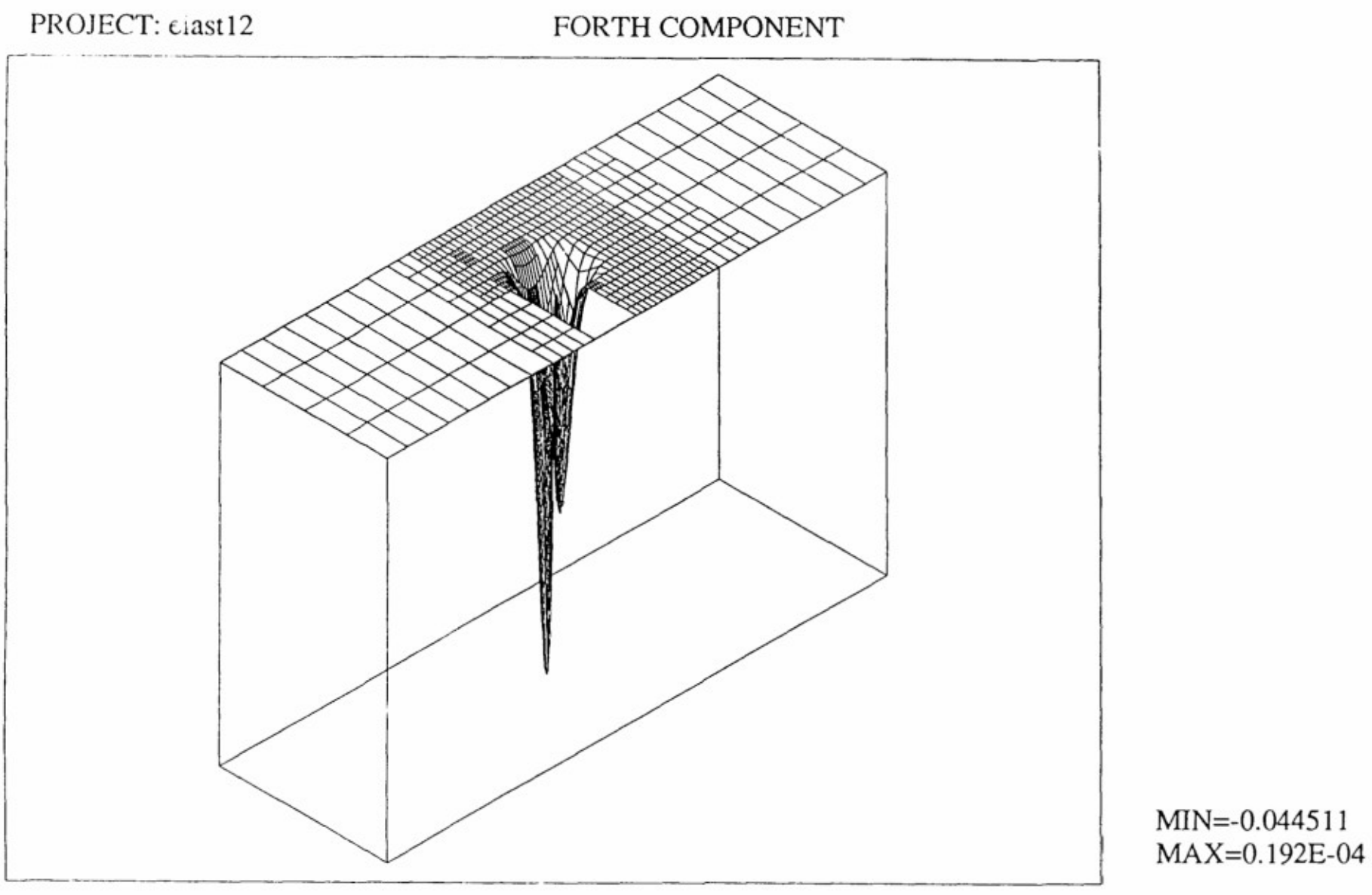

Fig. 21 Wave propagation in an elastic panel problem. The y component of the displacement vector at time $t = 0.25$ s.

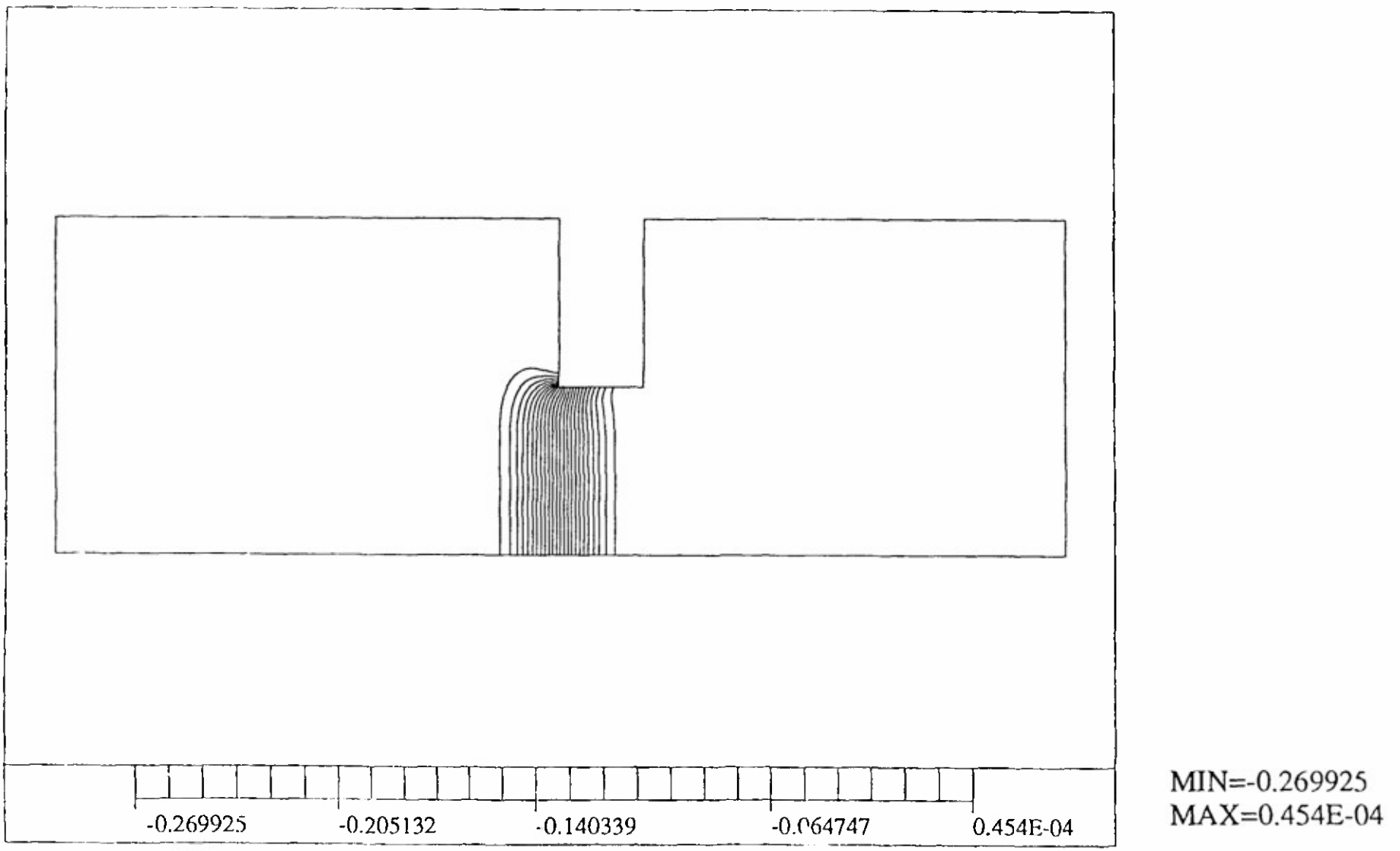

Fig. 22 Wave propagation in an elastic panel problem. x-displacement contours at time $t = 0.25\ s$.

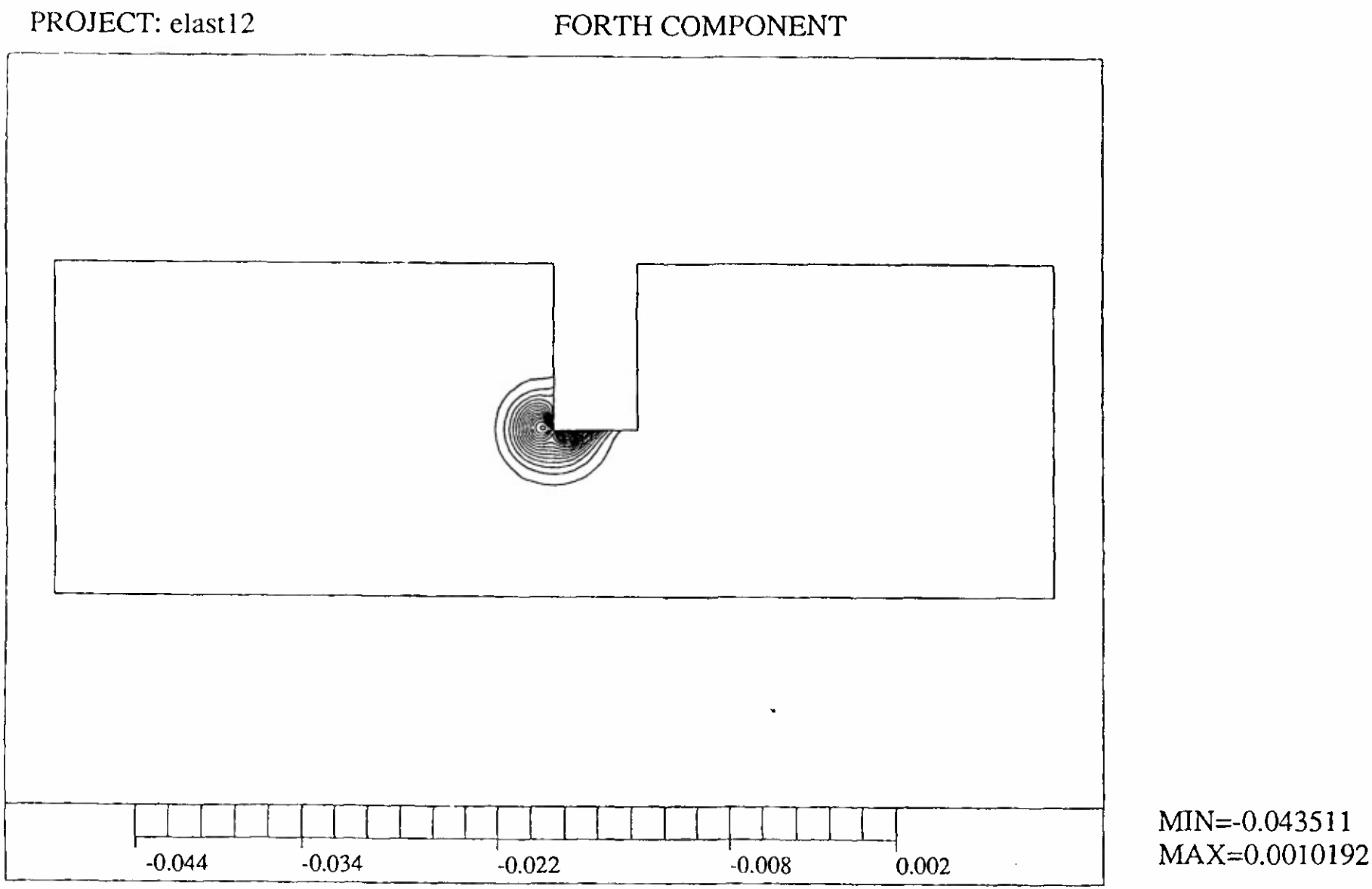

Fig. 23 Wave propagation in an elastic panel problem. y-displacement contours at time $t = 0.25\ s$.

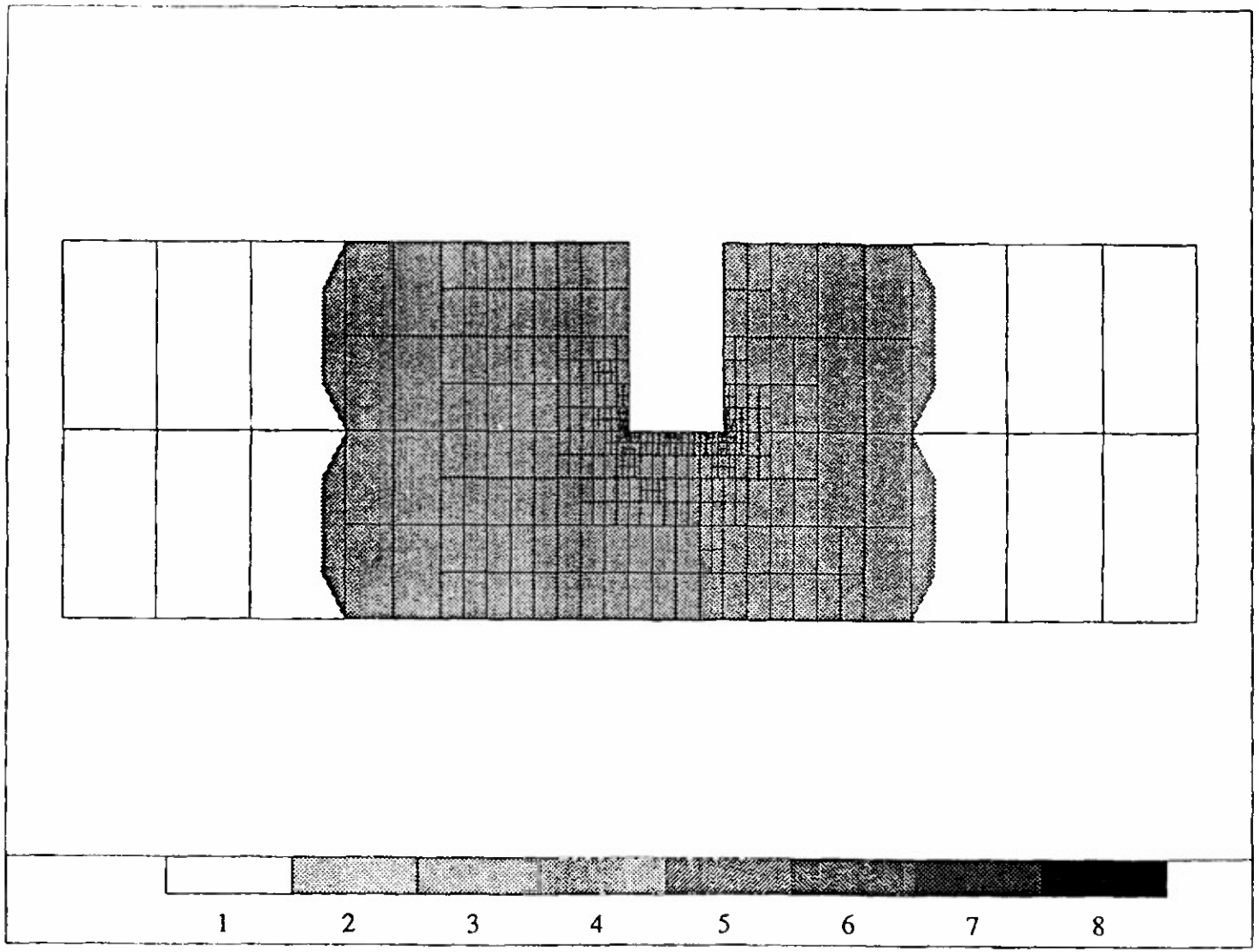

Fig. 24 Wave propagation in an elastic panel problem. An h adaptive finite element mesh at time $t = 0.5\ s$.

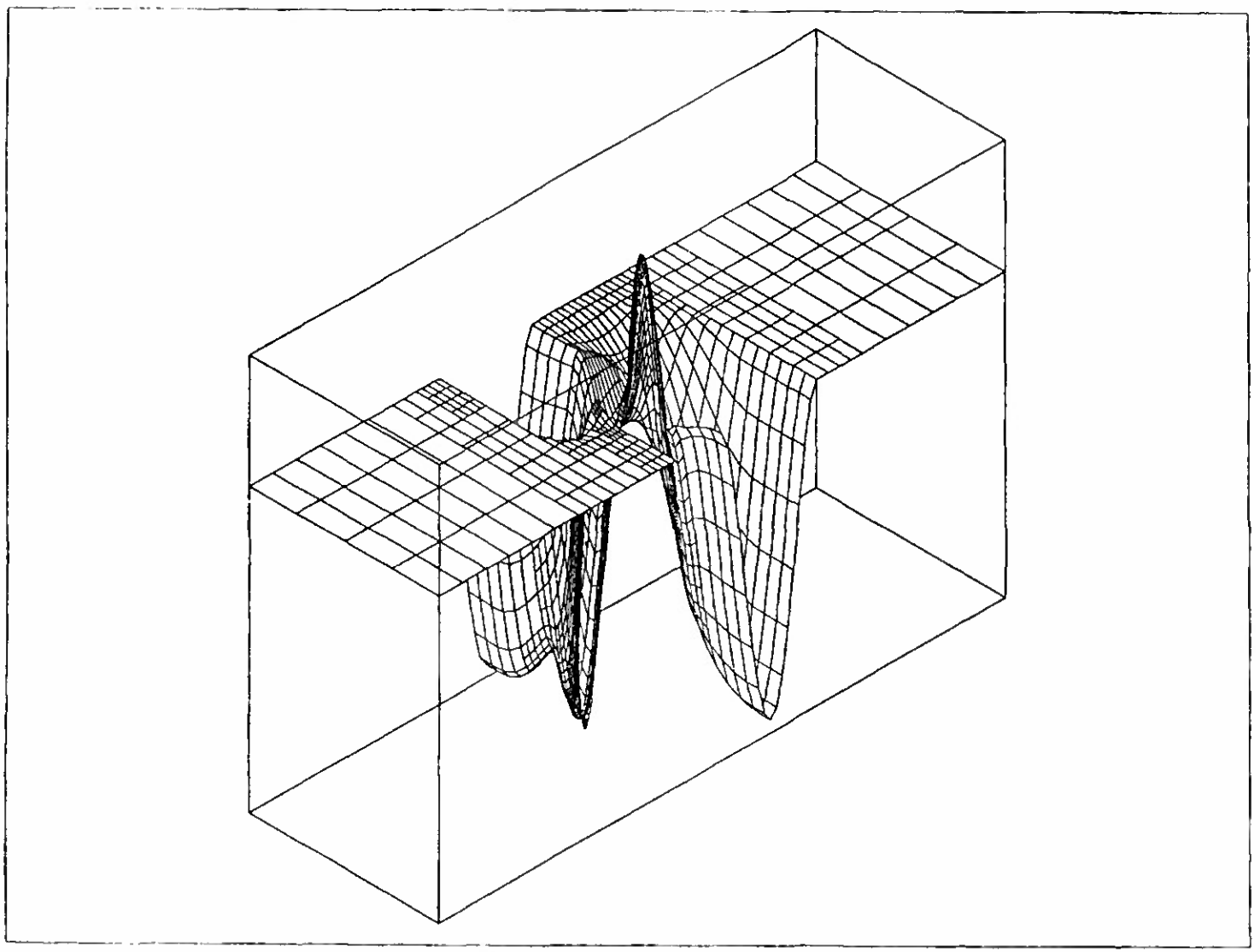

Fig. 25 Wave propagation in an elastic panel problem. The x component of the velocity vector at time $t = 0.5\ s$.

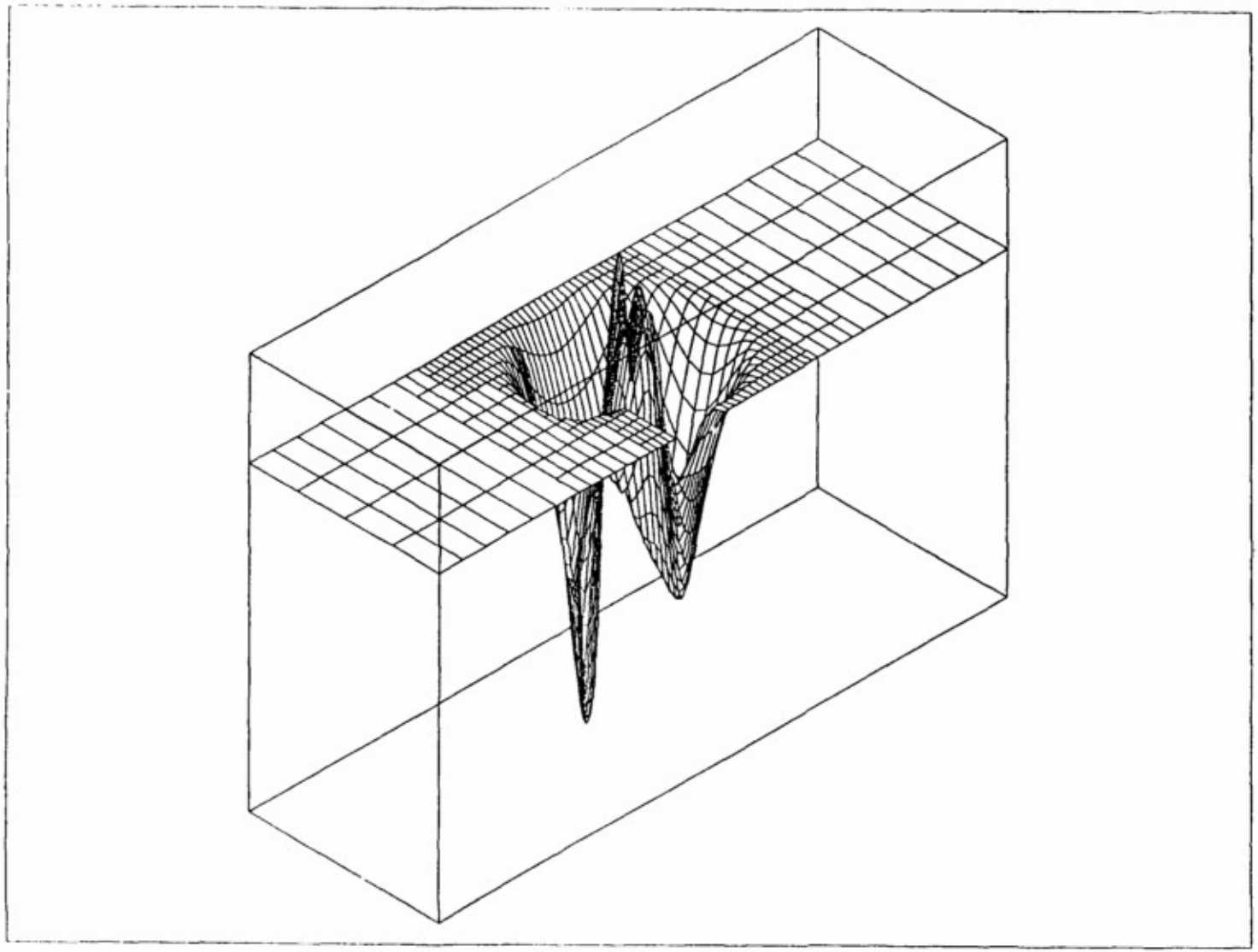

Fig. 26 Wave propagation in an elastic panel problem. The y component of the velocity vector at time $t = 0.5$ s.

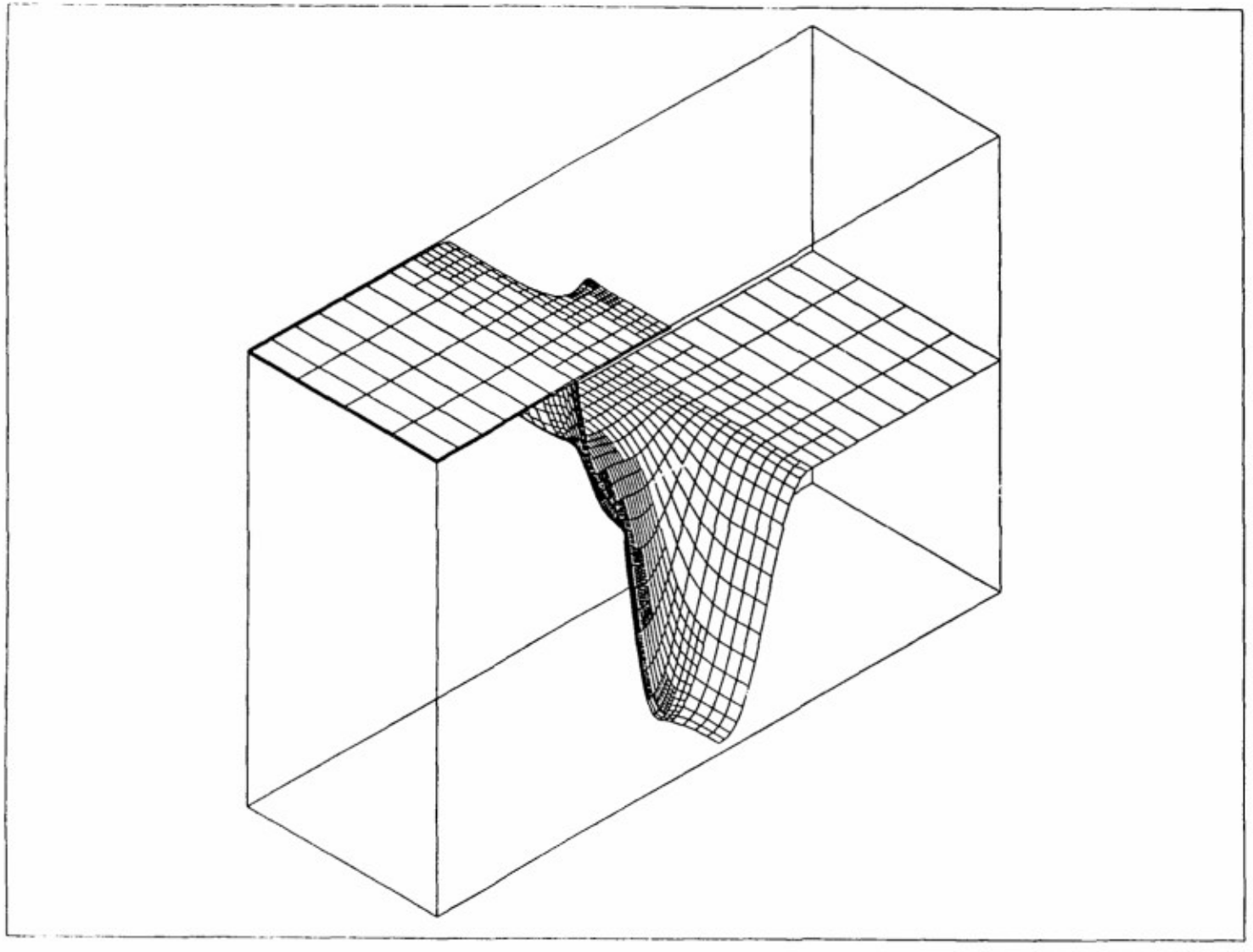

Fig. 27 Wave propagation in an elastic panel problem. The x component of the displacement vector at time $t = 0.5\ s$.

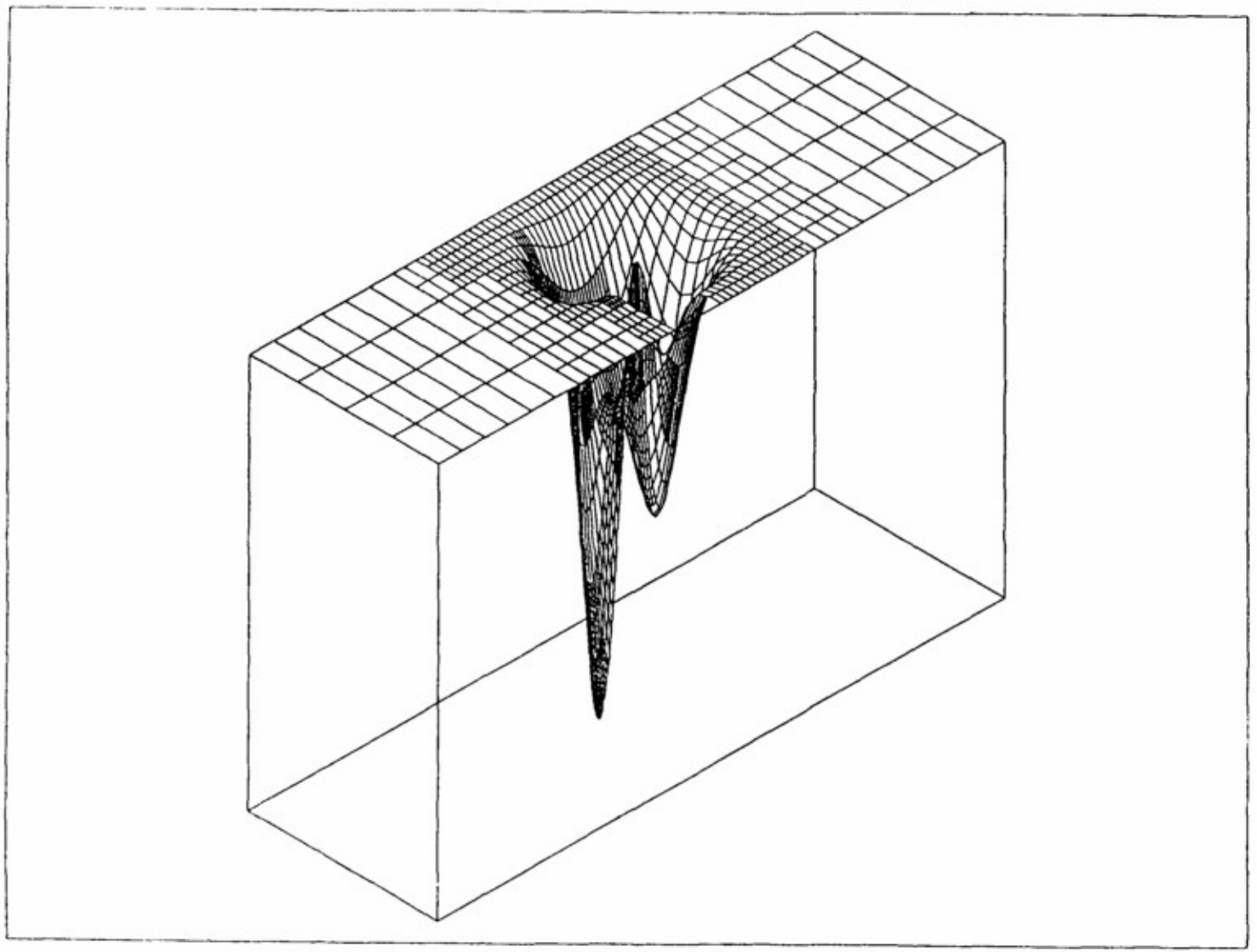

Fig. 28 Wave propagation in an elastic panel problem. The y component of the displacement vector at time $t = 0.5\ s$.

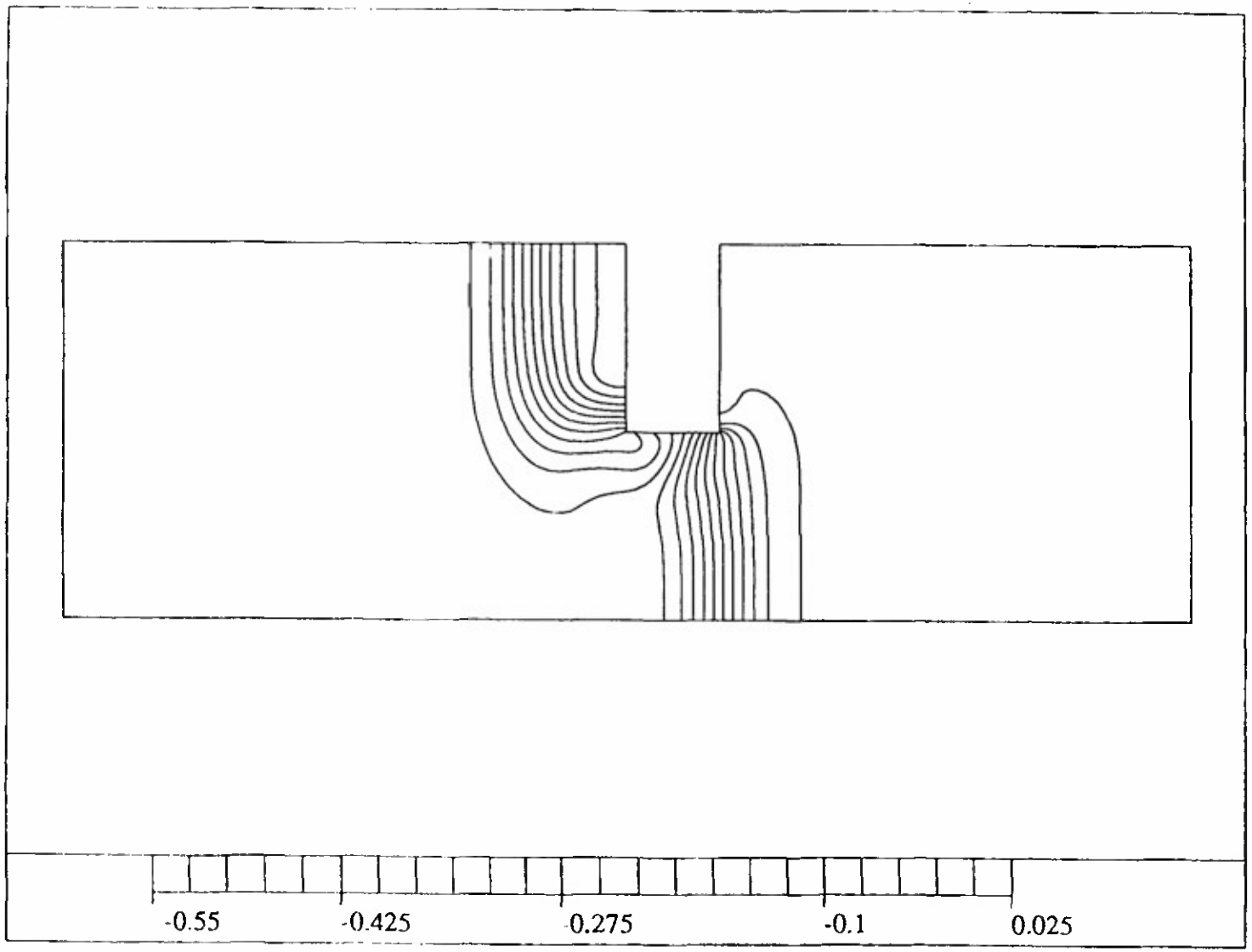

MIN=-0.545714
MAX=0.0042385

Fig. 29 Wave propagation in an elastic panel problem. x-displacement contours at time $t = 0.5\ s$.

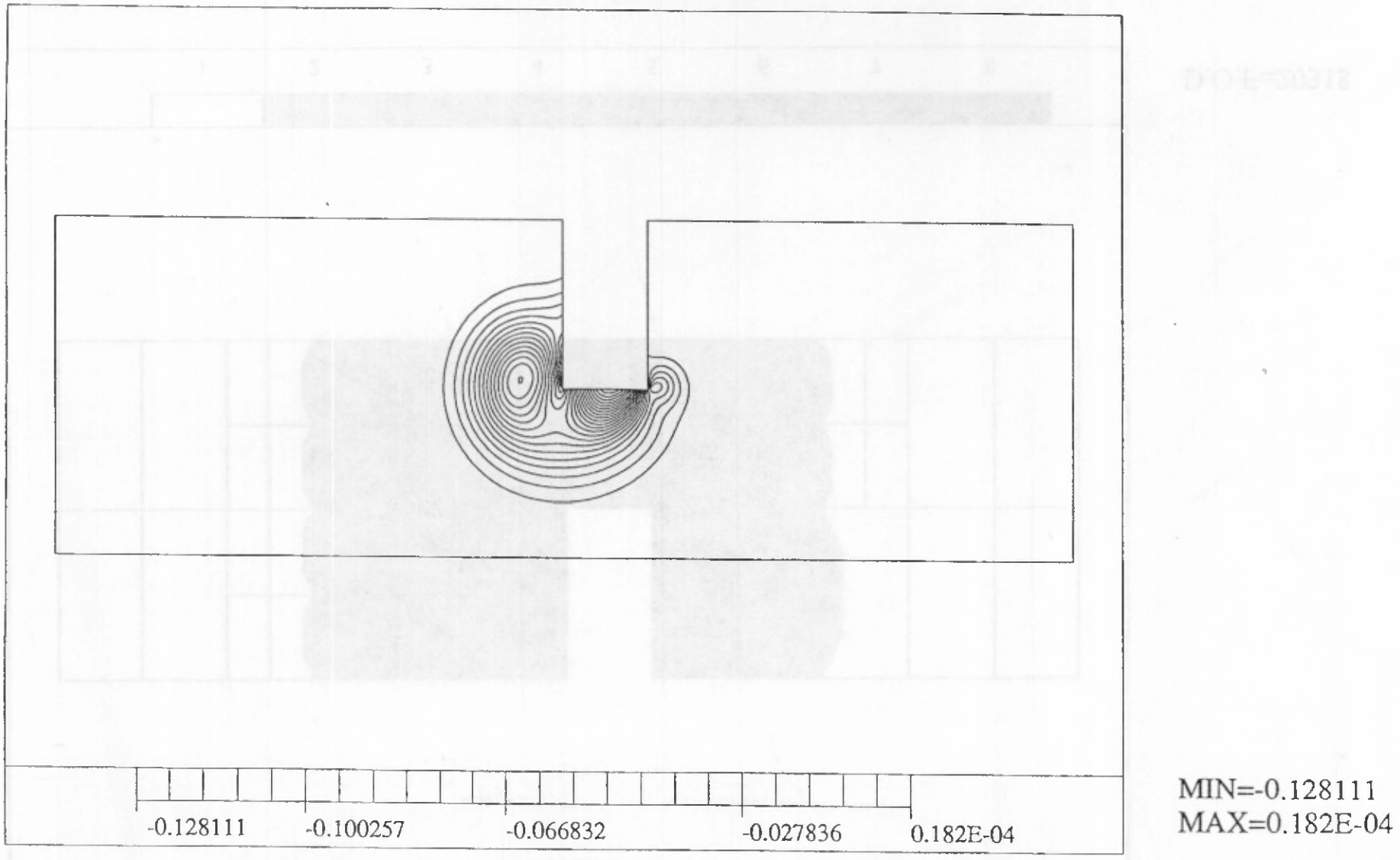

Fig. 30 Wave propagation in an elastic panel problem. y-displacement contours at time $t = 0.5$ s.

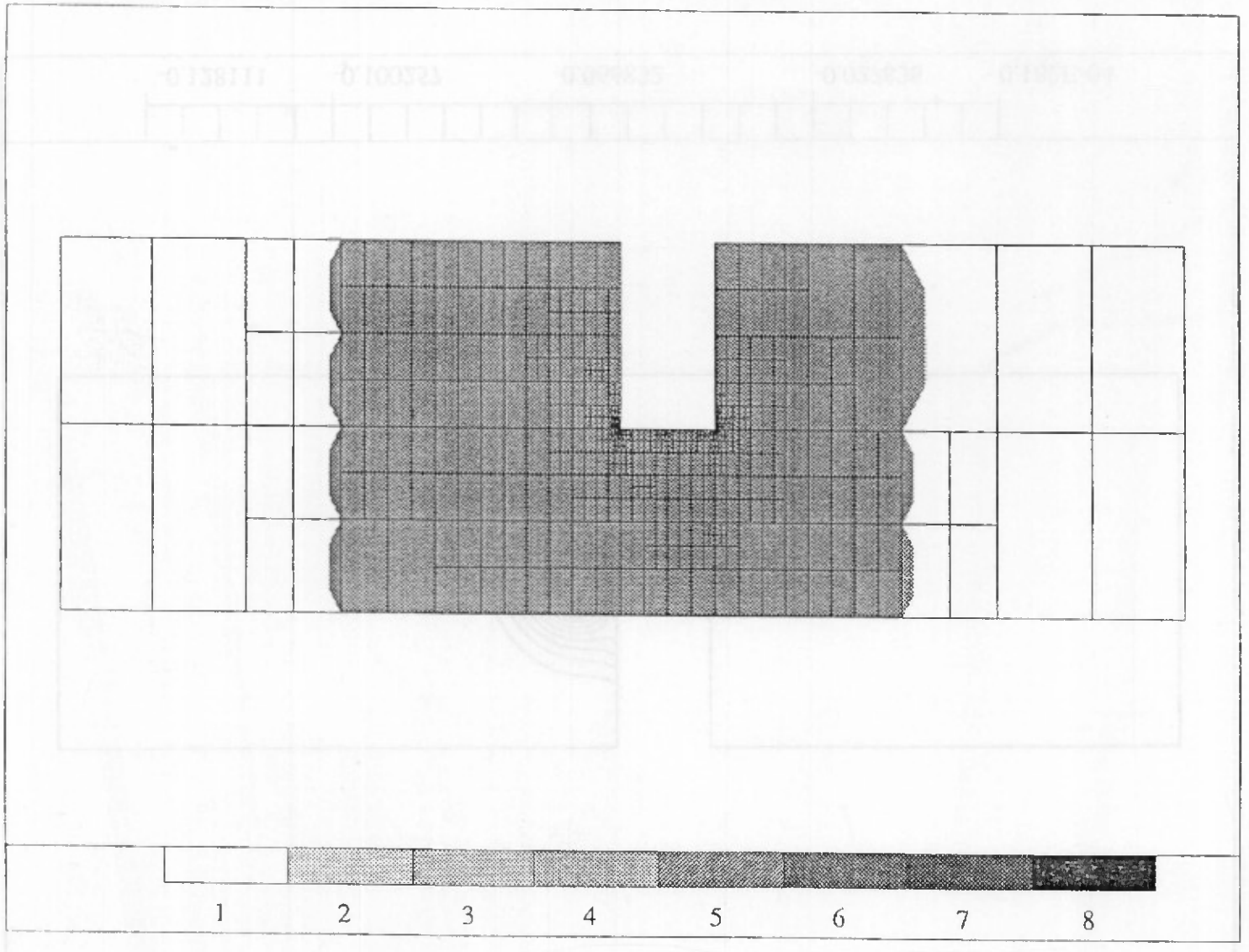

Fig. 31 Wave propagation in an elastic panel problem. An h adaptive finite element mesh at time $t = 0.75$ s.

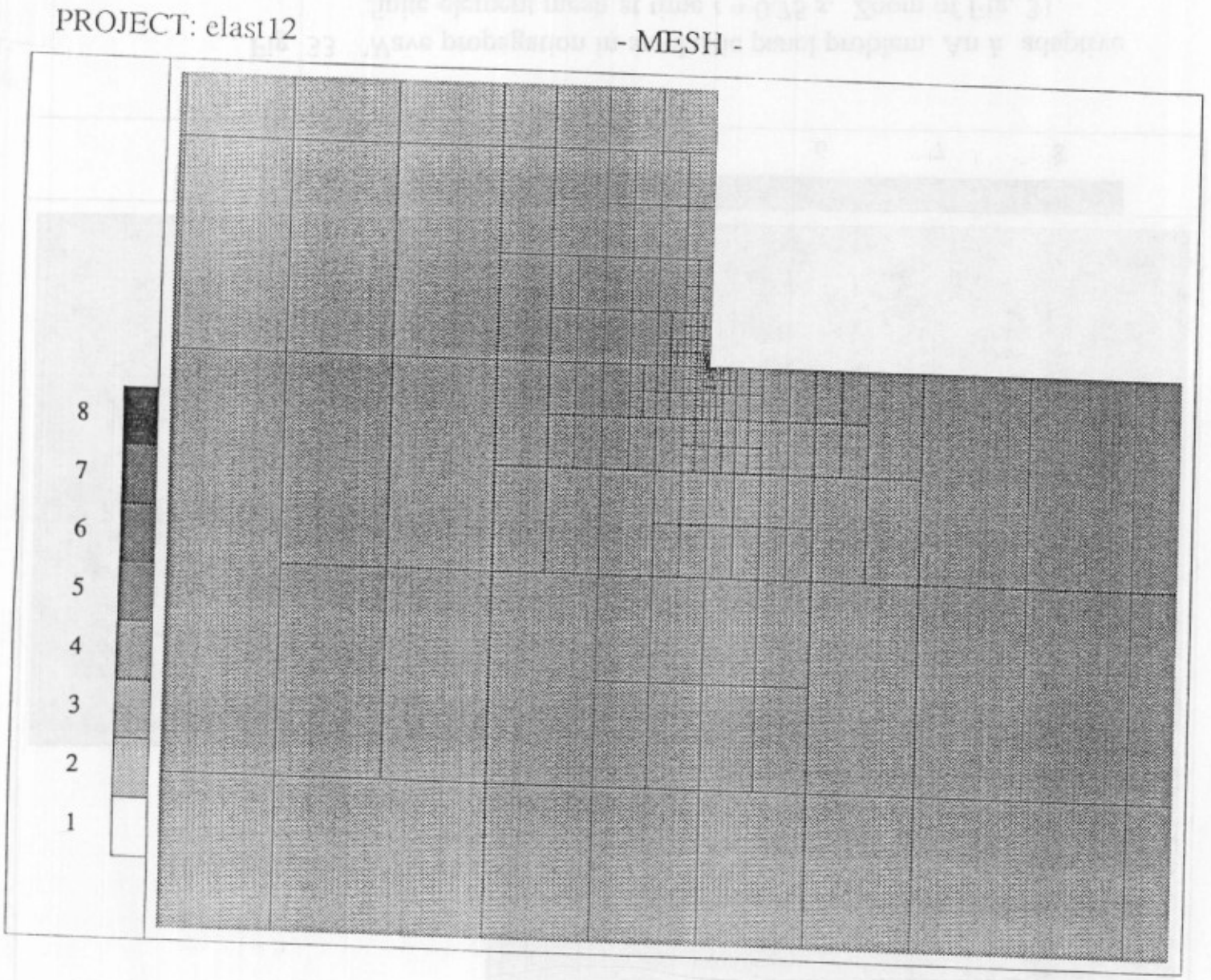

Fig. 32 Wave propagation in an elastic panel problem. An h adaptive finite element mesh at time $t = 0.75\ s$. Zoom of Fig. 31.

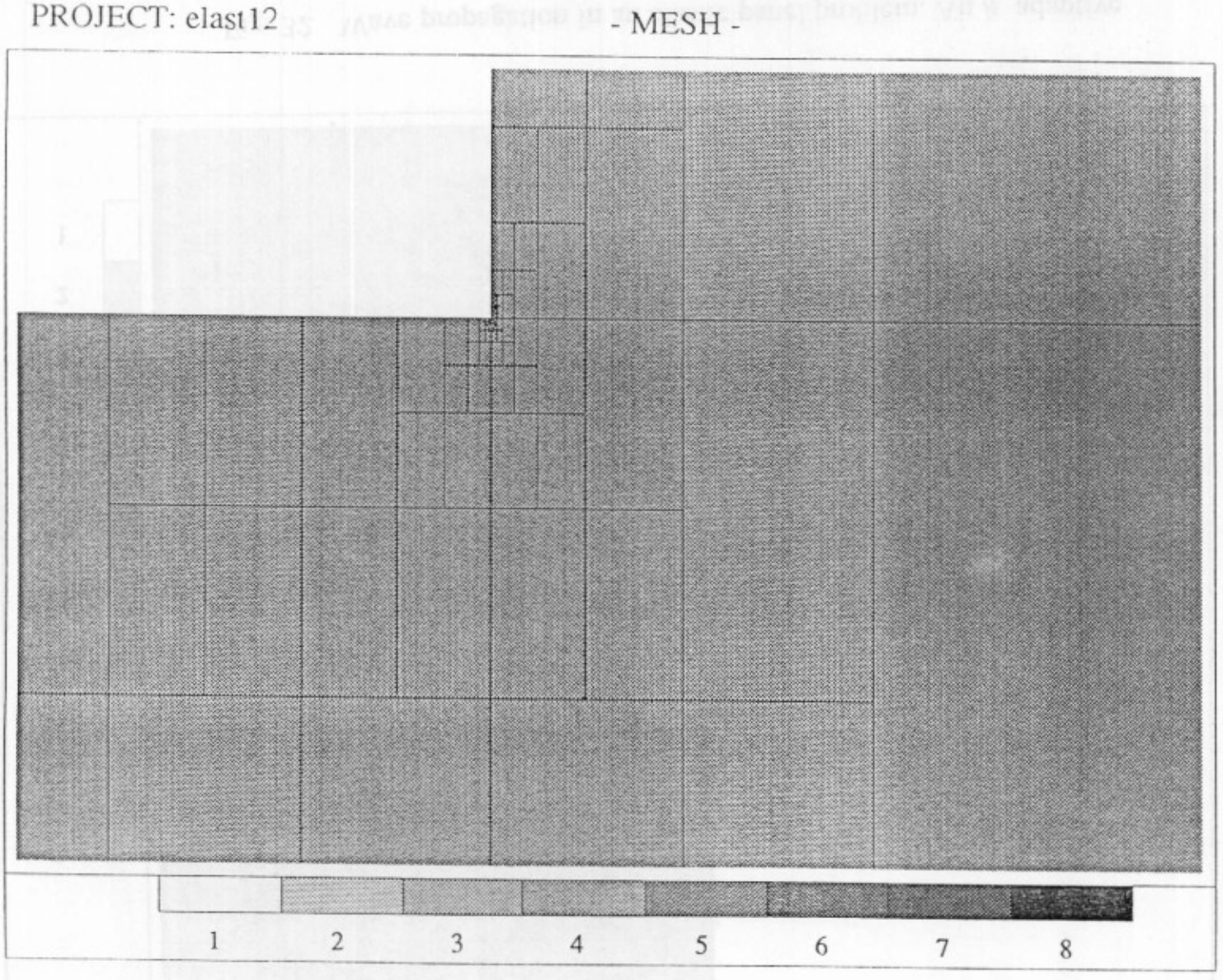

Fig. 33 Wave propagation in an elastic panel problem. An h adaptive finite element mesh at time $t = 0.75\ s$. Zoom of Fig. 31.

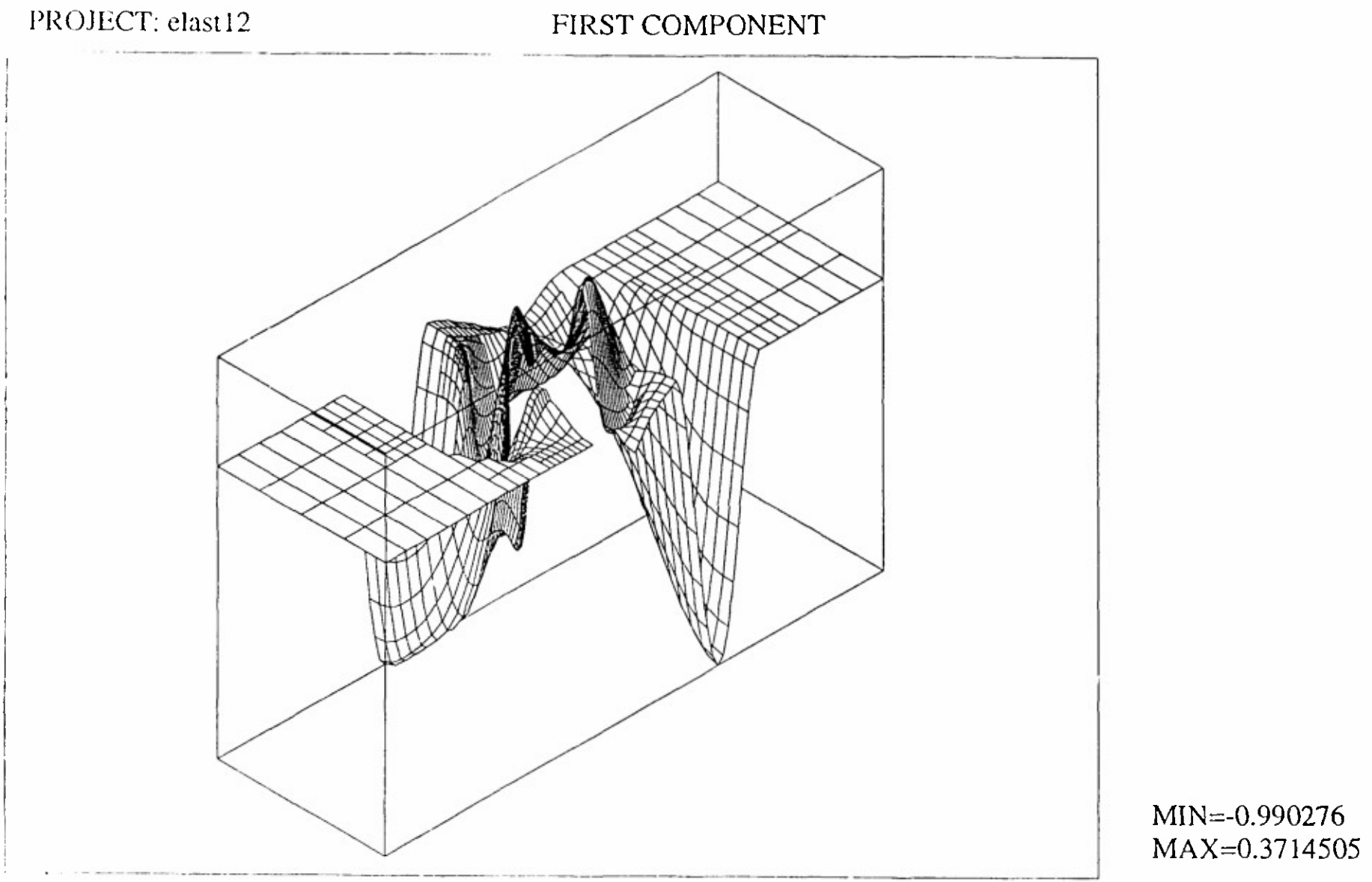

Fig. 34 Wave propagation in an elastic panel problem. The x component of the velocity vector at time $t = 0.75$ s.

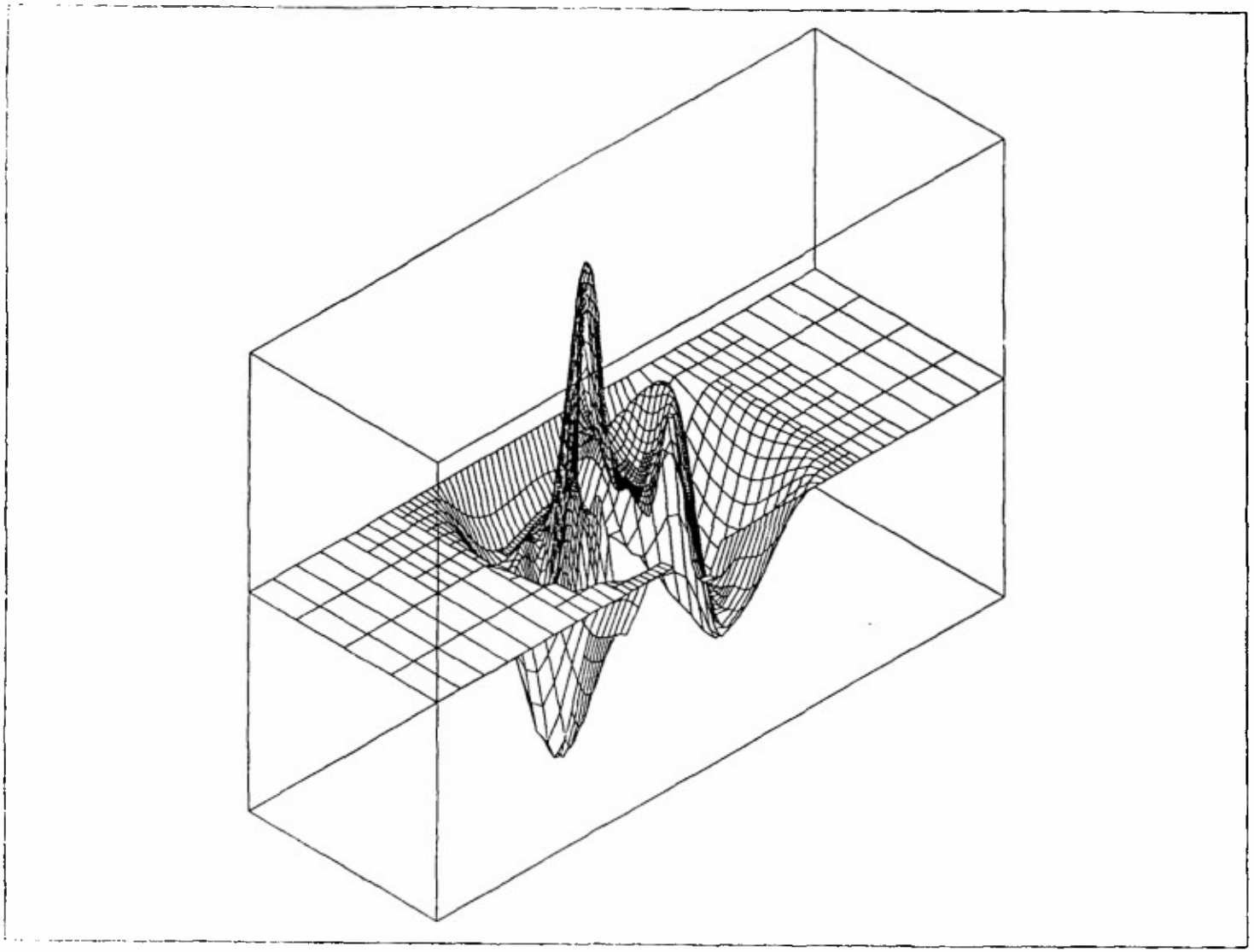

Fig. 35 Wave propagation in an elastic panel problem. The y component of the velocity vector at time $t = 0.75$ s.

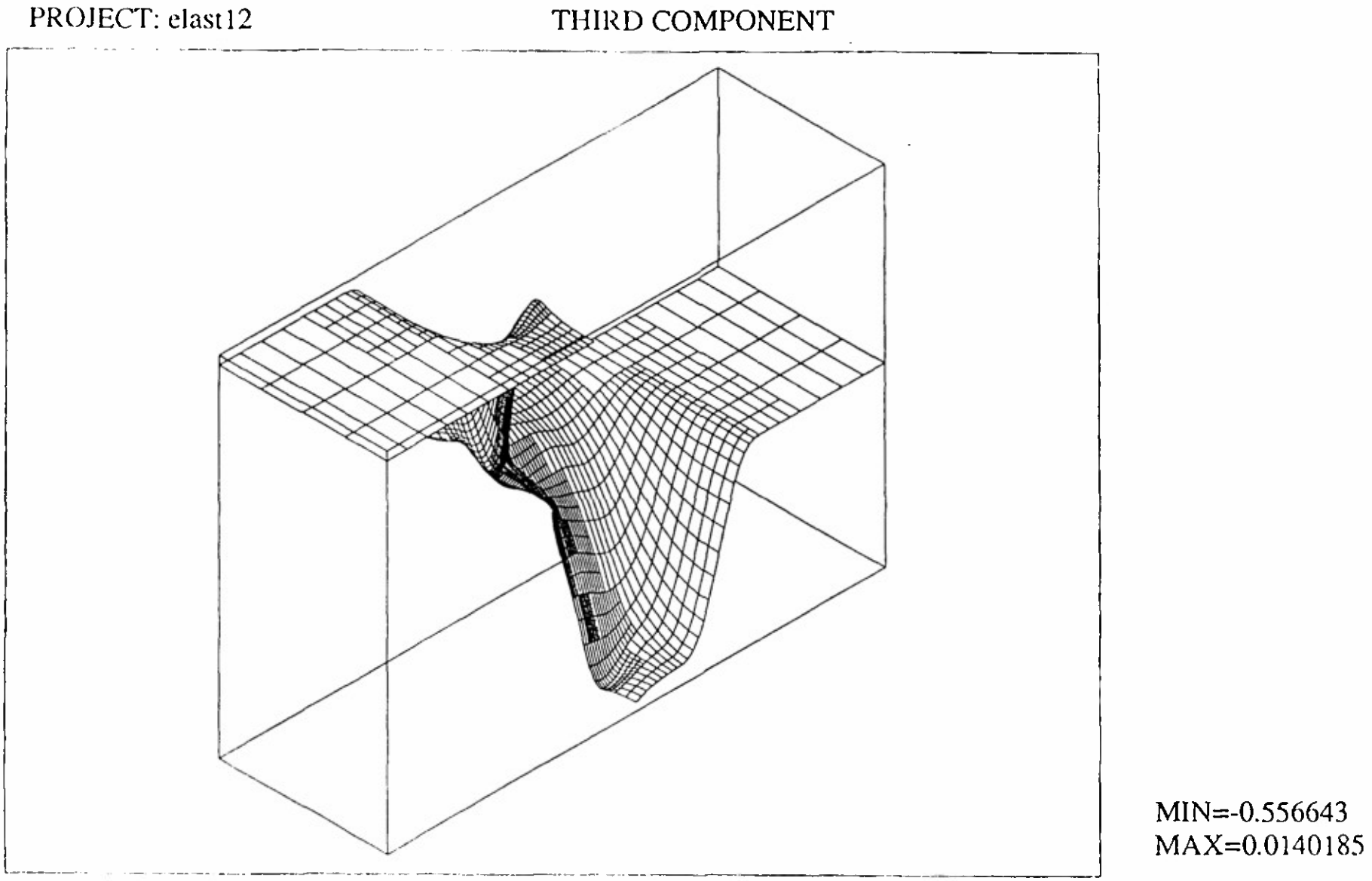

Fig. 36 Wave propagation in an elastic panel problem. The x component of the displacement vector at time $t = 0.75$ s.

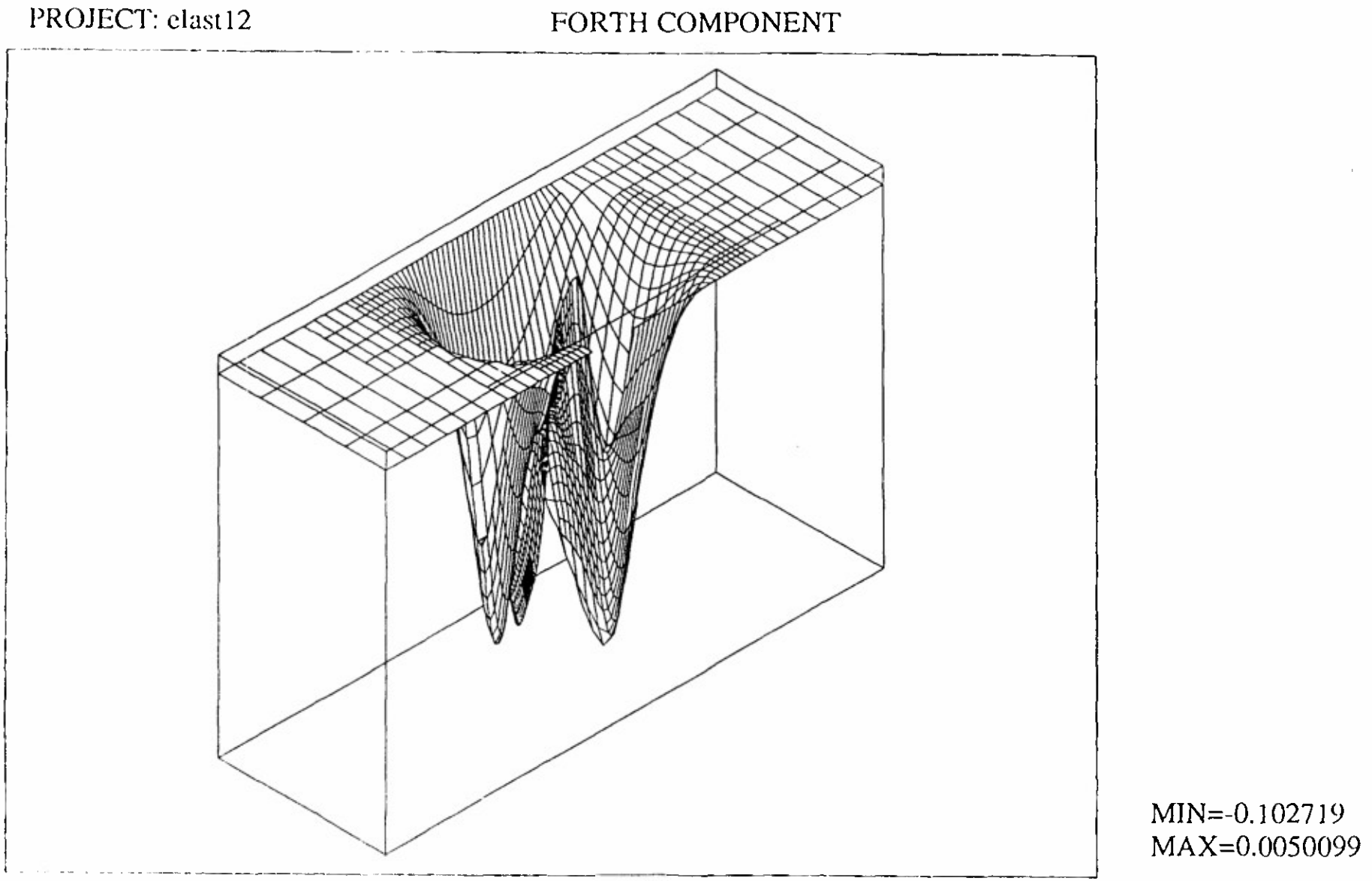

Fig. 37 Wave propagation in an elastic panel problem. The y component of the displacement vector at time $t = 0.75$ s.

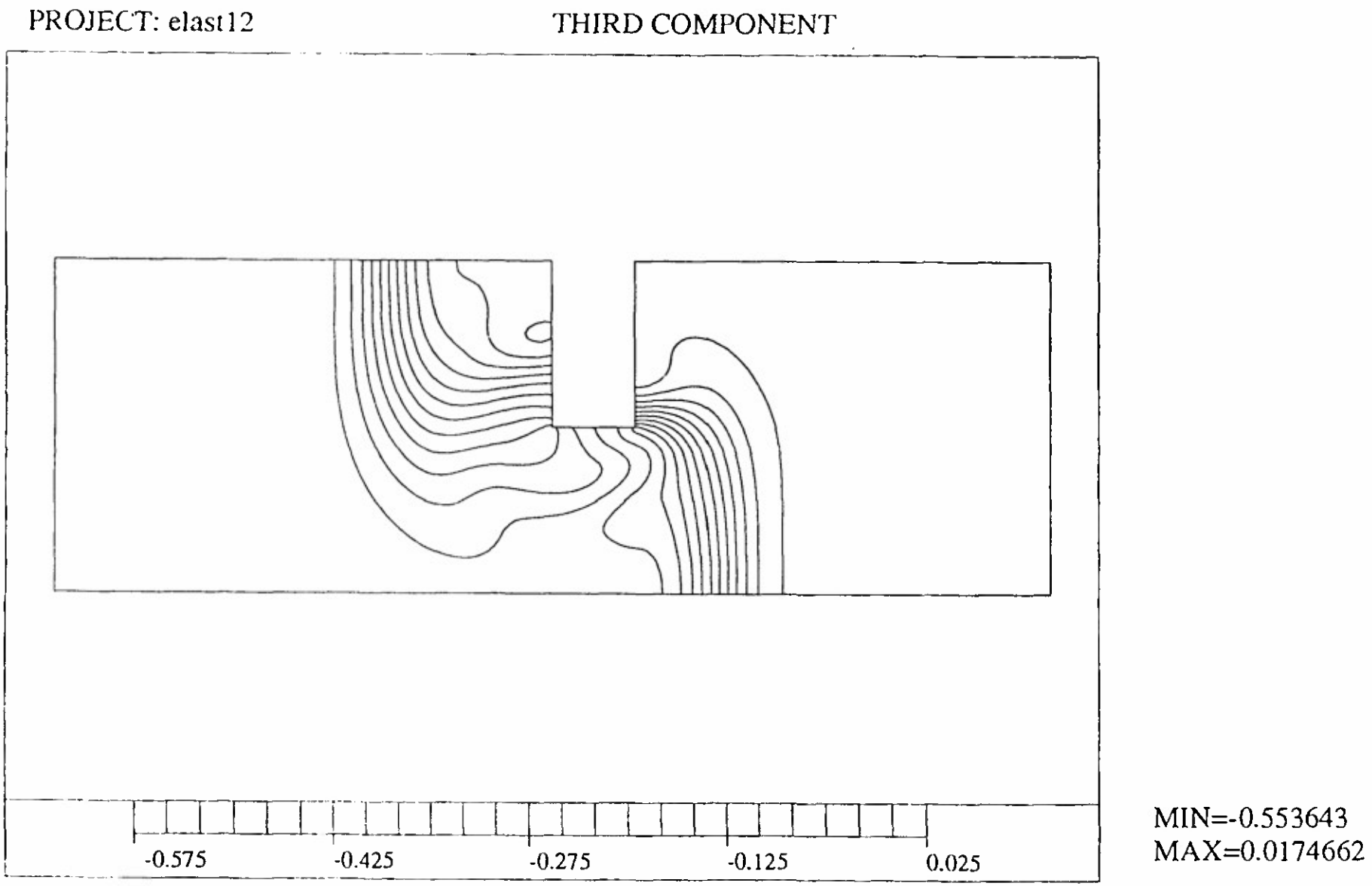

Fig. 38 Wave propagation in an elastic panel problem. x-displacement contours at time $t = 0.75$ s.

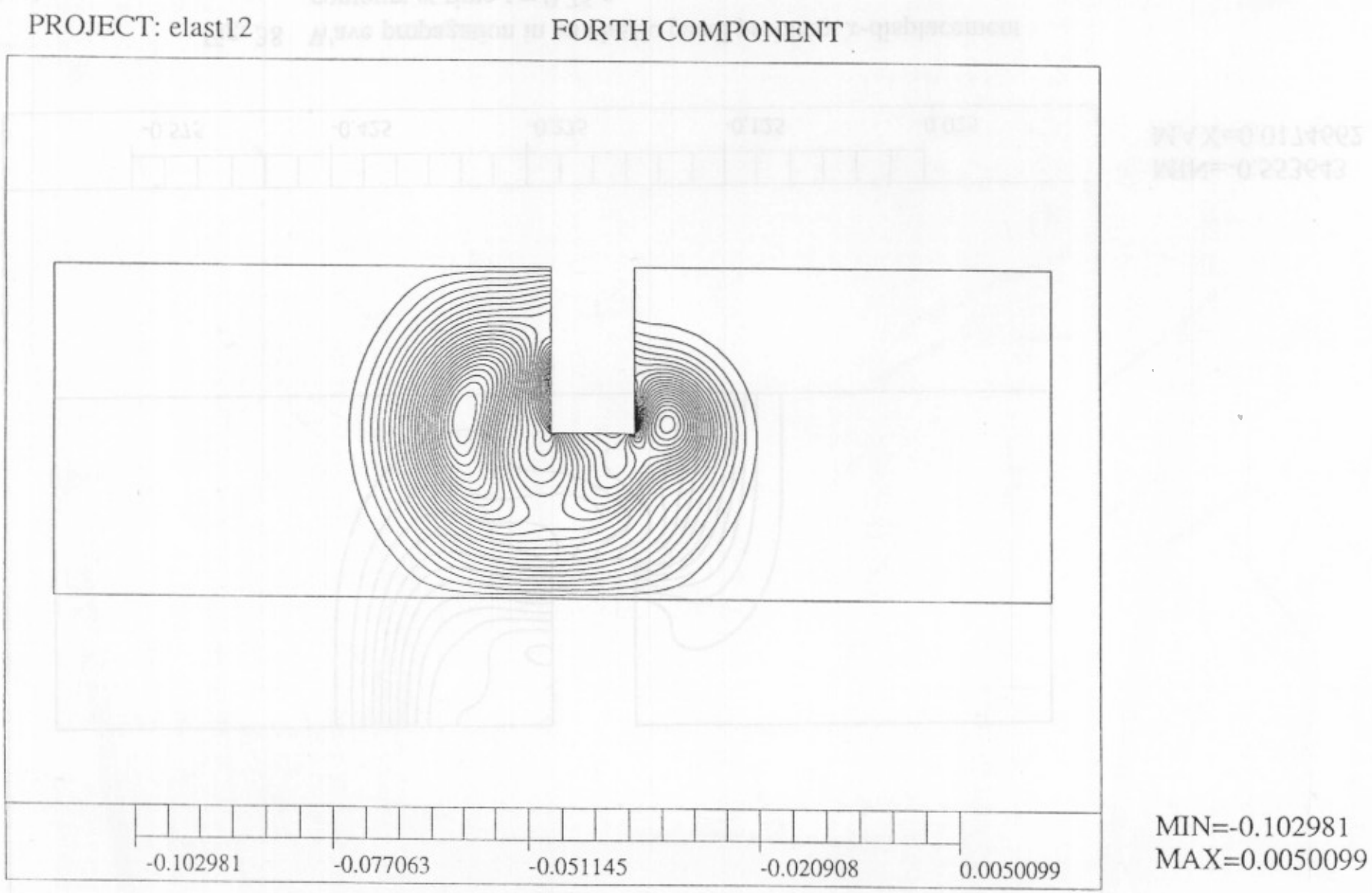

Fig. 39 Wave propagation in an elastic panel problem. y-displacement contours at time $t = 0.75\ s$.

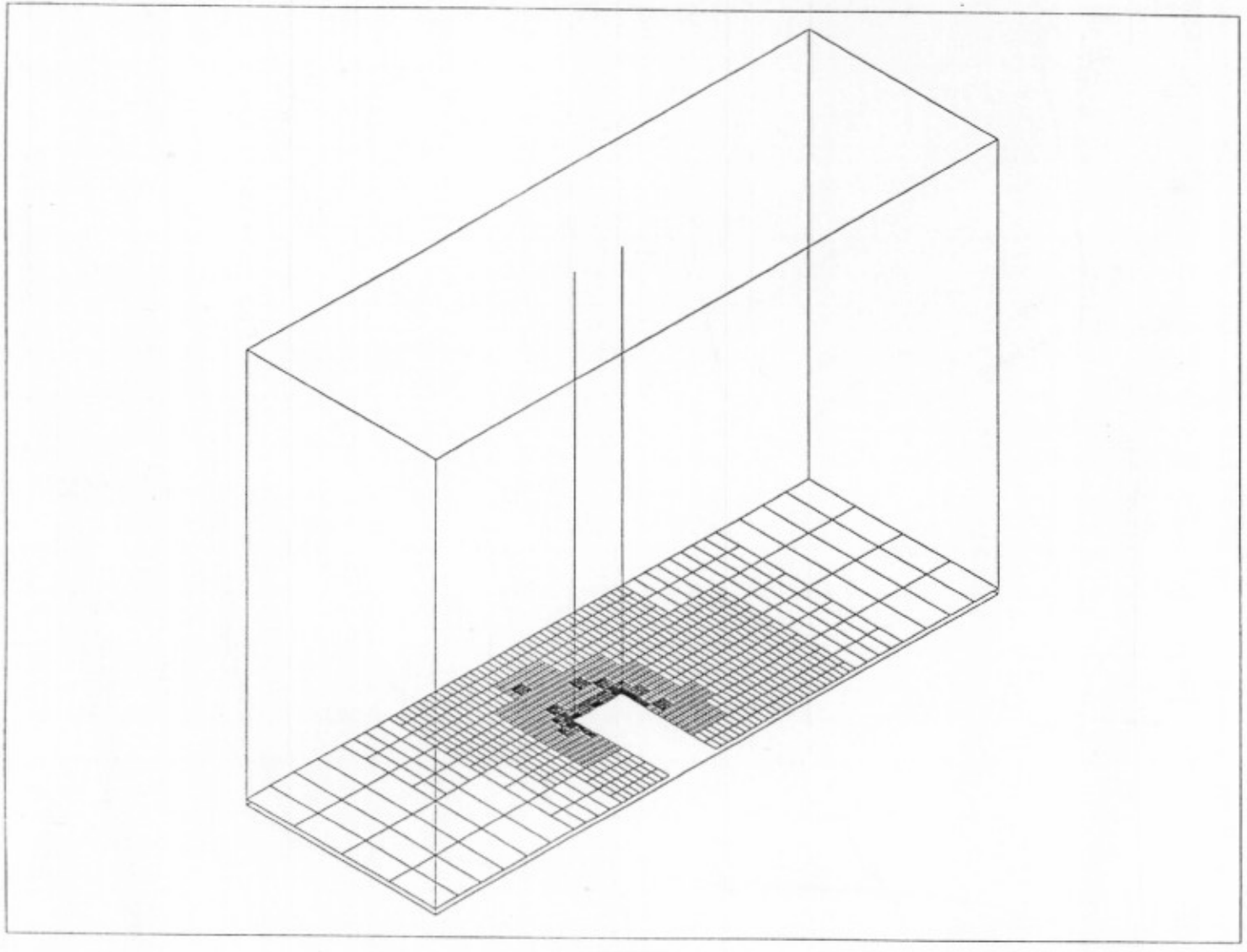

Fig. 40 Wave propagation in an elastic panel problem. The x -x component of the stress tensor at time $t = 0.75$ s.

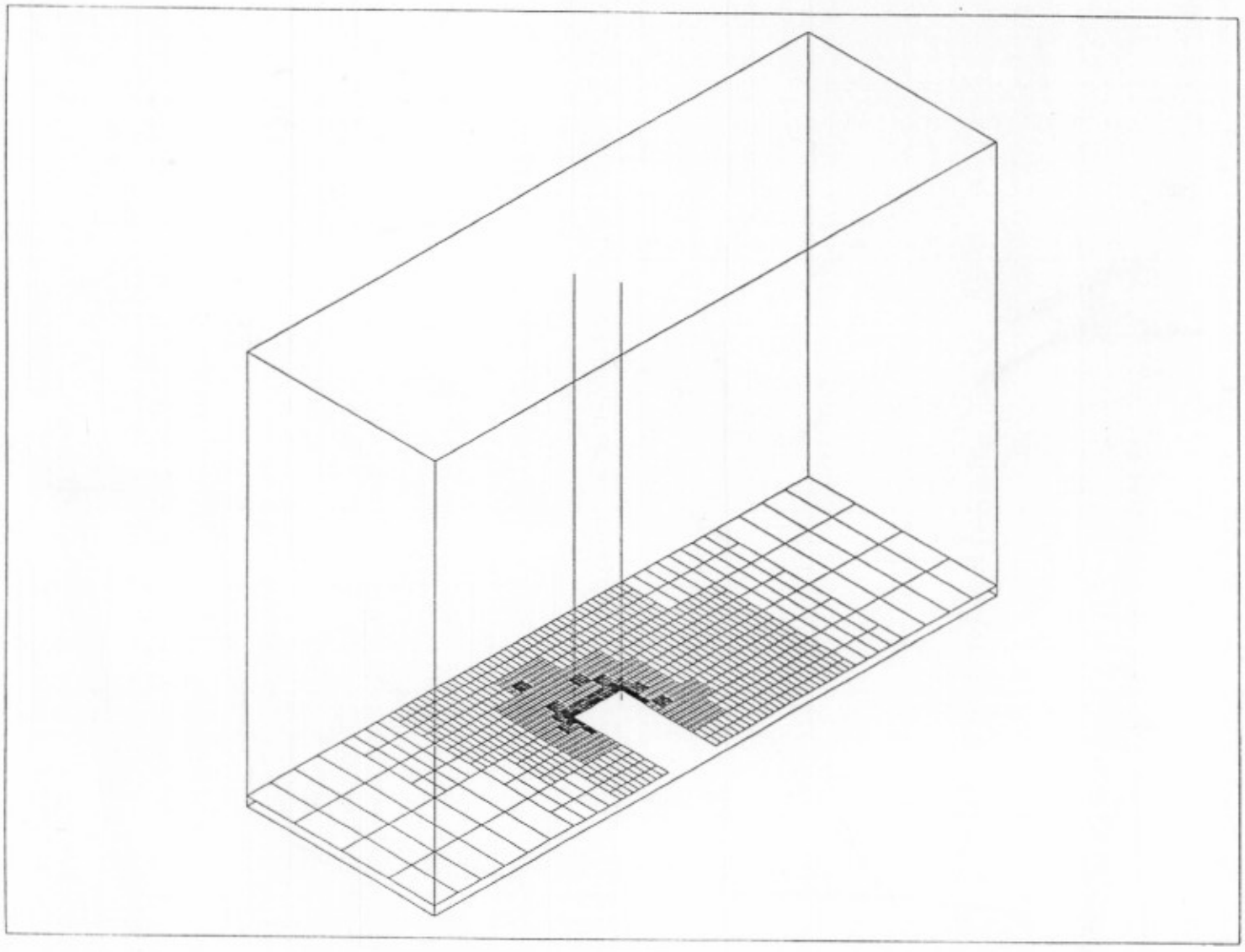

Fig. 41 Wave propagation in an elastic panel problem. The y -y component of the stress tensor at time $t = 0.75$ s.

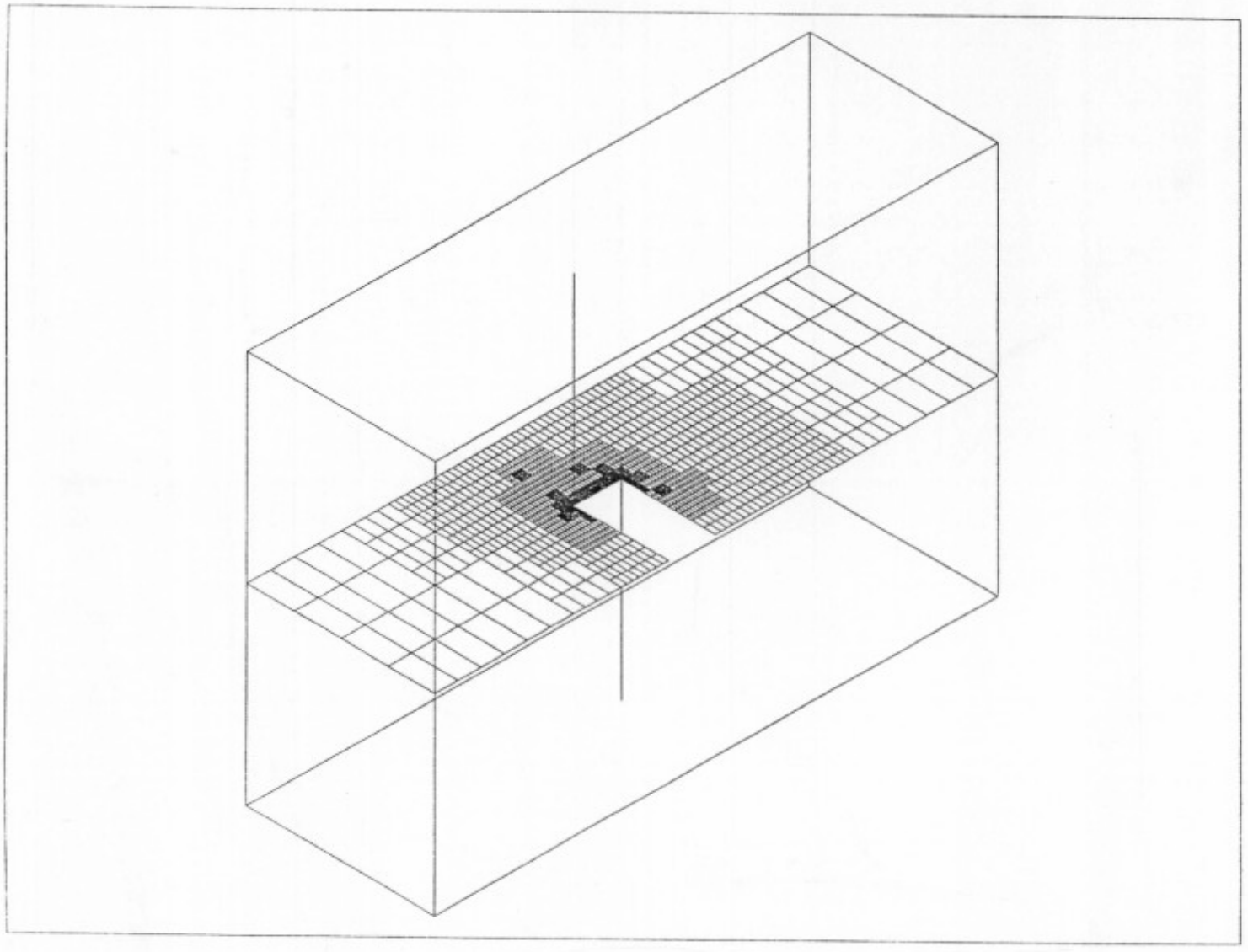

Fig. 42 Wave propagation in an elastic panel problem. The x -y component of the stress tensor at time $t = 0.75$ s.

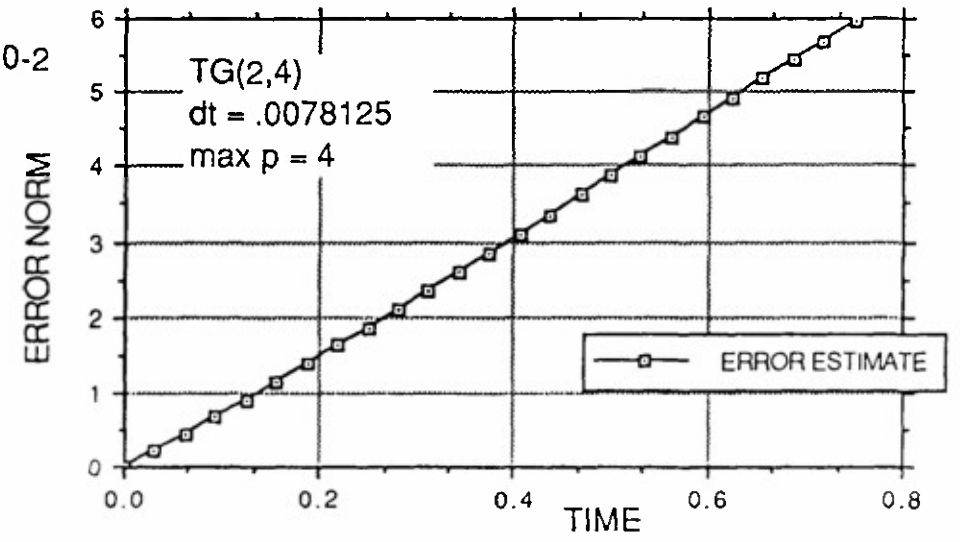

Fig. 43 Wave propagation in an elastic panel problem. The bound on the global energy norm of the error as a function of time.

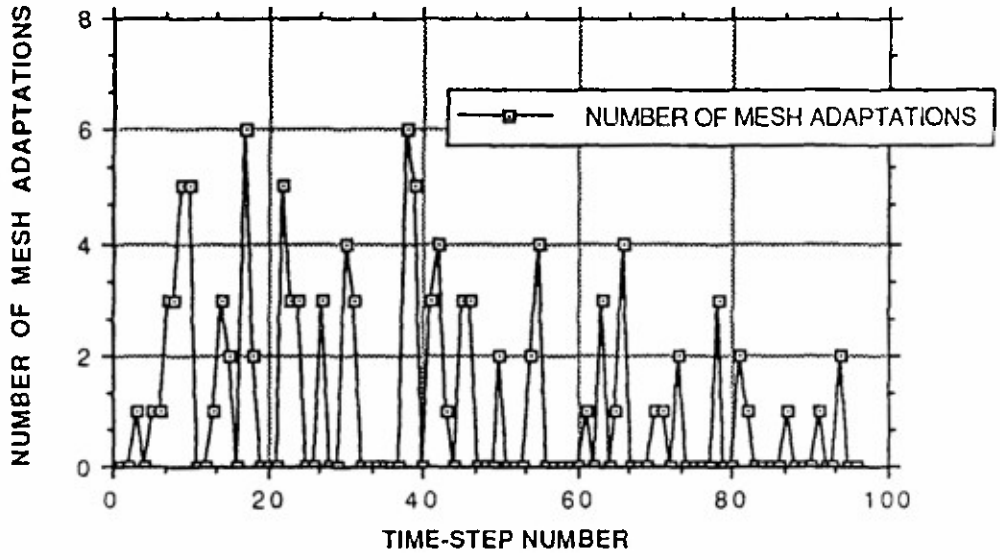

Fig. 44 Wave propagation in an elastic panel problem. The number of mesh adaptations as a function of time.